



UNIVERSITY  
OF TURKU

# THE BIOLOGICAL ROLE OF OMEGA SUBUNIT OF CYANOBACTERIAL RNA POLYMERASE

---

Juha Kurkela





UNIVERSITY  
OF TURKU

# THE BIOLOGICAL ROLE OF OMEGA SUBUNIT OF CYANOBACTERIAL RNA POLYMERASE

---

Juha Kurkela

## **University of Turku**

---

Faculty of Science and Engineering  
Department of Biochemistry  
Molecular Plant Biology  
Doctoral programme in Molecular Life Sciences

## **Supervised by**

---

Adjunct Professor, Taina Tyystjärvi  
Molecular Plant Biology  
Department of Biochemistry  
University of Turku  
Finland

## **Reviewed by**

---

Associate Professor, Takashi Osanai  
Department of Agricultural Chemistry  
Meiji University  
Japan

Dr, Franck Chauvat  
Department of Microbiology  
CEA Saclay  
France

## **Opponent**

---

Prof. Karl Forchhammer  
Interfaculty Institute of Microbiology  
University of Tübingen,  
Germany

The originality of this publication has been checked in accordance with the University of Turku quality assurance system using the Turnitin OriginalityCheck service.

Cover Image: Juha Kurkela

ISBN 978-951-29-8149-6 (PRINT)  
ISBN 978-951-29-8148-9 (PDF)  
ISSN 0082-7002 (Print)  
ISSN 2343-3175 (Online)  
Painosalama Oy, Turku, Finland 2020

*"All we have to decide is what to do with the time that is given us."  
J. R.R. Tolkien*

UNIVERSITY OF TURKU  
Faculty of Science and Engineering  
Department of Biochemistry  
Molecular Plant Biology  
JUHA KURKELA: The biological role of omega subunit of cyanobacterial  
RNA polymerase  
Doctoral Dissertation, 159 pp.  
Doctoral Programme in Molecular life Sciences  
September 2020

## ABSTRACT

Cyanobacteria are important primary producers performing oxygenic photosynthesis using CO<sub>2</sub> or HCO<sub>3</sub><sup>-</sup> as a carbon source. Active adjustment of gene expression according to environmental cues depends on the RNA polymerase (RNAP). The cyanobacterial RNAP core ( $\alpha_2\beta\beta'\gamma\omega$ ) recruits one of regulatory  $\sigma$  factors to form an RNAP holoenzyme that recognizes the promoter sequence and initiates transcription. The RNAP core structure of cyanobacteria is unique due to splitting of  $\beta'$  into  $\gamma$  and  $\beta'$  subunits. The small  $\omega$  subunit of RNAP, encoded by the *rpoZ* gene, has been found to be non-essential in many heterotrophic bacteria but has not been studied in cyanobacteria. To characterize the  $\omega$  subunit, an inactivation strain ( $\Delta rpoZ$ ) was constructed in the cyanobacterial model organism *Synechocystis* sp. PCC 6803. The  $\omega$  subunit was found to be non-essential in our standard growth conditions but essential in heat and in high CO<sub>2</sub>. The carbon concentrating mechanisms, carbon fixation and nitrogen acquisition genes were downregulated in  $\Delta rpoZ$  in standard conditions, whereas other household genes including transcription and translation machinery genes expressed normally. Although  $\Delta rpoZ$  grew well in standard conditions, light saturated photosynthetic activity was low and some photoprotective mechanisms were upregulated. The heat lethal phenotype of  $\Delta rpoZ$  was accompanied with a highly abnormal transcriptome but high amounts of rRNA in  $\Delta rpoZ$  indicated that the  $\omega$ -less RNAP stayed active upon heat treatment. In high CO<sub>2</sub>, more stationary phase specific RNAP-SigC holoenzyme was formed in  $\Delta rpoZ$  than in the control strain (CS), leading to downregulation of many photosynthesis, nitrogen acquisition and cell division genes. Thus,  $\Delta rpoZ$  did not enhance photosynthesis, readjust C/N balance or produce enough cell wall components in high CO<sub>2</sub>, which eventually led to accumulation of glycogen and cell doublets, and to growth arrest. Spontaneously arisen suppressor mutants,  $\Delta rpoZ$ -S1 and  $\Delta rpoZ$ -S2, contained point mutations in the *ssr1600* gene, which rescued acclimation to high CO<sub>2</sub> and to heat. Due to L24S and G43V mutations of Ssr1600, the amount of the Ssr1600 protein was low in the suppressor mutants. Our results revealed that Ssr1600 functions as an anti-SigC antagonist. In the suppressor strains, similar low amount of RNAP-SigC holoenzyme is formed as in the CS, and cells acclimate to high CO<sub>2</sub>.

**KEYWORDS:** Cyanobacteria, RNA polymerase,  $\sigma$  factor,  $\omega$  subunit, high CO<sub>2</sub>, photosynthesis, cell division, Ssr1600, anti- $\sigma$  factor antagonist, gene expression

TURUN YLIOPISTO

Luonnontieteiden ja tekniikan tiedekunta

Biokemian laitos

Molekulaarinen kasvibiologia

JUHA KURKELA: The biological role of omega subunit of cyanobacterial

RNA polymerase

Väitöskirja, 159 s.

Molekulaaristen biotieteiden tohtorihjelma

Syyskuu 2020

## TIIVISTELMÄ

Syanobakteerit ovat tärkeitä perustuottajia, jotka käyttävät hiilen lähteenä joko CO<sub>2</sub>:ta tai HCO<sub>3</sub><sup>-</sup>:ta. Syanobakteerit sopeutuvat ympäristön muutoksiin muuttamalla geenien ilmentymisestä vastaavan RNA-polymeraasin (RNAP) toimintaa. Syanobakteerien RNAP:n ytimeen ( $\alpha_2$ ,  $\beta$ ,  $\beta'$ ,  $\gamma$  ja  $\omega$ ) kiinnittyy transkription aloitusta varten yksi säätelevistä  $\sigma$ -alaysiköistä ja RNAP-holoentsyymi tunnistaa geenin promoottorialueen ja käynnistää transkription. Tutkimusten mukaan  $\omega$  on ainoa RNAP:n alaysikkö, joka ei ole välttämätön monilla heterotrofisilla bakteereilla. Syanobakteereissa  $\omega$ -alaysikön tehtäviä ei ole kuitenkaan tutkittu ja tästä syystä rakennettiin kanta, joka ei tuota  $\omega$ -alaysikköä ( $\Delta$ rpZ). Tavallisissa kasvatusolosuhteissa  $\Delta$ rpZ-kanta kasvoi hyvin, mutta kuumassa tai runsaassa CO<sub>2</sub>:ssa  $\Delta$ rpZ-kanta ei pystynyt kasvamaan. Solun perustoimintojen geneistä hiilen keräämiseen ja sitomiseen sekä typen sisäänottoon osallistuvat geenit ilmenivät vähemmän  $\Delta$ rpZ-kannalla kuin villityypin kannalla (WT), mutta muut ylläpitogeenit ilmenivät normaalisti. Vaikka  $\Delta$ rpZ-kanta kasvoi tavallisissa olosuhteissa, sen maksimaalinen fotosynteesiteho oli pienempi kuin WT:llä ja soluihin kertyi valolta suojaavia yhdisteitä. Kuumassa RNAP pysyi toiminnallisena ilman  $\omega$ -alaysikköä, mutta normaalia geenien ilmenemisen säätelyä ei tapahtunut. Kasvatettaessa soluja runsaassa CO<sub>2</sub>:ssa  $\Delta$ rpZ-soluihin muodostui paljon stationääriselle kasvuvaiheelle tyypillistä RNAP-SigC holoentsyymiä, jolloin monet fotosynteesistä, typen sisäänotosta ja solun jakautumisesta vastaavat geenit ilmenivät vähemmän kuin WT:llä. Geenien ilmentymisessä havaitut ongelmat estivät  $\Delta$ rpZ-kannan sopeutumisen lisääntyneeseen CO<sub>2</sub>:een: fotosynteesi ei tehostunut, typi/hiili tasapaino ei säätynyt, jolloin glykogeeniä kertyi soluihin, solun jakautuminen pysähtyi ja lopulta  $\Delta$ rpZ-solut kuolivat. Itsenäisesti muuttuneista  $\Delta$ rpZ-kannoista ( $\Delta$ rpZ-S1 ja  $\Delta$ rpZ-S2) löydettiin genomisekvensoinnin avulla *ssr1600*-geenistä pistemutaatiot, jotka mahdollistivat  $\Delta$ rpZ-S1- ja  $\Delta$ rpZ-S2-kantojen kasvun korkeassa CO<sub>2</sub>:ssa. Mutaatioiden seurauksena Ssr1600-proteiini hävisi lähes kokonaan  $\Delta$ rpZ-S1- ja  $\Delta$ rpZ-S2-soluista. Tutkimalla  $\Delta$ rpZ-S-kantoja tarkemmin havaittiin, että Ssr1600-proteiini säätelee SigC:n sitoutumista RNAP:hen.

ASIASANAT: Syanobakteerit, RNA-polymeraasi,  $\sigma$ -alaysikkö,  $\omega$ -alaysikkö, hiilidioksidi, fotosynteesi, solunjakautuminen, Ssr1600

# Table of Contents

<b>Abbreviations .....</b>	<b>8</b>
<b>List of Original Publications .....</b>	<b>10</b>
<b>1 Introduction.....</b>	<b>11</b>
1.1 Cyanobacteria in changing climate.....	11
1.2 The model cyanobacterium <i>Synechocystis</i> sp. PCC 6803.....	12
1.2.1 Structure and cell division .....	12
1.2.2 Carbon concentrating mechanisms and carbon fixation .....	14
1.2.3 Linear photosynthetic electron transfer chain and respiration .....	16
1.2.4 Alternative electron transfer routes and photoprotective mechanisms.....	18
1.2.5 Detection of available Ci and signaling of Carbon/Nitrogen balance .....	21
1.3 Cyanobacterial RNA polymerase .....	24
1.3.1 Structure and function .....	24
1.3.2 Regulatory $\sigma$ factors.....	26
1.3.3 Roles of different $\sigma$ factors in <i>Synechocystis</i> .....	28
1.3.4 Omega subunit.....	31
<b>2 Aims of the Study .....</b>	<b>33</b>
<b>3 Materials and Methods .....</b>	<b>34</b>
3.1 Cyanobacterial strains and growth experiments .....	34
3.2 Measurements of cell properties and photosynthesis .....	35
3.2.1 Light saturated photosynthetic activity and respiration .....	35
3.2.2 Electron transfer rate, P <sub>700</sub> redox transitions and 77 K fluorescence emission spectra .....	35
3.2.3 Pigments, $\alpha$ -tocopherol and lipids .....	36
3.2.4 Glycogen and glutathione.....	36
3.2.5 Cell number analysis and survival rates .....	36
3.2.6 Protein oxidation and cellular ROS content .....	37
3.3 Molecular biology techniques .....	37
3.3.1 Genome sequencing.....	37
3.3.2 Operon analysis .....	37
3.3.3 Total RNA, RT-qPCR and microarray analysis.....	37
3.3.4 SDS-PAGE, BN-PAGE and Western blot.....	38

3.3.5	Detection of sigma factors in RNA polymerase holoenzyme.....	39
3.3.6	Immunoprecipitation and silver staining.....	39
<b>4</b>	<b>Overview of the results.....</b>	<b>42</b>
4.1	The $\omega$ subunit of RNAP is non-essential in ambient air in <i>Synechocystis</i> .....	42
4.2	<i>Synechocystis</i> cells do not acclimate to high temperatures without the $\omega$ subunit of RNAP .....	44
4.3	Acclimation of <i>Synechocystis</i> to high CO <sub>2</sub> .....	46
4.4	The $\omega$ subunit of RNAP is obligatory for high CO <sub>2</sub> acclimation of <i>Synechocystis</i> cells.....	48
4.5	Suppressor mutations in the <i>ssr1600</i> gene encoding an anti- $\sigma$ factor antagonist rescue the acclimation capacity of $\Delta$ rpz to high CO <sub>2</sub> and to high temperature.....	52
<b>5</b>	<b>Discussion.....</b>	<b>54</b>
5.1	Role of the $\omega$ -subunit of the RNA polymerase core in <i>Synechocystis</i> .....	54
5.2	Mutations in the anti-SigC antagonist <i>Ssr1600</i> rescue $\Delta$ rpz in high CO <sub>2</sub> .....	58
5.3	A novel signaling cascade of high CO <sub>2</sub> acclimation in <i>Synechocystis</i> .....	61
<b>6</b>	<b>Conclusions and future perspectives .....</b>	<b>64</b>
	<b>Acknowledgements .....</b>	<b>67</b>
	<b>List of References.....</b>	<b>69</b>
	<b>Original Publications .....</b>	<b>85</b>

# Abbreviations

2-OG	2-oxoglutarate
2-PG	2-phosphoglycolate
3-PGA	3-phosphoglyceric acid
APC	Allophycocyanin
asRNA	anti-sense RNA
ATP	Adenosine triphosphate
CA	Carbonic anhydrase
CBB	Calvin-Benson-Bassham cycle
CCMs	Carbon concentrating mechanisms
Ci	Inorganic carbon
CO <sub>2</sub>	Carbon dioxide
Cyt-b6f	Cytochrome b6f complex
FD	Ferredoxin
FNR	Ferredoxin-nicotinamide adenine dinucleotide phosphate-reductase
FQR	Ferredoxin-plastoquinone reductase
G3P	Glyceraldehyde-3-phosphate
GS-GOGAT	Glutamine synthase-Glutamine-oxoglutarate amidotransferase
GSH	Glutathione
GSSG	Glutathione disulfide
HCO <sub>3</sub> <sup>-</sup>	Bicarbonate
NADPH	Nicotinamide adenine dinucleotide phosphate
P680	Primary electron donor of PSII
P680 <sup>+</sup>	Oxidized P680
P700	Primary electron donor of PSI
P700*	Excited P700
P700 <sup>+</sup>	Oxidized P700
PC	Phycocyanin
PBP <sub>s</sub>	Penicillin binding proteins
PG	Peptidoglycan
PQH <sub>2</sub>	Plastoquinole
PSI	Photosystem I

PSII	Photosystem II
QA	Plastoquinone A
QB	Plastoquinone B
RNAP	RNA polymerase
Rubisco	Ribulose-1.5-bisphosphate carboxylase/oxygenase
RuBP	1.5-ribulose-bisphosphate
ROS	Reactive oxygen species
<i>Synechocystis</i>	<i>Synechocystis</i> sp. PCC 6803

# List of Original Publications

This dissertation is based on the following original publications, which are referred to in the text by their Roman numerals:

- I Gunnelius L, Hakkila K, Kurkela J, Wada H, Tyystjärvi E and Tyystjärvi T. The omega subunit of the RNA polymerase core directs transcription efficiency in cyanobacteria. *Nucleic Acids Research*, 2014; 7: 4606-4614.
- II Gunnelius L, Kurkela J, Hakkila K, Koskinen S, Parikainen M and Tyystjärvi T. The  $\omega$  subunit of RNA polymerase is essential for thermal acclimation of the cyanobacterium *Synechocystis* sp. PCC 6803. *PLoS ONE*, 2014; 11: e112599.
- III Kurkela J, Hakkila K, Antal T and Tyystjärvi T. Acclimation to high CO<sub>2</sub> requires the  $\omega$  subunit of the RNA polymerase in *Synechocystis*. *Plant Physiology*, 2017; 1: 172-184.
- IV Kurkela J, Koskinen S, Reimann V, Ezu S, Hakkila K, Hess WR and Tyystjärvi T. An anti-SigC antagonist (Ssr1600) controls growth rate of the cyanobacterium *Synechocystis* sp. PCC 6803. Manuscript

Papers I and II have been published under the terms of the Creative Commons CC BY license.

Paper III has been reprinted by kind permission of American society of plant biologists.

# 1 Introduction

## 1.1 Cyanobacteria in changing climate

Ancient cyanobacteria evolved 2.7-2.2 billion years ago and invented the oxygenic photosynthesis involving two photosystems (Brocks et al. 1999; Kopp et al. 2005; Rasmussen et al. 2008; Lyons et al. 2014). This enabled the use of water as an electron source in photosynthetic light reactions and produced oxygen as a side product. Rise of oxygen levels was harmful for all obligate anaerobes and this caused an extinction wave on Earth (Hodgskiss et al. 2019). Life adapted to the new atmosphere, when aerobic organisms emerged and started to claim likely empty ecological niches (Battistuzzi et al. 2004). Accumulation of oxygen in the atmosphere lead to formation of the ozone layer in the stratosphere protecting cells against harmful UV-radiation (Cavalier-Smith 2006). Later, ancestors of plants and algae evolved by primary endosymbiosis, where a cyanobacterium was engulfed by an eukaryotic cell (Yoon et al. 2004; Hedges et al. 2004; Shih and Matzke 2013). Currently, cyanobacteria are successfully adapted to biomes where light is available. Cyanobacteria are common in marine environments and in fresh waters, but some species can live in deserts and glaciers and even in hot springs (Pentecost and Whitton 2012). This diverse bacterial group consists of both unicellular and multicellular filamentous species, and some can fix nitrogen. Currently, cyanobacteria have been estimated to be responsible for 1/3 of global CO<sub>2</sub> fixation (Bryant 2003).

During Earth's history, CO<sub>2</sub> levels have varied drastically. When ancient cyanobacteria emerged, estimations suggest that CO<sub>2</sub> levels were 20-100 times higher than nowadays and O<sub>2</sub> levels were negligible (Rye et al. 1995; Sheldon 2006). Later, CO<sub>2</sub> levels have decreased significantly at least in two periods of time. The first one occurred 1.8 to 1.0 billion years ago (Sheldon 2006) and the second one later, 0.4 billion years ago (Bernier 2003). During both periods, not only CO<sub>2</sub> levels decreased, but also O<sub>2</sub> levels increased simultaneously. In cyanobacteria, ribulose-1,5-bisphosphate carboxylase/oxygenase (Rubisco) function both as a carboxylase and oxygenase. In high CO<sub>2</sub>, low O<sub>2</sub> environment, Rubisco is efficient in carbon fixation, whereas in low CO<sub>2</sub>, high O<sub>2</sub> climate, the oxygenase function of Rubisco increases (Kacar et al. 2017). To reduce unfavorable photorespiration, carbon

concentrating mechanisms (CCMs) evolved in cyanobacteria when O<sub>2</sub> increased and CO<sub>2</sub> decreased in the atmosphere. CCMs (section 1.2.1) most probably emerged already 1.8-1.0 billion years ago, as traces of molecular components of CCMs have been found from 1.2 billion years old stromatolites (Kupriyanova et al. 2007).

For cyanobacteria, current CO<sub>2</sub> concentrations are actually low when considering the evolutionary history. However, the prominent problem of our time is that CO<sub>2</sub> levels are increasing with an increasing speed. For example, CO<sub>2</sub> concentration increase from 200 ppm to 250 ppm took ~800 000 years (Petit et al. 1999), but just in the last 100 years, the concentration has almost doubled – recent measurement from Mauna loa observatory showed 414 ppm of CO<sub>2</sub> in atmosphere (<https://www.noaa.gov/>, accessed: 8.6.2020). The main reason for the rapid increase of CO<sub>2</sub> levels has been the usage of fossil fuels. In line with CO<sub>2</sub> increase, global mean temperatures in oceans and on land has increased approximately one degree (IPCC report 2019) and it is not well known how these rapid alterations in atmosphere affect cyanobacteria. In general, increase in inorganic carbon (C<sub>i</sub>) concentrations or/and temperature accelerates the growth of cyanobacteria. In nutrient rich conditions, this can also lead to harmful cyanobacterial blooms. Elevated C<sub>i</sub> concentrations and temperature in aquatic environments can also cause changes in nutrient availability, and increased C<sub>i</sub>/nutrient ratio may lead to alternations in species composition (Van De Waal et al. 2010). Another outcome from CO<sub>2</sub> increase is acidification of aquatic environments. However, by fixing CO<sub>2</sub> cyanobacteria can decrease marine and freshwater acidification, thus helping acidification sensitive species (for a review, see Mostofa et al. 2016).

## 1.2 The model cyanobacterium *Synechocystis* sp. PCC 6803

### 1.2.1 Structure and cell division

Cyanobacterial research has focused on few model species including fresh water and marine species as well as single cell and filamentous strains. *Synechocystis* sp. PCC 6803 (*Synechocystis*) is a fresh water cyanobacterium (Rippka et al. 1979), and the glucose-tolerant substrain (Williams 1988) is widely used as a model organism. *Synechocystis* is non-diazotrophic, non-toxic species, and the glucose tolerant lab strain used as a control strain in this Thesis has lost the ability of phototactic movement (Trautmann et al. 2012). *Synechocystis* is naturally transformable and therefore an easy target for genetic modifications, and different growth modes, autotrophic, mixotrophic or heterotrophic, allow testing of diverse mutant lines. Heterotrophic growth conditions can be implemented by activating cell division with a short daily pulse of light (Anderson and McIntosh 1991). *Synechocystis* was the

first phototrophic organism sequenced (Kaneko et al. 1996), and later the genome has been re-annotated along with the addition of all plasmid sequences (Kaneko et al. 2003; Fujisawa et al. 2017). In total, the circular chromosome and seven plasmids contain 3.96 Mbp, and depending on the growth phase, the number of polyploidic chromosomes vary (Soppa et al. 2016).

According to the cell envelope structure (Fig 1), *Synechocystis* is classified as a gram-negative bacterium. The outermost layer of the cyanobacterial cell envelope is a carbohydrate rich capsule anchored to the outer membrane (Mohamed et al. 2005, Fig 1). The outer membrane consists of a lipopolysaccharide layer and a lipid layer, and numerous porin channels are embedded in this semi-permeable membrane (Nikaido 2003, Fig 2). The outer membrane and cell membrane are separated by a periplasmic space that contains a peptidoglycan (PG) layer (Silhavy et al. 2010, Fig 2). The cell membrane functions as a selective barrier and site of synthesis of many cellular components, and contains numerous channels and transporters (Nikaido 2003; Mills et al. 2020). Inside the cells, yet another membrane system, the thylakoid membranes, contains the photosynthetic and respiratory complexes (Figs. 1 and 2).

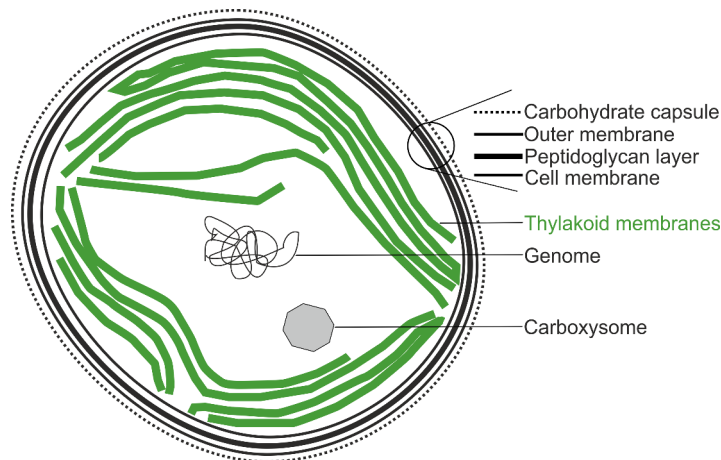


**Figure 1.** Schematic representation of a *Synechocystis* cell.

*Synechocystis* has a spherical shape and it divides by binary fission (Rippka et al. 1979). The cell division mechanism and regulation are not yet completely understood in cyanobacteria, but obviously have both similarities and differences to the better understood cell division mechanisms of *Escherichia coli* (for a review, see Booth and Lewis 2019). Cell division starts with septum site determination controlled by the Min system in *E. coli* (Rowlett and Margolin 2013). Homologs of the *minCDE* genes are found in *Synechocystis*. Although the *minCDE* genes are non-essential in *Synechocystis*, deletion mutants show exceptional cell morphologies

(Mazouni et al. 2004). Once the septum site is determined, the Z-ring is formed via polymerization of tubulin-like FtsZ proteins (Lutkenhaus 2007). The Z-ring provides a scaffold for other cell division proteins. A large protein complex called divisome is formed along the FtsZ filaments, and this complex stimulates further the cell division by constricting the cell to two halves (for a review, see den Blaauwen et al. 2017). The divisome components vary between bacterial species (Booth and Lewis 2019) and in *Synechocystis* at least FtsZ, ZipN, Ftn6 (Slr2073) and SepF (Sll1939) are essential divisome components (Koksharova and Wolk 2002; Mazouni et al. 2004; Marbouty et al. 2009a).

To complete the cell division, inward growth of cell membrane, synthesis of PG, and outer membrane closure occur in a coordinated manner. PG synthesis is well understood in *E. coli* and homologous proteins have been found in *Synechocystis* (Mazouni et al. 2004; Marbouty et al. 2009a, 2009b). PG synthesis begins in the cytoplasm and is completed in the periplasm. In the cytoplasm, Mur ligase family proteins orchestrate the synthesis of PG precursor Lipid II that is transported to the periplasmic space by three putative flippase proteins, RodA, FtsW and MurJ (Mohammadi et al. 2011; Sieger et al. 2013; Sham et al. 2014). In the periplasmic space, Lipid II is linked to a growing glycan chain by penicillin binding proteins (PBPs). In addition, PBPs catalyze various modifications in the newly formed PG layer (Booth and Lewis 2019). In *Synechocystis*, the cytoplasmic pathway has not been thoroughly characterized but there is some information about PBPs. Mutants devoid of Pbp5 and Pbp6 in *Synechocystis* form clusters of four cells because new cell division starts in daughter cells before the previous division has been completed (Marbouty et al. 2009b). In addition, two component response regulator RpaA has been shown to regulate some Min system and Mur family genes, as well as, *pbp2* in *Synechocystis* (Kizawa and Osanai 2020).

## 1.2.2 Carbon concentrating mechanisms and carbon fixation

*Synechocystis* and other cyanobacteria can uptake C<sub>i</sub> as CO<sub>2</sub> or as HCO<sub>3</sub><sup>-</sup>, the available form of C<sub>i</sub> being highly dependent on pH. CCMs are a vital part of C<sub>i</sub> uptake in *Synechocystis*, and actually many mutants with deficiencies in CCMs cannot grow in ambient air but require enhanced CO<sub>2</sub> levels (Ogawa et al. 1994; Shibata et al. 2001, 2002). CO<sub>2</sub> diffuses into *Synechocystis* cells through the membranes, and aquaporins have been suggested to facilitate diffusion (Kaplan 2017). In thylakoid membranes, *Synechocystis* possesses specialized NDH-complexes (for a review, see Battchikova et al. 2011) that facilitate CO<sub>2</sub> influx (Fig 2). The high affinity NDH-1<sub>3</sub> and low affinity NDH-1<sub>4</sub> complexes are located in the thylakoid membrane, but traces of NDH-1<sub>4</sub> have detected in the cell membrane as well (Xu et al. 2008a). Both NDH complexes contains a carbonic anhydrase-like

protein, CupA or CupB (Price et al. 2008; Kupriyanova et al. 2013). It has been suggested that CupA is associated with the NDH-1<sub>3</sub> complex (Zhang et al. 2004) and CupB with the NDH-1<sub>4</sub> complex (Xu et al. 2008a). According to the prevailing theory (Price et al. 2002), Cup proteins facilitate CO<sub>2</sub> to HCO<sub>3</sub><sup>-</sup> conversion using reducing power derived from NDH-complexes (Shibata et al. 2002) thus increasing the net influx of CO<sub>2</sub> and minimizing the efflux of CO<sub>2</sub>. Clear evidence of carbonic anhydrase activity of Cup proteins is still missing (Kaplan 2017).

Uptake of HCO<sub>3</sub><sup>-</sup> to the periplasmic space is poorly understood. PorB has been suggested to function as a HCO<sub>3</sub><sup>-</sup> channel, but inactivation of PorB has only a small effect on Ci uptake (Woodger et al. 2007). HCO<sub>3</sub><sup>-</sup> transport across plasma membrane is well understood (Fig 2), and three different transport systems are known in *Synechocystis*: BCT1 (Omata et al. 1999), SbtA (Shibata et al. 2002) and BicA (Xu et al. 2008b). BCT1 (encoded by the *cmpABCD* operon) is an ATP-dependent high affinity HCO<sub>3</sub><sup>-</sup> pump. SbtA and BicA are medium and low affinity Na<sup>+</sup>- HCO<sub>3</sub><sup>-</sup> symporters, respectively (Shibata et al. 2002; Burnap et al. 2013). In addition, *Synechocystis* contains some auxiliary mechanisms that support the function of SbtA and BicA (Fig. 2). Both symporters need an Na<sup>+</sup>-gradient that might be created by the Na<sup>+</sup>-H<sup>+</sup> antiporter, NhaS3 (Price et al. 2008; Kupriyanova et al. 2013) and/or by a specialized NDH-complex, Mnh (Omata et al. 1999). However, the role of NhaS3 remains controversial as some studies have localized it in the thylakoid membrane (Tsunekawa et al. 2009). The Mnh complex contains NdhD5 and NdhD6 subunits and its role is thought to be a redox driven Na<sup>+</sup> extrusion pump (Omata et al. 1999), and the *mnh* operon of *Synechocystis* is known to be low-Ci-responsive (Wang et al. 2004). Yet another supporting mechanism is PxcA (Fig 2), a H<sup>+</sup> transporter considered to be important maintaining H<sup>+</sup> homeostasis during CO<sub>2</sub> uptake (Sonoda et al. 1998).

Intracellular HCO<sub>3</sub><sup>-</sup> diffuses inside carboxysomes that are polyhedral proteinaceous cellular compartment containing Rubisco, carbonic anhydrase (CA), 1.5-ribulose-bisphosphate (RuBP) and 3-phosphoglyceric acid (3-PGA) (see a review by Turmo et al. 2017). CA speeds up HCO<sub>3</sub><sup>-</sup>/CO<sub>2</sub> conversion near Rubisco, and the carboxysome shell is suggested to limit influx of O<sub>2</sub>, thus highly favouring the carboxylase function of Rubisco and suppressing the oxygenase action (Kerfeld and Melnicki 2016). The protein shell of the carboxysome also provides a diffusion barrier to CO<sub>2</sub> efflux but allows HCO<sub>3</sub><sup>-</sup> influx (Dou et al. 2008; Cai et al. 2009). However, transport mechanisms of HCO<sub>3</sub><sup>-</sup>, RuBP or 3-PGA are not yet completely understood (Zhang et al. 2018).

*Synechocystis* is classified as a β-cyanobacterium, and it contains γ-CA (CcmM) and β-CA (CcaA) (So and Espie 2005). However, it remains unclear if both CAs function individually in certain conditions or if they work together. Enzyme kinetics studies performed with CcmM and CcaA *in vitro* show that CcmM is more active

than CcaA (McGurn et al. 2016). CCMs help to provide efficient carbon fixation in the Calvin-Benson-Bassham (CBB) cycle. The CBB cycle consists of three different phases (Fig 2), a carbon fixation phase (1), a reducing phase (2) and a regeneration phase (3). In the carbon fixation phase, CO<sub>2</sub> is fixed to RuBP by Rubisco and 3-PGA is produced. Then in the reducing phase, 3-PGA is converted via 1,3-bisphosphoglycerate to glyceraldehyde-3-phosphate (G3P). Finally, the regeneration phase synthesises RuBP from G3P in a series of reactions, and the cycle starts over again. The CBB cycle uses the high-energy phosphate compounds, adenosine triphosphate (ATP) and nicotinamide adenine dinucleotide phosphate (NADPH), produced by the photosynthetic electron transfer chain. In C<sub>i</sub> excess conditions or in nitrogen limitation, *Synechocystis* stores carbohydrates as glycogen (Ball and Morell 2003) or as polyhydroxybutyrate (Hein et al. 1998; Koch et al. 2020).

One of the most important functions of CCMs is to minimize the oxygenase activity of Rubisco. Oxygenation of RuBP generates 2-phosphoglycolate (2-PG) and 3-PGA. 2-PG is a toxic compound, and in *Synechocystis*, photorespiration occurs via a glycerate pathway or C<sub>2</sub> cycle. In both pathways 2-PG is metabolized to 3-PGA and in glycerate pathway also CO<sub>2</sub> is produced. (Eisenhut et al. 2006). In addition, 2-PG can be converted to CO<sub>2</sub> in a decarboxylation pathway (Eisenhut et al. 2008). Despite its toxic nature and energy demanding processing, 2-PG functions as an important signalling molecule in carbon metabolism (Jiang et al. 2018).

### 1.2.3 Linear photosynthetic electron transfer chain and respiration

Carbon fixation requires reducing power and energy in the forms of NADPH and ATP that are produced in cyanobacteria by the photosynthetic electron transfer chain (Fig. 2). In the linear electron transport chain (for a review, see Lea-Smith et al. 2016), the energy of light is converted to a chemical form. Light is mainly absorbed by photosynthetic pigments, phycocyanobilin and Chl *a*. In *Synechocystis*, phycobilisomes mainly absorb at 550-650 nm, whereas Chl *a* has a blue peak and a red peak. The phycobilisome antenna in *Synechocystis* consists of an allophycocyanin (APC) core and phycocyanin (PC) rods, both containing covalently bound phycocyanobilin as a pigment. The core contains three APCs, and six PC rods are connected to these via two linker proteins CpcG1 and CpcG2 (Kondo et al. 2009; Gwizdala et al. 2016). Once a photon is absorbed by the phycobilisome, photon energy resonates to Photosystem II (PSII) reaction centre P680 that becomes excited, and the charge separation P680<sup>+</sup> pheophytin<sup>-</sup> takes place in picosecond time scale (Vasilev et al. 2001). The strong oxidant P680<sup>+</sup> takes electrons from water via an oxygen evolving complex that splits water molecules to electrons, protons and oxygen. Then in a series of oxidation-reduction reactions, electrons move along the

electron transfer chain, first from pheophytin to a primary plastoquinone electron acceptor  $Q_A$  and further to a secondary electron acceptor  $Q_B$ .  $Q_B$  accepts two electrons, becomes protonated and then plastoquinol ( $PQH_2$ ) is released from the  $Q_B$  pocket to the plastoquinone pool (PQ) of the thylakoid membrane. In cyanobacteria, PSII functions as a dimer (Suga et al. 2017) and one phycobilisome serves one PSII dimer (Rakhimberdieva et al. 2001).

$PQH_2$  reduces electron acceptors in cytochrome  $b_6f$  complex (Cyt- $b_6f$ ), which then recycles one electron back to the PQ pool and transfers the other electron to the soluble electron carrier plastocyanin (PC) or to cytochrome  $c_6$  (Fig 2). In photosystem I (PSI), the reaction centre P700 is excited, and charge separation moves an electron from  $P700^*$  to chlorophyll  $a_0$  and PC/cyt  $c_6$  reduces the  $P700^+$ . From  $a_0^-$ , an electron moves to phyloquinone  $a_1$  and then via iron-sulfur clusters Fx, Fa and Fb to ferredoxin (FD). It is suggested that two active electron transfer branches work in PSI from P700 to Fx, one in PsaA subunit and another in PsaB subunit. (Guergova-Kuras et al. 2001)

FD reduces ferredoxin-nicotinamide adenine dinucleotide phosphate-reductase (FNR) in the cytoplasm and FNR recharges the energy carrier molecule nicotinamide adenine dinucleotide phosphate ( $NADP^+$ ) to NADPH (Fig 2). In cyanobacteria, PSI might be a dimer, trimer or tetramer (Rögner et al. 1990; Chitnis and Chitnis 1993; Chitnis et al. 1993; Zakar et al. 2018). The roles of PSI polymerization remain unclear, as a *Synechocystis* mutant lacking the PsaL protein contains only PSI monomers and the photosynthetic electron transfer chain functions well (Chitnis and Chitnis 1993). The function of the electron transfer chain generates a proton gradient across the thylakoid membrane, and the proton gradient powers an ATP-synthetase that phosphorylates ADP to ATP.

Respiration in cyanobacteria (see review, Lea-Smith et al. 2016) functions mainly in darkness and unlike in plants or algae, respiratory electron transfer chains are located mainly in the thylakoid membrane. In addition, a respiratory chain utilizing an alternative respiratory terminal oxidase might function in the cell membrane (Berry et al. 2002, Lea-Smith et al., 2013). In the thylakoid membrane, respiratory and photosynthetic electron transfer chains share electron carriers like PQ, Cyt- $b_6f$  and PC/cyt  $c_6$ . Succinate dehydrogenase (SDH) is thought to be the main electron donor to the PQ pool in respiration, but some NDH-1 and NDH-2 complexes have suggested to play minor roles as well (Mi et al. 1992; Howitt et al. 1999; Ohkawa et al. 2000). Terminal oxidases reduce molecular oxygen to water, the cytochrome *bd*-quinol oxidase takes electrons directly from the PQ pool whereas cytochrome *c* oxidase take electrons from the PQ pool via Cyt- $b_6f$  and PC/cyt  $c_6$  (Howitt and Vermaas 1998; Berry et al. 2002).

### 1.2.4 Alternative electron transfer routes and photoprotective mechanisms

In addition to linear electron transfer, cyclic electron transfer (CET) functions around PSI. CET routes are still poorly characterized in cyanobacteria, although several have been proposed (Fig 2). FNR or Fd might transfer electrons to NDH-1, which then donates electrons to the PQ pool (Peng and Shikanai 2011; Yamamoto et al. 2011; Peltier et al. 2016; Schuller et al. 2019). In addition NDH-2 and ferredoxin-plastoquinone reductase (FQR) might provide an alternative electron transfer route in which NADPH would be the donor for NDH-2 and Fd for FQR (Yeremenko et al. 2005; Lea-Smith et al. 2016). The cycles are completed when PQ transfers an electron back to PSI via the Cyt- $b_6/f$  and PC/cytochrome  $c_6$ . Cyclic electron transfer increases the proton gradient and thus contributes to ATP production without NADPH production or water splitting. The general theory is that cyclic electron flow helps in keeping the NADPH:ATP ratio optimal for CO<sub>2</sub> fixation.

Electron transfer in thylakoid membranes is adjusted according to changing light conditions. To do this, cyanobacteria possess many regulatory mechanisms, which directly control the input of excitation energy to the photosystems or change the stoichiometry of energy transferring complexes (for a review, see Mullineaux 2014). When light quality changes and becomes more favourable to either PSI or PSII, state transitions balance the energy distribution between the photosystems (McConnell et al. 2002). If light excitation exceeds the need, extra excitation energy must be quenched to minimize the accumulation of dangerous reactive oxygen species (ROS). A cyanobacteria-specific orange carotenoid protein (OCP) can dissipate excess energy as heat at the phycobilisome antenna (Wilson et al. 2007). OCP interacts with the phycobilisome core proteins, and the thermal dissipation capacity depends on the form of OCP (Wilson et al. 2008). In darkness, OCP is in an inactive orange form but illumination with blue-green light causes a conversion to an active red form (Wilson et al. 2008). To reduce energy dissipation, a fluorescence recovery protein helps to convert the red form to the orange form (Boulay et al. 2010).

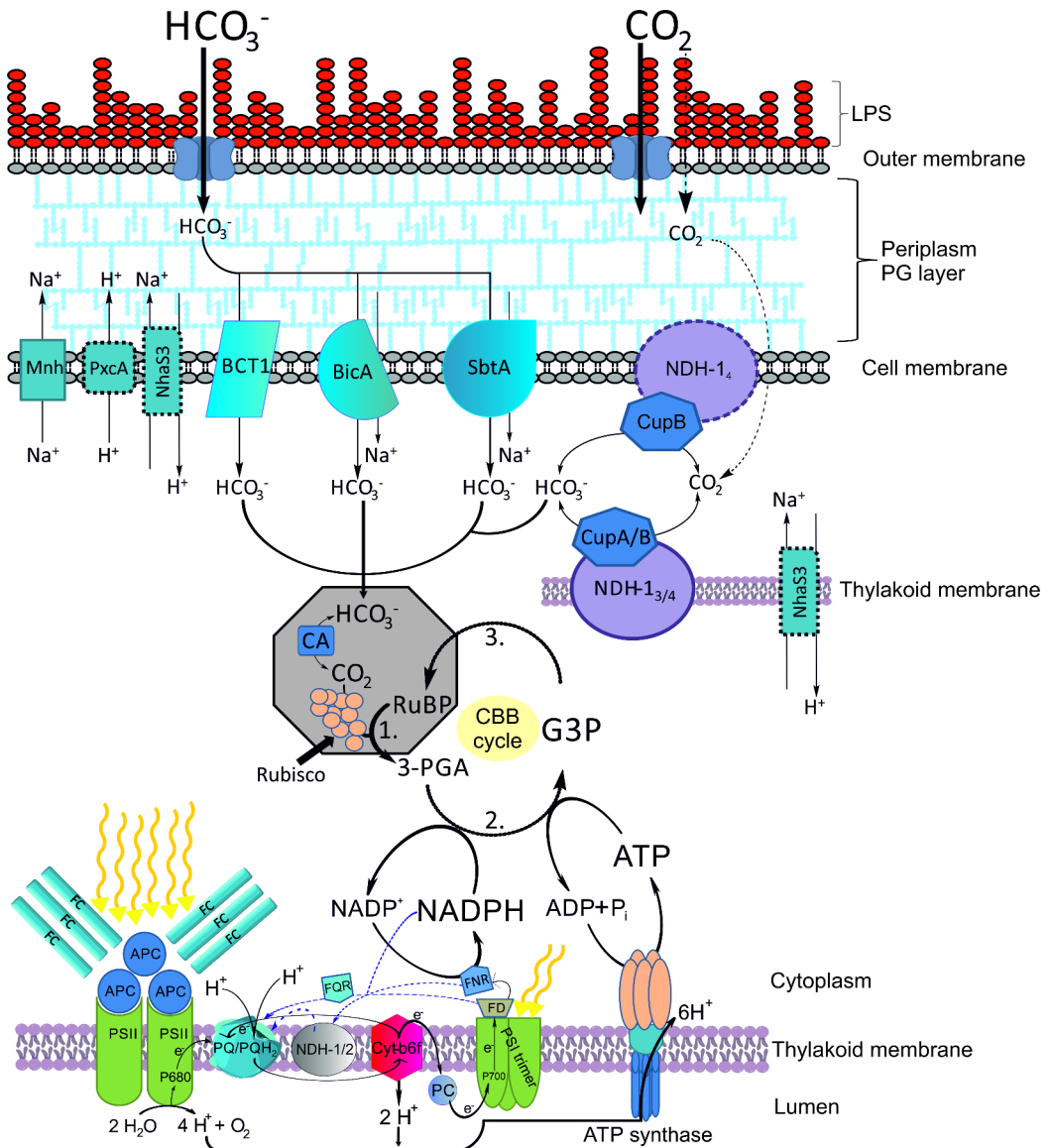


**Figure 2.** Schematic representation of carbon concentrating mechanisms, Calvin-Benson-Bassham cycle and linear photosynthetic electron transfer chain. The figure legend continues on the next page.

**Figure 2.** Outer membrane is composed of a lipopolysaccharide (LPS) layer and a lipid layer.  $\text{HCO}_3^-$  and  $\text{CO}_2$  diffuse into the periplasm via outer membrane porins. The peptidoglycan (PG) layer gives rigidity to the cell wall. The cell membrane harbors  $\text{HCO}_3^-$  transporters and their auxiliary complexes: specialized NDH-1 complex (Mnh), working as a redox driven  $\text{Na}^+$  pump, a  $\text{H}^+$  transporter (PxcA), an  $\text{Na}^+$ - $\text{H}^+$ -antiporter (NhaS3), an ATP-driven  $\text{HCO}_3^-$  pump (BCT1), the  $\text{HCO}_3^-$ - $\text{Na}^+$  symporters BicA and SbtA, and the  $\text{CO}_2$ -uptake specialized NDH-1<sub>4</sub> complex associated with the carbonic anhydrase like protein CupB. The thylakoid membrane harbors NDH-1<sub>4</sub>/CupB and NDH-1<sub>3</sub>/CupA complexes and possibly also NhaS3. The first reaction of carbon fixation occurs in carboxysomes (grey octagon) whereas the majority of the CBB cycle occurs in the cytoplasm (Carbonic anhydrase (CA), Rubisco (orange sphere), 1.5-ribulose-bisphosphate (RuBP), 3-phosphoglyceric acid (3-PGA) and glyceraldehyde-3-phosphate (G3P)). Phycobilisomes are formed from phycocyanin rods (PC) and allophycocyanin cores. Photosynthetic electron transfer chain consists of photosystem II (PSII), plastoquinone pool (PQ/PQH<sub>2</sub>), cytochrome-b6f-complex (Cyt-b6f), plastocyanin (PC), photosystem I (PSI), ferredoxin (FD), ferredoxin-nicotinamide adenine dinucleotide phosphate-reductase (FNR) and ATP synthase. Yellow arrows present sunlight. Suggested cyclic electron transfer routes are shown in dashed blue lines with ferredoxin:plastoquinone reductase (FQR) and NADPH-dehydrogenase 1 or 2 (NDH-1/2).

Cyanobacteria have also multiple other mechanism to cope with high light stress. The Flv1 and Flv3 proteins are involved in the Mehler-like reaction, where photoreduction of  $\text{O}_2$  to  $\text{H}_2\text{O}$  occurs without ROS production (Helman et al. 2003; Allahverdiyeva et al. 2011). In addition, the *flv4-sll0218-flv2* operon might be associated with the photoprotection of PSII (Zhang et al. 2009, 2012a; Bersanini et al. 2014). The protective pigments, especially carotenoids, and *a*-tocopherol are also important for high light acclimation (Maeda et al. 2005; Sozer et al. 2010). Carotenoids and *a*-tocopherol can non-enzymatically detoxify singlet oxygen. The importance of carotenoids was demonstrated by a mutant strain lacking all carotenoids, as it can only grow in light activated heterotrophic growth conditions and does not assemble a functional oxygen-evolving PSII complex (Sozer et al. 2010).

One additional photoprotective compound is glutathione that is especially in plants an important electron donor for various enzymes with antioxidant properties (Noctor et al. 2012). In *Synechocystis*, two enzymes, GshA and GshB, catalyse the synthesis of glutathione (GSH). Both of these proteins are important in oxidative stress but GshA is found to be essential also in standard growth conditions (Cameron and Pakrasi 2010, 2011b, 2011a; Narainsamy et al. 2013). GSH can donate electrons to glutaredoxins, glutathione peroxidases or to glutathione-S-transferases (Noctor et al. 2012). At least two glutaredoxins, Grx1 and Grx2, are found in *Synechocystis*, and especially Grx2 was shown to be important in  $\text{H}_2\text{O}_2$  stress and in protection against selenate toxicity (Marteyn et al. 2009). In addition, two genes encoding glutathione-S-transferases (*sll1545* and *slr0236*) were recently characterized from *Synechocystis* (Kammerscheit et al. 2019). The *sll1545* gene was essential for growth in standard conditions, but *slr0236* was not (Kammerscheit et al. 2019). However,

also Slr0236 plays a protective role in photo-oxidative stress (Kammerscheit et al. 2019). Eventually electron donation by GSH results in the oxidized form of glutathione, the dimeric disulfide (GSSG). GSSG is usually reduced back to GSH by an NADPH-dependent glutathione reductase but *Synechocystis* is lacking that enzyme (Marteyn et al. 2009). Instead, it has been suggested that GSSG gets electrons from NADPH via thioredoxin reductase and Grx1 (Marteyn et al. 2009).

## 1.2.5 Detection of available Ci and signaling of Carbon/Nitrogen balance

It remains unclear how cyanobacteria sense form and amount of available Ci, although recently some metabolites have been shown to have important roles in Ci signalling (Jiang et al. 2018; Selim et al. 2018; Forchhammer and Selim 2019). In general, CO<sub>2</sub> studies have focused on responses after cyanobacteria have been transferred from high, 3-5% CO<sub>2</sub> to ambient air (Wang et al. 2004; Eisenhut et al. 2007; Klähn et al. 2015; Orf et al. 2016) and less is known about the responses after the cells are transferred from ambient air to high CO<sub>2</sub>.

CCMs are regulated at least by four transcription factors: CmpR, NdhR, SbtB and CyAbrB2 (for a review, see Forchhammer and Selim 2019). CmpR is an activator of the *cmpABCD* operon encoding the HCO<sub>3</sub><sup>-</sup> pump (Omata et al. 2001). The DNA binding affinity of CmpR was suggested to increase when RuBP or 2-PG binds to CmpR (Daley et al. 2012). Later it was also shown in *Synechococcus elongatus* that CmpR co-crystallized with RuBP (Mahounga et al. 2018). Interaction with RuBP causes conformational changes in CmpR, which might activate the *cmpABCD* operon, but a detail molecular mechanism of regulation remains to be solved (Mahounga et al. 2018).

The NdhR transcription factor has been characterized to repress *ndhR*, *bicA* and *sbtA* genes, putative Na<sup>+</sup>/H<sup>+</sup> antiporter *slr1727* and *ndh3* operon (Figge et al. 2001; Jiang et al. 2018). Under Ci limitation or osmotic stress, NdhR binds to the promoter region with the consensus sequence TCAATG-(N<sub>10</sub>)-ATCAAT (Figge et al. 2001) and recently the molecular mechanism of promoter binding was resolved in detail (Jiang et al. 2018). NdhR protein can alternatively bind two central metabolites, 2-OG that accumulates when C/N balance is high (Carrieri et al. 2015), and the photorespiration product 2-PG whose accumulation is a signal of carbon deprivation (Hackenberg et al. 2012). The formation of the NdhR-2-PG complex changes the distance between two DNA binding domains in NdhR tetramer, which prevents the binding of NdhR to the major groove of DNA (Jiang et al. 2018). Since NdhR works as a repressor, the formation of NdhR-2-PG complex activates the expression of Ci uptake genes. In carbon sufficient conditions, the formation of NdhR-2-OG complex activates DNA binding of NdhR, thereby repressing CCM genes (Jiang et al. 2018).

It was recently found that the SbtA bicarbonate transporter could be regulated by the PII-like signaling protein SbtB (Selim et al. 2018). Interestingly, SbtB is lacking typical PII protein effector sites, and instead of 2-OG, SbtB binds cyclic AMP (cAMP) with high affinity and ADP/AMP with lower affinity (Selim et al. 2018). The current view on SbtB regulation is that in low carbon conditions, ADP/AMP activates SbtB, and the active SbtB induces localization of SbtA into the cell membrane (Selim et al. 2018). In high carbon, formation of the SbtB-cAMP complex prevents localization of SbtA to the cell membrane and thus reduces  $\text{C}_i$  uptake (Selim et al. 2018).

The CyAbrB2 (cyanobacterial AbrB-like protein) transcription factor has been studied with the knockout mutant  $\Delta\text{CyAbrB2}$  (Orf et al. 2016). Comparison of transcriptomes of  $\Delta\text{CyAbrB2}$  and the control strain have shown that some CCMs genes are downregulated in  $\Delta\text{CyAbrB2}$  in ambient air, whereas some photosynthetic genes are downregulated in high  $\text{CO}_2$  (Orf et al. 2016).

*Synechocystis* is a non-diazotrophic cyanobacterium utilizing ammonium, nitrate or urea as a nitrogen source (Watzer et al. 2019). *Synechocystis* prefers ammonium over nitrate or urea, but in laboratory conditions mainly nitrate is used as a nitrogen source in BG-11 growth medium. Combined nitrogen is actively transported to cytoplasm by the ABC-type nitrite/nitrate transporter NrtABCD (Flores et al. 2005), by ammonium/methylammonium permeases (Montesinos et al. 1998) or by the urea permease UrtABCDE (Valladares et al. 2002). Inside the cell, nitrate is converted to nitrite by nitrate reductase (NarB) and in sequential reaction to ammonium by nitrite reductase (NirA); both reactions require reducing power from photosynthesis, ferredoxin being the electron donor (reviewed by Flores et al. 2005). Ammonium is incorporated into carbon skeletons via the glutamine synthase (GS)-glutamine-oxoglutarate amidotransferase (GOGAT) cycle (reviewed by Bolay et al. 2018). The first step is the ligation of ammonium to glutamate by an ATP consuming reaction catalysed by GS forming glutamine, and then in subsequent reaction NADPH-dependent GOGAT converts glutamine and 2-OG to two molecules of glutamate (Meeks et al. 1977). As 2-OG is in the intersection of nitrogen and carbon metabolisms (Fig 3), 2-OG is a suitable sensor of carbon and nitrogen fluxes. In carbon limiting and nitrogen excess conditions, nitrogen can be stored as cyanophycin (Watzer and Forchhammer 2018).

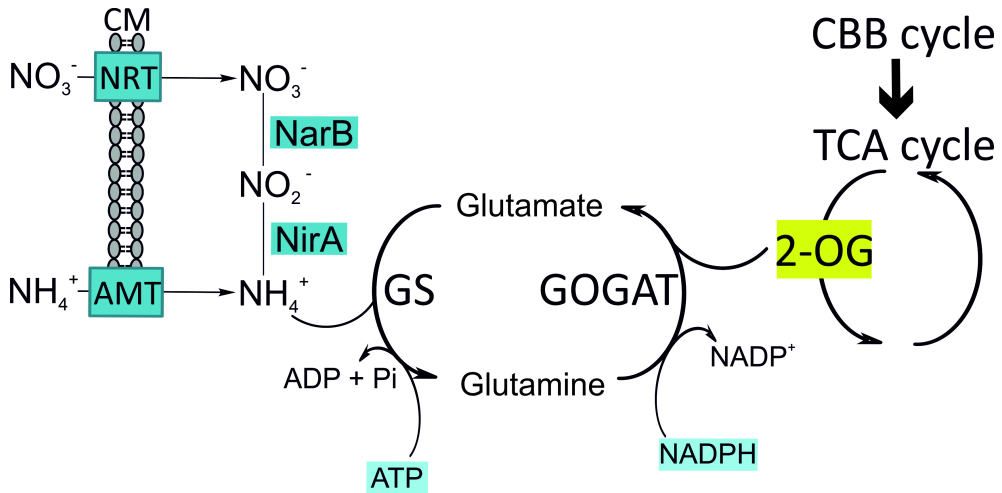


**Figure 3.** Nitrogen uptake and assimilation linked with CO<sub>2</sub> fixation. Cell membrane (CM) localized nitrite/nitrate transporter (NRT) and ammonium/methylammonium permease (AMT) transport nitrate (NO<sub>3</sub><sup>-</sup>) and ammonium (NH<sub>4</sub><sup>+</sup>), respectively, into the cytoplasm. Nitrogen assimilation occurs in the cytoplasm where nitrate reductase (NarB) and nitrite reductase (NirA) reduce NO<sub>3</sub><sup>-</sup> to NH<sub>4</sub><sup>+</sup>. In glutamate synthetase – glutamine-oxoglutarate-amidotransferase (GS-GOGAT) cycle NH<sub>4</sub><sup>+</sup> is incorporated to glutamate and in the consequent reaction, glutamine reacts with 2-OG (yellow) producing glutamate. 2-OG is derived from the tricarboxylic acid cycle (TCA cycle) and carbon skeletons to TCA cycle are derived from the Calvin-Benson-Bassham cycle (CBB cycle).

In *Synechocystis*, two main regulators of nitrogen metabolism are the PII-signalling protein (PII) and a global nitrogen transcription factor NtcA (for a recent review see Forchhammer and Selim 2019). PII is encoded by the *glnB* gene and forms trimeric complexes which can measure the amounts of 2-OG and ATP/ADP (reviewed by Forcada-Nadal et al. 2018). This means that PII is able to sense both the intracellular energy balance and the C/N balance. The mechanism of action of PII is the binding of effector molecules 2-OG, Mg<sup>2+</sup>-ATP or ADP into clefts between PII monomers, and depending on the combination of bound effector molecules, the T-loops of PII take various conformations, changing the interaction properties of PII (Zeth et al. 2014). In addition, none, one, two or three subunits of PII trimer can be phosphorylated; the non-phosphorylated form is prevailing in ammonium rich media and the highly phosphorylated form in nitrogen deficiency (Forchhammer and Selim 2019).

PII is involved in many nitrogen signalling pathways. It regulates directly nitrogen uptake, as it interacts with Amt1 and Nrt (Watzer et al. 2019). PII regulates also the nitrogen storing together with N-acetyl-glutamate kinase (NAGK) (Llácer et al. 2007; Lüddecke and Forchhammer 2013). NAGK is a key enzyme in arginine production, and arginine and aspartate forms a storage compound cyanophycin in nitrogen sufficient conditions (Maheswaran et al. 2006). In the arginine pathway, the

formation of a PII-NAGK complex inhibits the arginine feedback loop and allows high arginine production, activating cyanophycin production (Maheswaran et al. 2006). Another interaction protein of PII is acetyl-CoA carboxylase (ACCase) (Hauf et al. 2016). In this interaction, PII inhibits the activity of ACCase that catalyses an important step of fatty acid biosynthesis (Gerhardt et al. 2015). It is suggested that PII-ACCase interaction is controlling the carbon flux between TCA cycle and lipid biosynthesis. In high carbon conditions, the carbon flux is directed to lipid biosynthesis and consequently the production of 2-OG decreases. On the other hand, in high nitrogen conditions, PII-ACCase interaction diminishes due to low amount of 2-OG, and carbon flux increases towards TCA and GS-GOGAT cycle (Forchhammer and Selim 2019).

In addition to PII, NtcA and PipX regulate nitrogen metabolism. NtcA in *Synechocystis* regulates nitrogen transporters, enzymes involved in the GS-GOGAT cycle, as well as nitrate and nitrite reductases (Giner-Lamia et al. 2017). In addition, NtcA acts as a repressor of GS inhibitory proteins GifA and GifB (García-Domínguez et al. 2000). PipX is a small protein that could interact with both master regulators, PII and NtcA (Burillo et al. 2004; Espinosa et al. 2006, 2007). The PipX-NtcA complex has higher DNA binding affinity than NtcA alone (Forcada-Nadal et al. 2014). In nitrogen-rich conditions, cells might suffer momentarily of energy deficiency, as in addition to CO<sub>2</sub> uptake and fixation, nitrogen uptake and GS-GOGAT cycle consumes ATP (Zeth et al. 2014; Espinosa et al. 2018). The PII-ADP-complex is formed and binds to PipX reducing the formation of the NtcA-PipX complex, thus downregulating NtcA induced genes, and thereby limiting nitrogen assimilation. In low nitrogen conditions, the affinity of PipX is higher to the NtcA 2-OG complex than to the PII 2-OG complex (Zhao et al. 2010; Llácer et al. 2010).

## 1.3 Cyanobacterial RNA polymerase

### 1.3.1 Structure and function

The DNA dependent RNA polymerase (RNAP) is essential to all life on Earth and orchestrates one of the vital processes in the central dogma of biology. The multisubunit RNAP is an evolutionarily very old enzyme and still many subunits are conserved in eubacteria, archaea and eukaryotes. Cyanobacteria have only one type of RNAP (for review, see Riaz-Bradley 2019) producing all cellular RNAs including transfer RNA, ribosomal RNA, messenger RNA and small regulatory RNAs. The cyanobacterial RNAP core consists of two  $\alpha$  subunits, a  $\beta$  subunit, a  $\gamma$  subunit, a  $\beta'$  subunit and a  $\omega$  subunit (Schneider and Haselkorn 1988; Pollari et al. 2008; Imashimizu et al. 2011). The assembly of cyanobacterial RNAP has not yet been characterized, but in *E. coli*, assembly starts when two  $\alpha$  subunits form a homodimer

(Zhang and Darst 1998). Next, the  $\beta$  subunit is attached to the  $\alpha_2$  sub-complex and in the final step a heterodimer of  $\beta'$  and  $\omega$  attach to the  $\alpha_2\beta$  sub-complex, forming the functional RNAP core (Murakami et al. 2015). The core composition is unique for cyanobacteria, as the conserved  $\beta'$  subunit has been split to two parts in cyanobacteria (Schneider and Haselkorn 1988). The N-terminal part is the  $\gamma$  subunit and the C-terminal part is the  $\beta'$  subunit. In addition, the  $\beta'$  subunit carries a circa 600 amino acid long, cyanobacterial-lineage specific insertion (Minakhin et al. 2001). According to numerous structural studies in prokaryotes (Murakami et al. 2003, 2015; Murakami 2013; Kouba et al. 2019) and *in silico* models of *Synechocystis* (Pollari et al. 2008) and *Bacillus subtilis* (Johnston et al. 2009), RNAP adopts a crab-claw like shape where  $\beta'$  forms one “pincer” and  $\beta$  the other. The active centre and catalytic  $Mg^{2+}$  locate in the cleft between the pincers. Even though functional cyanobacterial RNAP has been purified (Imashimizu et al. 2011; Riaz-Bradley et al. 2020), crystal structures are still missing.

Transcription is divided to three phases: initiation, elongation and termination. For transcription initiation, the RNAP core recruits one of the regulatory  $\sigma$  factors, and specific regions of the  $\sigma$  factor recognise promoter elements and help to unwind the DNA in the promoter region (Riaz-Bradley 2019; Srivastava et al. 2020). The RNAP holoenzyme-promoter complex (closed complex) is energetically unfavourable, which causes conformational changes in the RNAP holoenzyme, leading to transition from a closed to an open complex (for a review, see Belogurov and Artsimovitch 2019). In the open complex, RNAP still sits on the promoter, but 13 to 15 bp of the double stranded DNA has been unwound and the first 10 nucleotides on nascent RNA are synthesized. The initiation phase proceeds to the elongation phase when all contacts between the promoter and RNAP are loosened, the  $\sigma$ -factor detaches from the RNAP core and the transcription bubble starts to move along DNA towards the 3'-end of the gene (Mazumder and Kapanidis 2019)

In the elongation phase, RNAP moves along double stranded DNA, where the template strand is directed inside the RNAP and RNA is polymerized in the active centre of the RNAP core. The template strand is directed to the primary channel, where the catalytic  $Mg^{2+}$  is also located. In detail, the double-psi beta-barrel folds of  $\beta$  and  $\beta'$  subunits bind active  $Mg^{2+}$  ions (Iyer and Aravind 2012). In polymerization, ribonucleotides enter into the active centre via secondary channel and  $Mg^{2+}$  catalyses the formation of the phosphodiester bond and pyrophosphate is released through the same channel (recent review Belogurov and Artsimovitch 2019).

RNA polymerization is completed in the termination phase that is not yet well understood in cyanobacteria. Many bacteria have a Rho-dependent termination strategy, but cyanobacteria do not have homologs of the Rho-protein (D'Heygere et al. 2013). Instead, cyanobacteria might use a Rho-independent mechanism, where a termination loop is formed. This self-annealing hairpin destabilizes the transcription

complex and ends the transcription (for review see Roberts 2019). In *Synechocystis*, only part of genes or operons have termination loops (Georg et al. 2009) suggesting that some other transcription termination mechanism might function as well. A third termination mechanism, currently named as Mfd-dependent termination, was recently described (Fan et al. 2016), although the function of Mfd in transcription-coupled DNA repair was shown earlier (Selby and Sancar 1993). Mfd functions as a DNA translocase, which simultaneously binds to DNA and RNAP, and in transcription termination Mfd moves along DNA and catches stalled RNAP and then uses ATP energy to dislocate RNAP from DNA (Fan et al. 2016). *Synechocystis* contains an Mfd homolog (*sll0377*), but the function remains to be studied.

RNAP might stall if an incorrect nucleotide is incorporated into nascent RNA or if template DNA is damaged. In such events, RNAP might backtrack one or few nucleotides, remove mismatched nucleotide and then continue RNA synthesis (Belogurov and Artsimovitch 2019). Proof-reading mechanisms might be intrinsic properties of RNAP or utilize auxiliary factors. The best known auxiliary factors (Gre in bacteria and analogous TFIIS in eukaryotes) stimulate RNAP backtracking and RNA cleavage (Borukhov et al. 1993; Kettenberger et al. 2003). However, cyanobacteria lack homologs of Gre proteins. Interestingly, the fidelity of the cyanobacterial RNAP has been shown to be higher than that of *E. coli* (Imashimizu et al. 2011). Recent analysis also showed that the cyanobacterial RNAP has an efficient one nucleotide backtracking and cleavage activity (Riaz-Bradley et al. 2020). In addition it has been shown that when two native *E. coli* amino acid residues in the  $\beta'$  subunit are changed to cyano-specific residues (A940V and G1136Q), the hydrolysis activity of the *E. coli* RNAP increases (Riaz-Bradley et al. 2020).

### 1.3.2 Regulatory $\sigma$ factors

RNA polymerase is the major regulatory hub for signalling in bacteria. Environmental changes relay information to a signalling network that orchestrates the recruitment of different  $\sigma$  factors by the RNAP core, triggering changes in the overall gene expression pattern. Cyanobacterial  $\sigma$  factors belong to the  $\sigma^{70}$  family (Osanai et al. 2008), whereas other bacteria might contain also  $\sigma$  factors belonging to a different family called  $\sigma^{54}$  family (Gruber and Gross 2003). The number of  $\sigma$  factors varies between cyanobacterial species and even more between different bacterial species, and the amount of  $\sigma$  factors is usually high in species that have complex physiology or in species that live in harsh environments (Gruber and Gross 2003). In cyanobacteria, the nomenclature of  $\sigma$  factors is not universal (Osanai et al. 2008; Srivastava et al. 2020), as for example in *Synechocystis*  $\sigma$  factors are labelled as “sig”, but in *Synechococcus elongatus* sp. PCC 7942 as “rpo”. Some close

homologues might also have different names – for example SigC of *Synechococcus* sp. PCC 7002 is a close homolog of SigE of *Synechocystis* (Caslake et al. 1997).

*Synechocystis* sp. PCC 6803 contains nine  $\sigma$  factors, the primary  $\sigma$  factor SigA, four group 2  $\sigma$  factors (SigB, SigC, SigD and SigE) that structurally resemble SigA, and four group 3  $\sigma$  factors (SigF, SigG, SigH and SigI) that are structurally divergent from group 1 and 2  $\sigma$  factors (Pollari et al. 2008; Imamura and Asayama 2009). Many factors control the formation of the RNAP holoenzyme. Different  $\sigma$  factors compete for the binding to the same RNAP core, and therefore the amounts of different  $\sigma$  factors affect their competition (Malik et al. 1987). Deletions of  $\sigma$ -factor(s) have been shown to increase the recruitment of the other  $\sigma$  factor(s) (Koskinen et al. 2016; Hakkila et al. 2019). In addition, the amount of the particular  $\sigma$  factor vary depending on environmental conditions, and the expression of  $\sigma$  factor genes can be controlled at the transcriptional or post-transcriptional level (for a recent review, see Srivastava et al. 2020). For some  $\sigma$  factors, the formation RNAP holoenzyme directly reflects the amount of that  $\sigma$  factor (Koskinen et al. 2016) whereas the recruitment of other  $\sigma$  factors is controlled at yet another level by anti- $\sigma$ -factors and their antagonists (Osanai et al. 2009; Bell et al. 2017; Bouillet et al. 2018) or by chemical modifications of  $\sigma$  factors (Türkeri et al. 2012; Kim et al. 2020).

Anti- $\sigma$ -factors are proteins that bind to  $\sigma$  factors and prevent the formation of RNAP holoenzyme (Bouillet et al. 2018). In some cases, anti- $\sigma$ -factors are controlled by anti- $\sigma$  factor antagonists, which can be further regulated via phosphorylation and dephosphorylation (Hecker et al. 2007; Bradshaw and Losick 2015). In cyanobacteria, two anti- $\sigma$  factors have been identified. In *Synechocystis*, the ChlH subunit of chlorophyll synthetase functions also as a SigE specific anti- $\sigma$  factor (Osanai et al. 2009) and SapG is proposed to be an anti- $\sigma$  factor of SigG in *Nostoc punctiforme* (Bell et al. 2017).

In promoter recognition, specific domains of the  $\sigma$  factor in the RNAP holoenzyme recognize conserved promoter elements. These interactions between  $\sigma$  factor and promoter elements define the initiation site of transcription and regulate gene expression levels. Various promoter elements have been characterized in *Synechocystis*. According to Asayama and Imamura, type 1 promoters show *E. coli*-like -35 (TTGACA) and -10 (TATAAT) hexamers as consensus sequences, type 2 promoters contain only -10 region and type 3 promoters comprise -32 (TAGGC) and -12 (GGTAA) elements (Asayama and Imamura 2008). Group 1 and 2  $\sigma$  factors were suggested to recognize type 1 and type 2 promoters whereas the type 3 promoter is specifically recognized by SigF (Asayama and Imamura 2008). An extended -10 element was as well found from *Synechocystis* (Mazouni et al. 1998) and later it was suggested that the RNAP-SigA holoenzyme recognizes that (Koskinen et al. 2018). In addition a -16 promoter element typical to Gram-positive bacteria has been found

from *Synechocystis* (Figge et al. 2000). A recent analysis showed that there is no clear consensus sequence for the -35 region in *Synechocystis* (Koskinen et al. 2018), but it has been suggested that spacing between -35 and -10 regions might be longer in *Synechocystis* than in *E.coli* (Mazouni et al. 1998). However, a detail biochemical analysis of promoter properties of different RNAP holoenzymes remains to be studied in cyanobacteria.

### 1.3.3 Roles of different $\sigma$ factors in *Synechocystis*

Acclimatory responses regulated by different  $\sigma$  factors in *Synechocystis* have been under extensive study. The primary  $\sigma$  factor SigA is essential (Imamura et al. 2003a) and it is responsible for the expression of housekeeping genes. SigA is highly conserved among cyanobacteria, forming a monophyletic clade (Osanai et al. 2008). It has been experimentally verified that SigA is regulated at transcriptional and translational levels, but detailed mechanisms are unknown (Tuominen et al. 2003). However, the anti-sense RNA (asRNA) slr0653-as4 might regulate *sigA* (Klotz et al. 2016). The  $\Delta$ sigBCDE strain lacking all group 2  $\sigma$  factors forms a large amount of the RNAP-SigA holoenzyme and in  $\Delta$ sigBCDE, genes encoding transcriptional and translational machineries are upregulated, and the RNA content of mutant cells is three times higher than in the control strain (Koskinen et al. 2018). Group 2  $\sigma$  factors are non-essential and a *Synechocystis* strain,  $\Delta$ sigBCDE, is fully viable in standard growth conditions, but sensitive to many stress conditions like bright light, heat, nitrogen deficiency and oxidative stresses (Koskinen et al. 2016, 2018; Antal et al. 2016; Hakkila et al. 2019; Valev et al. 2020).

SigB is upregulated at transcriptional level when cells are subjected to high salt, hyperosmotic stress, heat, light/dark transitions, superoxide or H<sub>2</sub>O<sub>2</sub> treatments (Kanesaki et al. 2002; Imamura et al. 2003b, 2003a; Tuominen et al. 2003; Nikkinen et al. 2012; Hakkila et al. 2019) and the amount of the SigB protein increases after high temperature, high salt or H<sub>2</sub>O<sub>2</sub> treatments (Imamura et al. 2003b; Koskinen et al. 2016; Hakkila et al. 2019). When the amount of the RNAP-SigB holoenzyme was measured in several stress conditions, the results showed a high RNAP-SigB holoenzyme level after heat and high salt (Koskinen et al. 2016) and H<sub>2</sub>O<sub>2</sub> (Hakkila et al. 2019b) treatments. In accordance with gene expression and holoenzyme data, SigB inactivation mutants grow poorly in increased salinity (Nikkinen et al. 2012; Tyystjärvi et al. 2013), after heat shock (Nikkinen et al. 2012) or in long heat treatment (Tuominen et al. 2006). The growth rate of  $\Delta$ sigB was slow also at low temperature, especially if grown in a diurnal light dark rhythm (Pollari et al. 2011).

In contrast to the SigB inactivation strain, the  $\Delta$ sigCDE strain containing SigB as an only functional group 2  $\sigma$  factor is more tolerant against salt stress (Nikkinen et al. 2012), light induced damage to PSII (Hakkila et al. 2013) and H<sub>2</sub>O<sub>2</sub> induced

stress (Hakkila et al. 2019) than the control strain. The photoinhibition-resistant phenotype was probably the outcome of a higher carotenoid content and overexpression of *flv4-sll0218-flv2* operon observed in  $\Delta$ sigCDE (Hakkila et al. 2013). It is also notable that the  $\Delta$ sigCDE strain contains more SigB than the control strain (Hakkila et al. 2019). In another study, a SigB overexpression strain (SigB-OE) was found to be more tolerant against elevated temperatures and butanol than the control strain (Kaczmarzyk et al. 2014). Tolerance can be explained by enhanced ROS scavenging of SigB-OE strain (Kaczmarzyk et al. 2014) and similarly the  $\Delta$ sigCDE strain containing more RNAP-SigB holoenzyme than CS, has enhanced H<sub>2</sub>O<sub>2</sub> tolerance (Hakkila et al. 2019). SigB-OE strain allocates carbon skeletons especially to PHB (Kaczmarzyk et al. 2014),  $\Delta$ sigCDE to carotenoids (Hakkila et al. 2013) and  $\Delta$ sigBCE (high SigD content) to glycogen (Antal et al. 2016). For  $\sigma$  factor double mutants,  $\Delta$ sigBD grows slowly at high temperatures (Tuominen et al. 2006) and  $\Delta$ sigBE after dark to light transition (Summerfield and Sherman 2007).

The *sigD* gene is light regulated (Imamura et al. 2003b; Tuominen et al. 2003) and amounts of the SigD protein and the RNAP-SigD holoenzyme increase in bright light (Imamura et al. 2003b; Koskinen et al. 2016). It has been proposed that SigD controls the upregulation of *psbA* genes in high light (Imamura et al. 2003a; Pollari et al. 2009) and the  $\Delta$ sigD strain is sensitive to PSII photoinhibition and show growth defects in high light (Tuominen et al. 2006; Pollari et al. 2008). Additionally, when both SigD and SigB are inactivated, mutant cells show more severe defects in photosynthesis and growth in bright light than single mutants (Pollari et al. 2009; Tyystjärvi et al. 2013). When SigD is the only remaining group 2  $\sigma$  factor (strain  $\Delta$ sigBCE), the amount of SigD is doubled compared to the control strain and mutant cells grow better in high light than the control strain cells (Hakkila et al. 2019a; Valev et al. 2020). SigD is, as well, important for induction of oxidative stress protection (Hakkila et al. 2014, 2019).

The *sigC* gene has been shown to respond to shifting between different growth phases or to nitrogen deficiency in several cyanobacteria (Caslake et al. 1997; Gruber and Bryant 1998; Imamura et al. 2003a; Asayama et al. 2004; Tuominen et al. 2008). In the stationary phase, *sigC* transcripts increase but the SigC proteins are less abundant than in the exponential phase (Imamura et al. 2003a). This points out that SigC might be regulated translationally and/or post-translationally. The RNAP-SigC holoenzyme was more abundant in darkness, and in heat or high salt treated cells than in standard conditions, although the amount of the SigC protein remained constant (Koskinen et al. 2016), suggesting that formation of RNAP-SigC holoenzyme is not only dependent on the amount of SigC protein. A single mutant lacking SigC shows defects in the stationary growth phase (Asayama et al. 2004), in mild heat treatments or when inorganic carbon level is below that in the ambient air (Gunnelius et al. 2010). The knockout strain  $\Delta$ sigBDE where SigC is the only

functional group 2  $\sigma$  factor contains the normal amount of the SigC protein. Enhanced formation of the RNAP-SigC holoenzyme during nitrogen starvation causes a slow recovery of growth after nitrogen is reintroduced (Antal et al. 2016, Heilmann et al. 2017).

SigE activates sugar catabolism genes (Osanai et al. 2005, 2007, 2011). In the  $\Delta$ sigE strain many genes encoding enzymes of glycolysis, oxidative penthose phosphate pathway or glycogen catabolism were downregulated (Osanai et al. 2005c). The  $\Delta$ sigE also showed reduced activity of several key enzymes of sugar metabolism (Osanai et al. 2005c). In contrast, a SigE overexpression strain (SigE-OE) enhances the expression of sugar catabolic genes, and the glycogen content is low in SigE-OE (Osanai et al. 2011). Furthermore, SigE-OE produces high amounts of polyhydroxybutyrate at the expense of glycogen production (Osanai et al. 2013). The H subunit of Mg-chelatase has been shown to act as an anti- $\sigma$  factor for SigE (Osanai et al. 2009). In darkness, lower Mg<sup>2+</sup> content of the cell induces dissociation of SigE-ChlH complex, which enables formation of the RNAP-SigE holoenzyme thus activating sugar catabolism genes (Osanai et al. 2009). In addition to darkness, also high salinity induces formation of the RNAP-SigE holoenzyme (Koskinen et al. 2018). The *sigE* gene is induced in nitrogen deprivation (Muro-Pastor et al. 2001) and it is rapidly downregulated after nitrogen addition (Heilmann et al. 2017). It has been previously suggested that SigE could be under the control of NtcA (Muro-Pastor et al. 2001; Osanai et al. 2006), but this connection remains controversial (Giner-Lamia et al. 2017). It has been shown that glycogen accumulates during nitrogen starvation (Schwarz and Forchhammer 2005; Antal et al. 2016), and simultaneous activation of sugar catabolic enzymes might be unexpected. However, metabolomic analysis has showed that despite the increase in glycogen, many downstream products of sugar catabolism also increased during nitrogen starvation (Osanai et al. 2014a). In addition to SigE, Rre37 controls sugar catabolism (Azuma et al. 2011; Osanai et al. 2014b).

From group 3  $\sigma$ -factors SigF is non-essential (Flores et al. 2018) and involved in pilus formation, cell motility, outer membrane vesicle formation and in extracellular polysaccharide formation (Bhaya et al. 1999; Asayama and Imamura 2008; Flores et al. 2018). Another group 3  $\sigma$  factor, SigG, is the only essential alternative  $\sigma$  factor in *Synechocystis*, but its biological role is not known (Huckauf et al. 2000; Imamura et al. 2003a; Matsui et al. 2007). Gene expression data have revealed that the *sigG* gene is upregulated in Ci limitation (Wang et al. 2004) and downregulated in heat-shock or in acid acclimation (Huckauf et al. 2000; Zhang et al. 2012b). So far, no strong phenotype has been detected for  $\Delta$ sigH (Huckauf et al. 2000), although *sigH* is upregulated at the transcriptional level in many conditions including Ci limitation and low pH (Zhang et al. 2012b). The *sigI* is upregulated upon exposure to high

cadmium concentrations (Houot et al. 2007), but there are no further studies related to this subject.

### 1.3.4 Omega subunit

The role of the  $\omega$  subunit of RNAP has been under research since its discovery in 1970 (Heil and Zillig 1970), but the precise function(s) and whether they are the same in all bacteria still remain unclear. The  $\omega$  subunit is encoded by the *rpoZ* gene and it is homologous with the archeal RpoK and the eukaryotic RBP6 subunit of RNAP (Minakhin et al. 2001). RpoK and RBP6 are essential proteins, but in bacteria the  $\omega$  subunit is non-essential (Gentry and Burgess 1989; Kojima et al. 2002; Mathew et al. 2005; Santos-Beneit et al. 2011). The  $\omega$  subunit is small, and its size varies between 7 and 11.5 kDa. All  $\omega$  subunits contain three conserved  $\alpha$  helices, but the N- and C-terminal regions show high variation between the bacterial species (Minakhin et al. 2001; Vassilyev et al. 2002; Zuo et al. 2013; Mao et al. 2018). In addition, the loop between the conserved  $\alpha$  helices 2 and 3 is highly variable (Mao et al. 2018). The  $\omega$  subunit mainly interacts with the  $\beta'$  subunit, but many of these interactions are taxon specific, for example less interactions are detected in *E. coli* than in *Thermus* species, and the lineage specific insertion between  $\alpha$  helices 2 and 3 in actinobacteria interacts with the  $\beta'$  subunit (Vassilyev et al. 2002; Zuo et al. 2013; Mao et al. 2018).

A chaperone like role, where  $\omega$  assists the  $\beta'$  subunit to join in the  $\alpha_2\beta$  sub-complex as the final step of the RNAP core formation and/or a role as a structure stabilizing protein have been suggested (Mukherjee et al. 1999; Ghosh et al. 2001; Minakhin et al. 2001; Richard et al. 2003; Mao et al. 2018). These functions resemble the putative functions of RpoK and RBP6 in archaeal and eukaryotic RNAPs. Physiologically the  $\omega$  subunit has been shown to be important in heat stress (Minakhin et al. 2001; Santos-Beneit et al. 2011), which would fit to the chaperone like role of  $\omega$  and also to a structural role as an RNAP integrity stabilizing subunit. However, the  $\omega$  subunit is non-essential in numerous bacterial species, including *E. coli*, *Streptomyces kasugaensis*, *Streptomyces coelicolor*, *Mycobacterium smegmatis*, *Staphylococcus aureus* and *Rhodobacter capsulatus* and  $\omega$ -less strains of those bacteria grow well at least in optimal conditions (Gentry and Burgess 1989; Kojima et al. 2002; Mathew et al. 2005; Santos-Beneit et al. 2011; Weiss et al. 2016; Westbye et al. 2017) questioning the structural importance or indispensable chaperon function. However, some  $\omega$  mutants are lethal in *E. coli* (Sabareesh et al. 2010; Sarkar et al. 2013) and in *Mycobacterium tuberculosis* the  $\omega$  subunit was suggested to be essential (Mao et al. 2018).

Characterization of  $\omega$ -less bacterial strains has revealed quite pleiotropic phenotypes. Originally, the  $\omega$  subunit was connected to stringent response in *E. coli*

(Vrentas et al. 2005). However the mechanisms of stringent response are not conserved in bacteria, and the importance of  $\omega$  in stringent response is still under debate (Vrentas et al. 2005; Ross et al. 2013, 2016; Weiss et al. 2016). Alterations of cell wall, capsule and cell morphology seem to be common for  $\omega$ -less strains. The  $\omega$ -less strains of *M. smegmatis* and *S. aureus* both show defects in biofilm production, and in *M. smegmatis* also sliding motility was reduced (Mathew et al. 2005; Weiss et al. 2016). Impaired biofilm production was observed in *E. coli*, when an  $\omega$ -less strain was grown in a minimal medium (Bhardwaj et al. 2018). The formation of aerial hyphae was impaired in  $\omega$ -less strains of *Streptomyces* species (Kojima et al. 2002; Santos-Beneit et al. 2011). In addition, *Streptomyces* bacteria produced less species specific antibiotics when  $\omega$  was deleted (Kojima et al. 2002; Santos-Beneit et al. 2011).

It has been proposed that the  $\omega$  subunit interacts with N- and C-terminal parts of  $\beta'$  to secure the structure of RNAP (Minakhin et al. 2001). In cyanobacteria, one of these regions possibly interacting with the  $\omega$  subunit would be in the  $\gamma$  subunit and the other one in the  $\beta'$  subunit, making the role of  $\omega$  in cyanobacteria an open question.

## 2 Aims of the Study

The general aim of this study was to reveal the role of the  $\omega$  subunit of RNAP in cyanobacteria. As the  $\beta'$  subunit of RNAP in cyanobacteria has been split to two parts, putative chaperon-like function would not be identical to the one where  $\omega$  has been suggested to assist  $\beta'$  to join to the RNAP core subassembly. Other studies have pointed to a potential regulatory role of the  $\omega$  subunit affecting the expression of housekeeping genes, which in cyanobacteria include numerous photosynthesis related genes missing from heterotrophic bacteria.

Specific aims of this Thesis were:

- 1) To construct an  $\omega$ -less strain of *Synechocystis* and to study if the deletion of the  $\omega$  subunit affects growth, basic cellular functions or gene expression in standard growth conditions (Papers I, III and IV).
- 2) To compare heat acclimation of the  $\omega$ -less strain to that of the control strain as  $\omega$ -less strains of some heterotrophic bacteria are heat sensitive (Paper II).
- 3) To test performance of the  $\omega$ -less strain in high CO<sub>2</sub>, as CCMs and carbon fixation genes were downregulated in the  $\omega$ -less strain in ambient air (Papers III and IV).
- 4) To find out why the  $\omega$ -less strain does not acclimate to high CO<sub>2</sub>.
- 5) To figure out what are the spontaneously raised suppressor mutations rescuing the high CO<sub>2</sub> and high temperature acclimation capacity of the  $\omega$ -less strain, and further on what are the mechanism(s) leading to the rescue (Paper IV).

## 3 Materials and Methods

### 3.1 Cyanobacterial strains and growth experiments

A glucose-tolerant, non-motile strain of *Synechocystis* sp. PCC 6803 (Williams 1988) was used as control strain (CS). All mutant strains, excluding the suppressor mutants (Table 1), were generated via homologous recombination using antibiotic resistance cassettes as selection markers; details are described in Papers I, III and IV. After selection of completely segregated lines, glycerol stocks of each strain were prepared and stored at -80 °C. The mutant strains were maintained on BG-11 plates supplemented with appropriate antibiotics for 1-2 months and then the cultures were renewed from stocks. The  $\Delta$ rpz strain was maintained on plates with kanamycin only for a couple of weeks because suppressor mutations regularly appear in  $\Delta$ rpz. Suppressor mutants were generated by maintaining the  $\Delta$ rpz strain on selective BG-11 plates for 3-4 months and then subcultures of the  $\Delta$ rpz strain growing well in high CO<sub>2</sub> were spread on selective plates, single colonies were picked up and single cell originated suppressor lines showing similar high CO<sub>2</sub> growth as CS were selected (Paper IV).

For the experiments, all strains were grown without antibiotics in liquid BG-11 medium supplemented with 20 mM HEPES-NaOH, pH 7.5, for 1-5 days under continuous illumination at the photosynthetic photon flux density of 40  $\mu\text{mol m}^{-2}\text{s}^{-1}$  at 32 °C in ambient air; these conditions are referred to as the standard growth conditions (Papers I, II, III and IV). For high CO<sub>2</sub> treatments, the growth chamber air was supplemented with 3 % CO<sub>2</sub> (Papers III and IV). Heat acclimation was tested by growing cells at 38 °C or at 40 °C in ambient air (Paper II). Acclimation to pH was studied by supplementing BG-11 medium with 20 mM HEPES-NaOH, pH 6.8, 7.5 or 8.3 (Paper III). Growth was also tested in non-buffered BG-11 medium (Paper III). In some experiments, nitrate (17.6 mM NaNO<sub>3</sub>) was replaced with ammonium (17.6 mM NH<sub>4</sub>Cl) as a nitrogen source (Paper III). Growth experiments were performed by setting the optical density at 730 nm to 0.1 and then measuring OD<sub>730</sub> daily; dense cultures were diluted before measurements.

**Table 1.** *Synechocystis* sp. PCC 6803 mutants used in this Thesis.

Strain	Plasmid		Modification		Used
$\Delta$ rpoZ	pUC19-rpoZ:Kn		$\omega$ subunit knockout		Papers I,II,III,IV
$\Delta$ rpoZ+rpoZ	pAll:Sm		$\omega$ subunit complementation strain		Papers I, II, III
CS-RNAP-His*	pMA-T-His-tag:Cm		control strain containing a 9 AA His-tag in $\gamma$ subunit		Papers III, IV
$\Delta$ rpoZ-RNAP-His	pMA-T-His-tag:Cm		$\Delta$ rpoZ containing a 9 AA His-tag in the $\gamma$ subunit		Papers III, IV
$\Delta$ rpoZ-S1-RNAP-His	pMA-T-His-tag:Cm		$\Delta$ rpoZ-S1 containing a 9 AA His-tag in the $\gamma$ subunit		Paper IV
$\Delta$ rpoZ-S2-RNAP-His	pMA-T-His-tag:Cm		$\Delta$ rpoZ-S2 containing a 9 AA His-tag in the $\gamma$ subunit		Paper IV
Target	Mutation	Change	Location	Nomenclature	
Ssr1600	L24S	TTG/TCG	2024196	$\Delta$ rpoZ-S1	Paper IV
Ssr1600	G53V	GGG/GTG	2024253	$\Delta$ rpoZ-S2	Paper IV

\*Koskinen et al. 2016

## 3.2 Measurements of cell properties and photosynthesis

### 3.2.1 Light saturated photosynthetic activity and respiration

Clark type oxygen electrode (Hansatech Ltd) was used to measure oxygen evolution (photosynthetic activity) and oxygen consumption (respiration). Photosynthetic activity was measured under saturating light (PPFD 2,000  $\mu\text{mol m}^{-2} \text{s}^{-1}$ ), the whole electron transfer chain was measured in the presence 10 mM  $\text{NaHCO}_3$ , and PSII activity was measured in the presence of 0.5 mM 2,6-dichloro-p-benzoquinone (DCBQ) and 0.5 mM ferricyanide. Respiration was measured by following oxygen consumption after 5 min of dark adaptation. Detailed information is available in Papers I, III and IV.

### 3.2.2 Electron transfer rate, $P_{700}$ redox transitions and 77 K fluorescence emission spectra

Light response properties of mutant strains were analyzed by measuring the relative electron transfer rate (ETR) with Multi-color-PAM device (Walz). A standard protocol was used where light intensity increased from 0 to 500  $\mu\text{mol photons m}^{-2}\text{s}^{-1}$  and ETR was calculated as  $\text{PPFD m}^{-2}\text{s}^{-1} * 0.84 * 0.5 * \Phi_{\text{PSII}}$  (Paper III). A Joliot-type spectrometer (JTS-10) was used to measure  $P_{700}$  oxidation and re-reduction kinetics of

$P_{700}^+$  as described in (Paper III). Fluorescence emission from PSII and PSI was measured at 77 K by exciting the sample with blue light (440 nm) and by measuring the emission spectrum with an Ocean Optics S2000 spectrometer (Papers I and III).

### 3.2.3 Pigments, $\alpha$ -tocopherol and lipids

The Chl *a*, carotenoids and  $\alpha$ -tocopherol were extracted from intact cells with methanol. Chl *a* content was measured as in (Mackinney 1941, Papers I and III) and carotenoids and  $\alpha$ -tocopherol were quantified by series 1100 high performance liquid chromatography (HPLC) device with diode array detector and fluorescence detector (Agilent Technologies), installed with a reverse-phase C18 column (LiChroCART 125-4, Hewlet Packard). HPLC program was run according to (Lehtimäki et al. 2011).  $\beta$ -carotene, echinenone, myxoxanthophyll and zeaxanthin were detected at 490 nm and  $\alpha$ -tocopherol by fluorescence (excitation = 295 nm, emission = 340 nm). *In vivo* absorption spectra were measured to detect Chl *a*, carotenoids and phycocyanobilins (Papers I and III). For lipid extraction and purification, a method established by Bligh and Dyer (Bligh and Dyer 1959) was used. Lipids were then separated with thin-layer chromatography and analyzed by gas chromatography (Wada and Murata 1989, Paper I)

### 3.2.4 Glycogen and glutathione

Glycogen was degraded with  $\alpha$ -amylase to glucose and the glucose content of samples was detected as described earlier (Antal et al., 2016, Paper III). Total glutathione concentration was measured using a DNTB method where the disappearance of DNTB and occurrence of TNB is measured at 412 nm as a function of time (Owens and Belcher, 1965). Glutathione concentrations of the samples were calculated from 10 min reactions using a glutathione standard (Paper III).

### 3.2.5 Cell number analysis and survival rates

Flow cytometry and microscopy imaging were used to estimate the number of cells in different mutants. Flow cytometry experiments were done with LSRFortessa™ cell analyzer (BD Bioscience) with 12  $\mu$ l/min flow rate. Microscopy images were taken with Nikon Eclipse Ti2-E-microscope and Nikon DS-Fi3-camera. The workflow is described in detail in Paper IV.

Cell survival rate was analyzed by growing cells first at 40 °C for 24 h and then cell concentration was diluted to  $OD_{730}=0.1$ . Samples were further serially diluted (1:10, 1:100, 1:1000 and 1:10 000) and 20 drops (10  $\mu$ l) were spotted on BG-11 plates. Plates were incubated in standard growth conditions and after one-week

colonies were counted. Colony forming units (CFUs) were then calculated as CFUs/1 ml cell culture with  $OD_{730} = 0.1$

### 3.2.6 Protein oxidation and cellular ROS content

To get an estimate on the amount of oxidative damage in cells, the amount of carbonylated proteins were analyzed as in Hakkila et al. 2014 (Paper III). Cellular ROS species were detected *in vivo* with a commercial fluorescence indicator CM-H2DCFDA (Invitrogen) as described in Paper III. According to the manufacturer, the indicator detects peroxyxynitrate, hydroxyl and hydroperoxyl radicals and hydrogen peroxide. In addition, singlet oxygen was measured *in vivo* with chemical trapping by histidine (Paper III). The method is described by Rehman et al. 2013.

## 3.3 Molecular biology techniques

### 3.3.1 Genome sequencing

Genomic DNA was extracted as described in Paper IV. The quantity and quality of DNA were checked with Biodrop  $\mu$ LITE (Biodrop, UK) and with agarose gel electrophoresis. The sequencing services at GATC Biotech AG were used for whole genome sequencing. Sequencing was executed with an Illumina HiSeq machine with paired-end sequencing, and the read length was 125 nt. After sequencing, quality was checked, and alignment was mapped to PCC-M reference genome. Insertion and deletions along with point mutation sites were analyzed with the help of variant analysis made in GATC.

### 3.3.2 Operon analysis

To study whether two adjacent genes are in the same operon, a reverse transcription-PCR method was applied (Paper I). Total RNA was extracted as described earlier (Tyystjärvi et al. 2001) and treated with TURBO DNase (Paper I). In the next step, 900 ng of RNA was used as a template in cDNA synthesis with Superscript III kit (Invitrogen). cDNA was used as a template in PCR reaction using primer pairs designed so that the forward primer anneals to one gene and the reverse primer to the other gene; for details see Paper I.

### 3.3.3 Total RNA, RT-qPCR and microarray analysis

Total RNA was extracted using the hot-phenol method (Tyystjärvi et al. 2001), quantified with the Biodrop  $\mu$ LITE (Biodrop, UK) spectrophotometer and visualized

with ethidium bromide staining on 1.2 % agarose gels as described (Papers I, II, III). In paper III, RNA was treated with a TURBO DNase (Invitrogen) before analysis.

DNA microarray experiments were performed as described in Papers I, II and IV. In papers I and II, cells were collected in pre-cooled Falcon tubes and RNA was isolated by the hot-phenol method (Tyystjärvi et al. 2001). Isolated RNA was purified with RNeasy Mini Kit (Qiagen). An Agilent 8 x 15K custom *Synechocystis* sp. PCC 6803 array (Eisenhut et al. 2007) contained probes for the 3,264 protein coding genes of *Synechocystis* sp. PCC 6803 and hybridizations, data collection and processing were done as described earlier (Hakkila et al. 2013). In paper IV, cells were collected using Falcon tubes containing 2 ml of water frozen at -70 °C for rapid cooling of the samples. RNA was isolated using PGTX extraction buffer (Pinto et al. 2009) to get better yield of small RNAs than with the hot-phenol method. The DNA microarray analysis was performed with an Agilent 8 × 60K array and 2 µg of RNA was labelled with Cy3 (Paper IV). Then hybridization was done with 600 ng of the labelled RNA per array. Arrays, data normalization, transcript mapping and identification of antisense transcripts were done according to Georg et al. 2009.

Gene expression was also analyzed by using real-time quantitative PCR (Paper IV). Here RNA was isolated by using the hot-phenol method (Tyystjärvi et al. 2001, Paper IV), and 1 µg of RNA was used for cDNA synthesis (Superscript III Reverse transcriptase kit, Invitrogen). The expression of the *ssr1600* gene and the reference gene *rnpB* were analyzed, RT-qPCR was performed with Sensifast™ SYBR & Fluorescein Kit (Bioline) and run with Bio-Rad IQ5 machine (Paper IV).

### 3.3.4 SDS-PAGE, BN-PAGE and Western blot

Total, soluble or membrane proteins were extracted and quantified with the Lowry method as described in Pollari et al. 2011 (Papers I, II, III and IV). Proteins were separated either with 10 % Next™ mini gels (Papers I, II, III and IV) or with 12 % SDS-PAGE gels (acrylamide:bis-acrylamide 37.5:1) with a 6 % stacking gel (Paper IV). The 10 % Next™ mini gels were run in Mini-Protean II™ (Bio-rad) or in Mini-Protean® Tetra System (Bio-rad) and custom gels were run in Protean® II xi cell system (Bio-Rad).

Thylakoid protein extraction for blue native gel electrophoresis was done according to Hagio et al. 2000 (Paper III). In BN-PAGE, protein complexes of 70 µg of thylakoid samples were separated in 5 % to 12 % (w/v) gradient gel as described in Paper III.

Studied proteins were quantified and detected by using Western blotting (Papers I, II, III and IV). After SDS-PAGE or BN-PAGE proteins were transferred from gels to Immobilon-P-PVDF-membrane (Millipore) with Trans-blot® (Bio-Rad) device. Primary antibodies used are listed in Tables 2-4, and the secondary antibody was the

goat anti-rabbit IgG (H+L) alkaline phosphatase conjugate (Zymed). For detection CDP-star-chemiluminescence reagent from two different providers, New England Biolabs (Paper I and II) and Perkin Elmer (Paper III and IV) was used. Since the chemiluminescence from Perkin Elmer gave stronger signal than equivalent from New England Biolabs, protein amounts loaded on gels were decreased, primary antibodies were diluted as shown in Tables 2-4, and secondary antibody was diluted to 1:50 000 or to 1: 10 000, respectively.

### 3.3.5 Detection of sigma factors in RNA polymerase holoenzyme

Two different techniques were used to analyze the amount of a particular  $\sigma$ -factor in the RNAP holoenzyme. The first technique was based on separating free and RNAP bound SigA factors by size filtrating the native soluble proteins according to protein size (Paper I). 250  $\mu$ g of soluble proteins were first filtrated trough Amicon Ultra-0.5 ml 100 K column and the flow trough was filtered with a 30 K column. The >100 kDa fraction contained  $\sigma$ -factors bound to RNAP and 30-100 kDa fraction contained free SigA factors and  $\alpha$  subunits (Paper I).

The second technique was His-mediated RNAP pulldown, which required transformation of a His-tag to the  $\gamma$  subunit of RNAP in all studied strains (Table 1). Soluble proteins were isolated from CS-RNAP-His,  $\Delta$ rpoZ-RNAP-His,  $\Delta$ rpoZ-S1-RNAP-His and  $\Delta$ rpoZ-S2-RNAP-His and 900  $\mu$ g of proteins were incubated with magnetic cobalt coated beads (Dynabeads<sup>®</sup>, Invitrogen). RNAP-His-cobalt bead complexes were harvested using a magnetic rack and RNAP-His complexes were eluted from cobalt beads with a buffer containing 300 mM imidazole as described in Koskinen et al. 2016 (Paper III). The amounts of specific  $\sigma$ -factors and the  $\alpha$ -subunit were analyzed by SDS-PAGE and Western blotting (see 3.3.4).

### 3.3.6 Immunoprecipitation and silver staining

Total of 800  $\mu$ g of soluble proteins were mixed with 2.5  $\mu$ l of the affinity purified Ssr1600 primary antibody. After 2 h incubation at 32 °C, magnetic  $\mu$ MACS Protein A (Miltenyi Biotec) beads were added to collect Ssr1600-antibody complex into magnetic  $\mu$ Columns (Miltenyi Biotec) placed in  $\mu$ MACS<sup>™</sup> Separator (Miltenyi Biotec). The Ssr1600-protein-antibody complexes were eluted from  $\mu$ Columns with pre-heated (95 °C) Laemmli's buffer. In some experiments, as indicated, soluble proteins were either denatured with Laemmli's buffer at 95 °C for 10 min prior to immunoprecipitation or treated with alkaline phosphatase (NEB) for 10 min at 37 °C after immunoprecipitation. Eluted and treated proteins were separated with SDS-PAGE, and Ssr1600 was recognized with Western blotting, or eluted proteins were

silver stained using Pierce™ Silver Stain kit (Thermo Scientific) according to the manufacturer's instructions (Paper IV).

**Table 2.** Commercial antibodies from Agrisera used in this Thesis.

Antibody	Dilution used for Western blot	Total proteins used for Western Blot ( $\mu$ g)	Used in Paper	Agrisera product number
Allophycocyanin	1:3000	1.6	I, II	AS08277
Phycocyanin	1:3000	1.6	I, II	AS08278
CP43	1:6000	5	I, II	AS111787
RbcL	1:5000	5	I, II	AS03037
PsaB	1:5000	10	I	AS10695
HspA	1:6000	50	I	AS08278
RpS1	1:2000	10	III	AS08309
RpL1	1:4000	15	III	AS111738
AtpE	1:2000	60 membrane proteins	I	AS101586
IsiA	1:500	5	III	AS06111

**Table 3.** Custom made antibodies used in this Thesis.

Antibody	Dilution used for Western blot	Total proteins used for Western Blot ( $\mu$ g)	Used in Paper	Peptide	Described in	Produced by
$\alpha$ subunit	1:8000	50 or 10	I - IV	CKSYTDQPQIGRLTA	Paper I	Agrisera
$\beta$ subunit	1:8000	50 or 15	I, II, III	CIRVQPHSPDNPAEK	Paper I	Agrisera
$\beta'$ subunit	1:6000	15	III	EQVNEAMGITGSAPAR	Koskinen et al. 2016	Agrisera
$\gamma$ subunit	1:5000	50 or 25	III	DQWVEIEDQIYAEDS	Koskinen et al. 2016	Agrisera
$\omega$ subunit	1:6000	25 or 20	I, II, III	CVAATEGKEKKVRKI	Paper I	Agrisera
SigA	1:1000	50	I, II, III, IV	CMSDELTRPEIISDN	Paper I	Agrisera
SigB/SigD	1:1000	65	IV	RTIRLPIHITEKLNKIKK	Koskinen et al. 2016	Agrisera
SigC	1:10000	15	IV	RRDRIRDYYENLG	Gunnelius et al. 2010	Innovagen
SigE	1:1000	40	IV	LRRPQVARRLKGWL	Koskinen et al. 2016	Innovagen
Ssr1600	1:5000	35	IV	CLHNSLAEAIATTEG	Paper IV	Agrisera

**Table 4.** Received antibodies used in this Thesis.

<b>Antibody</b>	<b>Dilution used for Western blot</b>	<b>Total proteins used for Western Blot (<math>\mu</math>g)</b>	<b>Used</b>	<b>Described in</b>	<b>Gift from</b>
Flv2	1:1000	50	Paper I, III	P. Zhang et al. 2009	E.M. Aro
Flv3	1:1000	40	Paper I, III	P. Zhang et al. 2009	
Flv4	1:1000	70	Paper III	P. Zhang et al. 2009	
NdhJ	1:1000	10 or 2	Paper I, III	P. Zhang et al. 2004	
NdhK	1:2000	10 or 2	Paper I, III	P. Zhang et al. 2004	
NdhD3	1:1000	50	Paper I	P. Zhang et al. 2004	
OCP	1:1500	10	Paper III	Wilson et al. 2007	D. Kirilovsky
SigF	1:1000	65	Paper IV	Imamura et al. 2003	M. Asayama
SigG	1:1000	65	Paper IV	Imamura et al. 2003	
SigH	1:2000	65	Paper IV	Imamura et al. 2003	
SigI	1:500	65	Paper IV	Imamura et al. 2003	

## 4 Overview of the results

### 4.1 The $\omega$ subunit of RNAP is non-essential in ambient air in *Synechocystis*

In cyanobacteria, the role of the small  $\omega$  subunit of RNAP has not been studied earlier. The  $\omega$  subunit inactivation strain,  $\Delta rpoZ$ , was constructed by inserting a kanamycin resistance cassette in the antisense orientation to the middle of the *rpoZ* (ssl2982) gene (Fig. 4), and a complementation strain  $\Delta rpoZ+rpoZ$  was constructed by replacing the coding sequence of the *psbAII* gene with the *rpoZ* coding sequence in the  $\Delta rpoZ$  strain (Paper I). The  $\Delta rpoZ$ ,  $\Delta rpoZ+rpoZ$  and the control strain (CS) grew similarly in standard growth conditions (ambient air, 32 °C, moderate light) indicating that just like in many heterotrophic bacteria, the  $\omega$  subunit of RNAP is non-essential in cyanobacteria (Paper I). Analysis of basic cellular properties of the  $\Delta rpoZ$  strain revealed that this strain has abnormalities in cell division leading to the accumulation of cell doublets (Paper IV). However, when one cell doublet was calculated as two cells, the same OD<sub>730</sub> corresponds to approximately the same number of cells in the CS and in  $\Delta rpoZ$  (Paper IV) and OD<sub>730</sub> can be used for cell content comparisons.

The amount of the RNAP core was normal in the  $\Delta rpoZ$  strain of *Synechocystis* but the amount of the SigA  $\sigma$  factor was lower in  $\Delta rpoZ$  than in CS, and less RNAP-SigA holoenzyme was detected in  $\Delta rpoZ$  than in CS when size fractionation columns were used to separate RNAP-bound and free SigA proteins (Paper I). Recruitment of  $\sigma$  factors was also analyzed by adding a His-tag to the  $\gamma$  subunit of RNAP in CS and  $\Delta rpoZ$  strains, and then collecting RNAP complexes with cobalt beads and analyzing the amount of different  $\sigma$  factors by western blotting (Papers III and IV). Similar amounts of the RNAP-SigA holoenzyme were measured in CS and  $\Delta rpoZ$  with pulldown technique (Paper III) and no differences were found in the amounts RNAP holoenzymes bearing other  $\sigma$  factors in standard growth conditions (Paper IV). The discrepancy of SigA results between the techniques remains to be solved. The size fraction method takes longer time than the pulldown technique, and the RNAP-SigA holoenzyme might be less stable without than with the  $\omega$  subunit. Furthermore, the growth history of cells was different, as for the size fractionation studies, cells were grown over one night and for pulldown experiment for three days.

Furthermore, if the SigA protein would make a complex with another protein, it might belong to the RNAP fraction in the size fractionation technique but not with the pulldown technique.

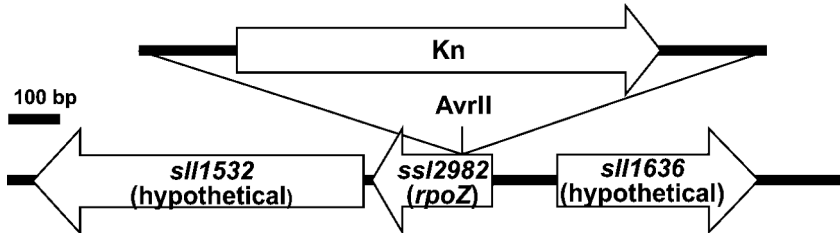


**Figure 4.** Genomic region of the *rpoZ* gene and the construction of the  $\Delta rpoZ$  strain.

The RNA contents of  $\Delta rpoZ$  and CS strains were similar (Papers I and III). The transcriptome of  $\Delta rpoZ$  was compared to that of CS, first by using a custom *Synechocystis* microarray (Eisenhut et al. 2007) containing probes for protein coding regions of 3264 genes (Paper I). Later we used a microarray and detection system (Georg et al. 2009) that in addition to mRNAs recognized putative small RNAs, and produced strand specific data (Paper IV). In general, numerous highly expressed genes were downregulated in  $\Delta rpoZ$ , whereas many low or moderately expressed genes were upregulated in  $\Delta rpoZ$  (Papers I and IV). More specifically, genes coding for subunits of CCMs (*ccmK2K1LMN*; *ndhA-C, E, G-K, M-N, S, ndhF4/D4*; *bicA*; *sbtAB*; *ndhF3-ndhD3-cupA-cupS*), carbon fixation (*rbcSLX*), ATP synthetase (*atpABCDEFG*), nitrate/nitrite transporters (*ntrABCD*) and urea transporter were downregulated in  $\Delta rpoZ$ . However, highly expressed genes encoding transcription and translation machineries, subunits of photosynthetic light reactions or light harvesting antenna structures were not affected in  $\Delta rpoZ$  in ambient air (Papers I and IV). The upregulated genes comprise some heat shock genes and many transposons, but the vast majority belonged to categories hypothetical or unknown (Papers I and IV). In addition, numerous asRNAs were upregulated in  $\Delta rpoZ$  in ambient air (Paper IV).

The promoter regions of differentially expressed genes in  $\Delta rpoZ$  were analyzed (Paper I). Both up and downregulated genes in  $\Delta rpoZ$  contained a typical *E. coli* type -10 region, consisting of TA<sup>T</sup>/AAAT sequence, but only the first A and last T were highly conserved. Some downregulated genes in  $\Delta rpoZ$  contained an extended -10 region, which is common to highly expressed genes of *E. coli* as well. The -35 region showed only low information content whether the gene was up or downregulated in  $\Delta rpoZ$  and no similarity with the *E. coli* -35 regions was detected. Altogether, the gene expression studies point to differences in the selection of promoters by the

native RNAP-SigA and by the  $\omega$ -less RNAP-SigA as only a particular set of genes was affected (Papers I and IV).

It was surprising that  $\Delta$ rpoZ grew normally in ambient air even though genes encoding proteins for CCMs and CO<sub>2</sub> fixation were downregulated (Papers I and IV). Western blot analyses further confirmed that Rubisco and Ndh contents were 35 % and 18 % lower, respectively, in  $\Delta$ rpoZ than in CS (Paper I). Although the  $\Delta$ rpoZ strain grew well in ambient air, some physiological differences were detected between  $\Delta$ rpoZ and CS. The light saturated photosynthetic activity was 20 % lower in  $\Delta$ rpoZ than in CS, even though the same amounts of PSII and PSI complexes were measured in  $\Delta$ rpoZ and CS. In addition, the energy distribution between PSII and PSI was found to be similar in  $\Delta$ rpoZ and CS, and PSI functioned normally in  $\Delta$ rpoZ (Paper III). Thus, lower carbon fixation capacity of the  $\Delta$ rpoZ most probably decreased the light saturated photosynthetic activity of the mutant strain (Papers I and III). The respiration rate was slightly higher in  $\Delta$ rpoZ than in CS, and  $\Delta$ rpoZ produced more glycogen than CS (Paper III).

One apparent phenotype of  $\Delta$ rpoZ was the upregulation of many photoprotective mechanisms. The  $\Delta$ rpoZ strain contained 13 % more carotenoids and 56 % more glutathione than CS in ambient air (Papers I and III). Carotenoids and glutathione both have antioxidant properties and especially carotenoids quench efficiently singlet oxygen (Latifi et al. 2009). In accordance with the high carotenoid content, less singlet oxygen was measured in  $\Delta$ rpoZ than in CS (Paper III). To estimate the amount of other ROS, a ROS sensitive fluorescent dye (CM-H<sub>2</sub>DCFDA) was loaded into cells and fluorescent signal was measured. CM-H<sub>2</sub>DCFDA detects hydrogen peroxide, hydroxyl and hydroperoxyl radicals, and peroxyxynitrite, and the results showed that  $\Delta$ rpoZ contains less these ROS than CS (Paper III). In accordance with a lower ROS content, less protein carbonylation in ambient air was detected in  $\Delta$ rpoZ than in CS (Paper III). However, less flavodiiron proteins (Flv2, Flv3 and Flv4) were measured in  $\Delta$ rpoZ than in CS (Paper I, Hakkila et al. 2013).

## 4.2 *Synechocystis* cells do not acclimate to high temperatures without the $\omega$ subunit of RNAP

Heat stress increases the misfolding of proteins and formation of protein aggregates (Schramm et al. 2019). Heat tolerance of  $\Delta$ rpoZ was tested, as the  $\omega$  subunit has been suggested to play a chaperone like role in other bacteria and some  $\omega$ -less strains are heat sensitive (Mukherjee et al. 1999; Ghosh et al. 2001; Minakhin et al. 2001; Richard et al. 2003; Santos-Beneit et al. 2011; Mao et al. 2018). The  $\Delta$ rpoZ cells acclimate, but slowly, to mild heat stress (38 °C), whereas at 40 °C  $\Delta$ rpoZ hardly grew at all, and the cultures completely bleached in two days (Paper II). The

complementation strain  $\Delta rpoZ+rpoZ$  grew like CS at 40 °C (Paper II). CS tolerates 42 °C well, so obviously  $\Delta rpoZ$  is sensitive to high temperatures.

For microarray analysis, CS and  $\Delta rpoZ$  were grown for three days at 32 °C to  $OD_{730}=1$  and these dense cultures were treated at 40 °C for 24 h (Paper II). Dense cultures of  $\Delta rpoZ$  tolerated heat treatment better than diluted ones (Paper II). Circa two times more genes were up or downregulated in  $\Delta rpoZ$  than in CS when the transcriptome at 40 °C was compared to that of the same strain under standard growth conditions at 32 °C (Paper II). Many genes responding to the 40 °C treatment in  $\Delta rpoZ$  belonged to gene categories hypothetical or unknown, and 80% of the heat-responsive genes of  $\Delta rpoZ$  did not respond to heat in CS. For known heat responsive genes, *slr1674*, *hypA1* and *clpB1* were upregulated in  $\Delta rpoZ$  compared to CS after heat treatment and in addition, nitrogen uptake genes including *nrtABCD*, *amt123* and *urtABCD* were upregulated in heat treated  $\Delta rpoZ$  cells but not in CS.

In CS, the amounts of  $\alpha$ ,  $\beta$  and  $\omega$  subunits of RNAP decreases after 24 h heat treatment, but in  $\Delta rpoZ$ , amounts of RNAP core proteins remained at 40 °C similar as at 32 °C (Paper II). Interestingly, the amount of SigA decreased in CS, but not in  $\Delta rpoZ$  upon heat treatment. In accordance with potentially higher formation of the RNAP-SigA holoenzyme,  $\Delta rpoZ$  cells contained more ribosomal RNA than CS at 40 °C. Taken together, the results indicate that the  $\omega$ -less RNAP remains active at high temperature, but does not properly adjust the gene expression according to the environmental cues.

The light saturated photosynthetic activity of  $\Delta rpoZ$  at 40 °C was lower than that of CS (Paper II). The heat treatment also induced partial degradation of phycocyanin rods but not allophycocyanin cores of the phycobilisome antenna in  $\Delta rpoZ$  (Paper II). In accordance with that, *nblA1* and *nblA2* genes encoding phycobilisome degradation proteins were upregulated in  $\Delta rpoZ$  but not in CS upon 40 °C treatment. Otherwise, the amounts of photosynthetic complexes were similar in CS and in  $\Delta rpoZ$  at 40 °C.

The  $\Delta rpoZ$  strain demonstrated occasionally elevated growth at 40 °C, and later it was discovered that  $\Delta rpoZ$  regularly generates suppressor mutations (Paper IV, chapter 5.5). The suppressor mutants can grow almost like CS at 40 °C or in 3 %  $CO_2$  (see chapter 5.4), even though the suppressor mutants lack the  $\omega$  subunit (Fig. 5). After noticing regular appearance of suppressor mutants, all cell patches of the  $\Delta rpoZ$  strain used in experiments were routinely tested for heat lethality.

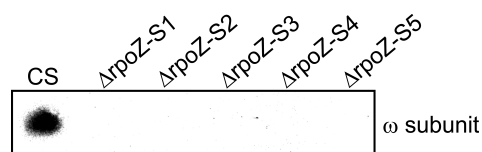


**Figure 5.** The amount of the  $\omega$  subunit in CS and in  $\Delta rpoZ$  suppressor mutants.

### 4.3 Acclimation of *Synechocystis* to high CO<sub>2</sub>

Transcriptional changes upon transfer of cyanobacteria from high CO<sub>2</sub> to ambient air are already well known (Wang et al. 2004; Eisenhut et al. 2007; Klähn et al. 2015), whereas transcriptional changes upon transfer of cells from ambient air to high CO<sub>2</sub>, have only been studied in *Microcystis aeruginosa* cells transferred from ambient air to 0.145 % CO<sub>2</sub> (Sandrini et al. 2015). However, typically high CO<sub>2</sub> conditions for *Synechocystis* are induced by enriching the growth chamber air with 1-5 % of CO<sub>2</sub> or by bubbling growth vessels with CO<sub>2</sub> enriched air (Wang et al. 2004; Eisenhut et al. 2007; Allahverdiyeva et al. 2011; Kopf et al. 2014; Orf et al. 2016; Sengupta et al. 2019). Therefore, transcriptomes of *Synechocystis* cells were analyzed after 1 h or 24 h of growth in air supplemented with 3 % CO<sub>2</sub> (high CO<sub>2</sub>). In total, 6.7 % of genes were differentially expressed after one hour incubation in high CO<sub>2</sub> compared to ambient air (Paper IV). In this comparison, the majority of upregulated genes belonged to functional groups of cellular processes, regulatory functions, translation and transport/binding proteins whereas many downregulated genes belonged to photosynthesis and respiration group, which includes the CCM genes (Fig. 6A). The category hypothetical included numerous up or downregulated genes, whereas genes in category unknown were more often upregulated than downregulated after 1 h of high CO<sub>2</sub> treatment (Fig. 6).

The C/N balance is maintained in cells with various regulatory systems and in high CO<sub>2</sub> this was observed as downregulation of outer membrane porin and Ci uptake genes (*porB*, *sbtA*, *bicA* *cmpABCD*, *ndhD3*, *cupA*) and auxiliary systems of CCMs (*nhaS3*, *ndhD5*, *ndhD6*). Almost all genes encoding subunits of NDH-1 complexes were downregulated (*ndhABC*, *D2*, *E*, *F3*, *GHIJK*) in high CO<sub>2</sub>. Interestingly, the negative regulator of many CCM components, *ndhR*, showed strong downregulation after 1 h in high CO<sub>2</sub>, yet genes repressed by NdhR were not upregulated. The *cmpR* transcription factor activating the *cmp* operon was downregulated as well. In contrast to carbon uptake, nitrogen uptake genes (*nrtABCD*, *amt1*, *urtA*, *amiC*) and nitrogen assimilation genes (*narB*, *nirA*) were upregulated after 1 h in high CO<sub>2</sub>. In addition, genes encoding glutamine synthetase inactivating factors GifA and GifB were downregulated, and glutamine synthetase genes (*glnA*, *glnN*) were upregulated, suggesting enhanced GS-GOGAT cycle activity in high CO<sub>2</sub>. Cyanate lyase, too, was upregulated at the transcriptional level, pointing to increased nitrogen requirement in high CO<sub>2</sub> (Paper IV). The phosphate uptake systems were also upregulated, but more slowly than nitrogen uptake (Paper IV).

After 24 h of high CO<sub>2</sub> treatment, 6.2 % of genes were differently regulated compared to the 1 h high CO<sub>2</sub> treatment (Fig. 6B). In general, many genes were transiently upregulated upon high CO<sub>2</sub> treatment, as the results show that translation machinery genes, ATP synthase and nitrogen transporter genes were downregulated

after 24 h of high CO<sub>2</sub> treatment, while the same genes were upregulated after 1 h of high CO<sub>2</sub> treatment (Paper IV). Interestingly, *glnB* encoding the nitrogen regulatory protein PII was not differently regulated after 1 h of high CO<sub>2</sub>, but after 24 h of high CO<sub>2</sub> treatment it was upregulated. It is also noticeable that many genes that were downregulated after the 1 h high CO<sub>2</sub> treatment, remained downregulated after the 24 h treatment. This group includes the majority of CCM and NDH genes. Genes encoding RNAP core subunits and the primary  $\sigma$  factor SigA were downregulated after long CO<sub>2</sub> treatment (Paper IV), and cells contained less RNAP in high CO<sub>2</sub> than in ambient air (Paper III).

The growth rate increased in high CO<sub>2</sub>, and the doubling times during the first 24 h in ambient air and in high CO<sub>2</sub> were  $11.3 \pm 0.0$  h and  $8.4 \pm 0.1$  h, respectively (Paper III). Photosynthesis was enhanced in high CO<sub>2</sub>, which could be seen as higher light saturated photosynthetic activity, as a higher electron transfer capacity, and higher PSII and PSI activities in high CO<sub>2</sub> than in ambient air (Paper III). Only minor changes were detected in the transcripts of PSI or PSII genes (Paper IV). The light harvesting capacity of cells increased in high CO<sub>2</sub>, as the amount of chlorophyll and phycocyanobilins increased (Paper III), and some chlorophyll synthesis and phycobilisome genes were moderately upregulated in the beginning of the high CO<sub>2</sub> treatment (Paper IV). Obviously, cells produced extra carbon skeletons, as glycogen was accumulating in high CO<sub>2</sub> (Paper III).

In high CO<sub>2</sub>, many photoprotective mechanisms decreased in CS. The NDH-1 complexes and flavodiiron proteins (*flv3*, *flv2*, *flv4*) were downregulated both at transcript (Paper IV) and protein (Paper III) levels. The amount of glutathione decreased in high CO<sub>2</sub> (Paper III), whereas carotenoids first decreased but later returned to the ambient air level (Paper III). However, the ROS content of cells did not increase in high CO<sub>2</sub> and the amount of oxidative damage to proteins remained at a similar level as in ambient air (Paper III). Apparently efficient carbon fixation in high CO<sub>2</sub> functions as a strong electron sink and the alternative electron transport routes or other protective mechanisms are needed less than in ambient air.

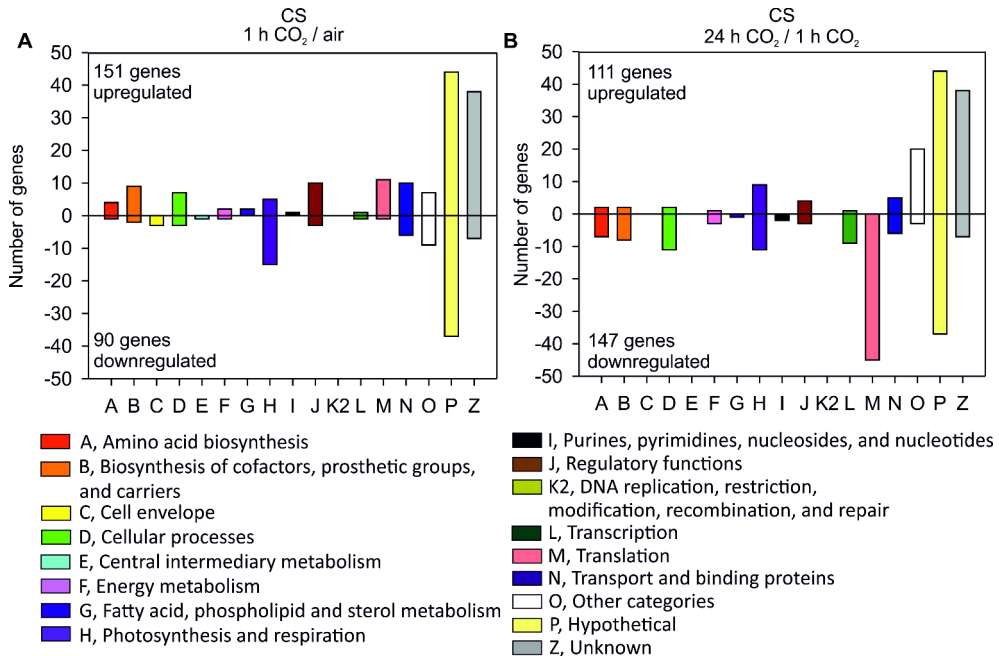


**Figure 6.** Upregulated and downregulated genes in CS after high CO<sub>2</sub> treatment. **(A)** Differently regulated genes after 1 h of high CO<sub>2</sub> treatment compared to ambient air. **(B)** Genes expressed differently after 24 h vs. 1 h of high CO<sub>2</sub> treatments. The genes were arranged to functional categories according to Cyanobase, and a gene was considered up or downregulated if log<sub>2</sub> of the foldchange was ≥ 1 or ≤ -1, respectively.

#### 4.4 The $\omega$ subunit of RNAP is obligatory for high CO<sub>2</sub> acclimation of *Synechocystis* cells

The  $\Delta$ rpz strain turned out to be very interesting for CO<sub>2</sub> acclimation studies, as it had the majority of CCM genes downregulated in ambient air (Papers I and IV). Contrary to expectations,  $\Delta$ rpz showed growth defects in high CO<sub>2</sub> (Papers III and IV). After the first day in high CO<sub>2</sub>,  $\Delta$ rpz reached OD<sub>730</sub> of 0.4, but in following days, growth was not accelerated like in CS, and after three days, OD<sub>730</sub> was 4.0 in CS, but only 1.2 in  $\Delta$ rpz and thereafter  $\Delta$ rpz cells did not grow further (Paper III). When high CO<sub>2</sub> grown  $\Delta$ rpz cells were collected on third day by centrifugation, the supernatant was light blue, indicating a partial lysis of  $\Delta$ rpz cells in high CO<sub>2</sub>.

The dissolved CO<sub>2</sub> causes acidification of water, and *Synechocystis* cells grow only slowly and only for a short time if pH drops to 6.0 (Kurian et al. 2006). For experiments, the BG-11 medium was buffered with 20 mM HEPES, pH 7.5. In high CO<sub>2</sub>, pH first dropped to 7.1 and then increased to 7.4 (Paper III). Without buffering, pH decreased from 7.8 to 7.2 during the first 24 h when CS was grown in high CO<sub>2</sub> and then gradually increased to pH 8.2 within three days (Paper III). The  $\Delta$ rpz strain did not practically grow at all in unbuffered BG-11 medium in high CO<sub>2</sub>, but cells

affected the pH of the growth medium, as after the initial drop of pH to 6.8, it increased to 7.8. The form of  $\text{C}_i$  is pH dependent and *Synechocystis* prefers neutral or slightly alkaline pH, where  $\text{HCO}_3^-$  is the most abundant form (Kurian et al. 2006). To test if  $\Delta\text{rpoZ}$  prefers  $\text{CO}_2$  or  $\text{HCO}_3^-$  as carbon source, growth was analyzed in BG-11 buffered to pH 8.3 or to pH 6.8 and cells were grown in ambient air. In both conditions,  $\Delta\text{rpoZ}$  grew like CS, which pointed out that the form of  $\text{C}_i$  is not the problem for  $\Delta\text{rpoZ}$ , but the amount of  $\text{C}_i$ . Supporting data was acquired from the experiment where high  $\text{C}_i$  conditions were established by adding 10 mM  $\text{Na}_2\text{CO}_3$  into BG-11. Addition of  $\text{Na}_2\text{CO}_3$  increased the growth of CS, but  $\Delta\text{rpoZ}$  grew only poorly (Paper III).

One potential reason for growth problems of  $\Delta\text{rpoZ}$  in high  $\text{CO}_2$  could be that the  $\omega$ -less RNAP would not function efficiently enough to produce RNAs needed for fast growth. In  $\Delta\text{rpoZ}$ , similar amounts of RNAP core proteins were measured in ambient air and high  $\text{CO}_2$ , whereas in CS, the amounts of RNAP core subunits decreased in high  $\text{CO}_2$  (Paper III). As the same amount of total proteins were loaded, it might be that the difference between the RNAP content of CS and  $\Delta\text{rpoZ}$  cells is smaller, as very abundant phycobilisomes were upregulated more in CS than in  $\Delta\text{rpoZ}$  in high  $\text{CO}_2$  (Paper III). Anyway, the total RNA content did not differ between CS and  $\Delta\text{rpoZ}$  in high  $\text{CO}_2$  (Paper III), suggesting that RNAP was functional in  $\Delta\text{rpoZ}$  but  $\omega$ -less RNAP was not able to adjust gene expression correctly.

To analyze the  $\sigma$  factor content of the RNAP holoenzyme, a His-tag was added to the  $\gamma$  subunit of RNAP in CS (Koskinen et al. 2016) and  $\Delta\text{rpoZ}$  (Paper III). RNAP complexes were collected with magnetic cobalt beads, and the  $\sigma$  factor content of collected RNAPs was analyzed with western blotting. The results showed that the amount of the RNAP-SigA holoenzyme increased in both strains upon high  $\text{CO}_2$  treatment (Paper III). Interestingly, the stationary phase specific RNAP-SigC holoenzyme decreased in CS and increased in  $\Delta\text{rpoZ}$  in high  $\text{CO}_2$ , leading to 4-fold more abundant RNAP-SigC holoenzyme in  $\Delta\text{rpoZ}$  than in CS in high  $\text{CO}_2$  (Paper IV). The RNAP-SigC holoenzyme content was similar in  $\Delta\text{rpoZ}$  and CS in ambient air (Paper IV). When SigC was measured from total proteins, no differences were seen between strains or conditions, pointing out that the recruitment of SigC by the RNAP core is not only dependent on the amount of SigC protein, but is regulated by an as yet unknown factor. The amount of the stress specific RNAP-SigB holoenzyme and the high light inducible RNAP-SigD holoenzyme were low in CS and  $\Delta\text{rpoZ}$  in ambient air and further decreased in high  $\text{CO}_2$  (Paper IV). Similar amount of the RNAP-SigE holoenzyme were detected in CS and  $\Delta\text{rpoZ}$  in ambient air and in high  $\text{CO}_2$ , although the amount of SigE protein was lower in  $\Delta\text{rpoZ}$  than in CS in high  $\text{CO}_2$  (Paper IV).

To see how the modified  $\sigma$  factor profile of the RNAP holoenzyme in  $\Delta\text{rpoZ}$  affects, the transcriptome of  $\Delta\text{rpoZ}$  was compared to that of CS after 1 h or 24 h

treatment in high CO<sub>2</sub> (Paper IV). Many of the CCM genes stayed downregulated in  $\Delta$ rpoZ also in high CO<sub>2</sub> (Paper IV). Numerous genes encoding subunits of photosynthetic light reactions and phycobilisome antenna were downregulated in  $\Delta$ rpoZ compared to CS after 24 h of high CO<sub>2</sub> treatment (Paper IV). However, the amounts of PSII and PSI complexes were not lower in  $\Delta$ rpoZ than in CS in high CO<sub>2</sub>, and the actual PSII content was higher (Paper III) whereas the phycobilisome antenna was reduced by 30% (Paper III). The light saturated photosynthetic activity and light response curve measurements revealed that  $\Delta$ rpoZ did not enhance photosynthetic light reactions in high CO<sub>2</sub> like CS, and also light saturated PSII activity was low (Paper III). 77 K measurements showed that the energy distribution between PSII and PSI was similar in CS and  $\Delta$ rpoZ in high CO<sub>2</sub>, but the PSI peak of  $\Delta$ rpoZ was shifted four nm towards shorter wavelengths, suggesting alterations in PSI trimer composition. This was confirmed by BN-PAGE analysis showing more PSI monomers and less PSI trimers in  $\Delta$ rpoZ than in CS in high CO<sub>2</sub> (Paper III). In accordance with that, microarray data reveal downregulation of *psaL* in high CO<sub>2</sub> in  $\Delta$ rpoZ (Paper IV). PsaL protein is needed for PSI trimer formation in *Synechocystis* (Chitnis and Chitnis 1993). Not only photosynthetic electron transfer was slow in  $\Delta$ rpoZ in high CO<sub>2</sub>, but the slower dark re-reduction of P700<sup>+</sup> in  $\Delta$ rpoZ than in CS suggests slow dark respiration in  $\Delta$ rpoZ (Paper III). Photosynthesis is only slightly upregulated in  $\Delta$ rpoZ in high CO<sub>2</sub> compared to ambient air, which could explain why  $\Delta$ rpoZ cells do not grow faster in high CO<sub>2</sub> than in ambient air, but does not explain why cells die after a few days.

Oxidative stress could cause growth problems. The  $\Delta$ rpoZ strain contained more carotenoids and glutathione than CS in ambient air (Paper I). However, like in CS the levels of these protective compounds decrease in high CO<sub>2</sub> in the  $\Delta$ rpoZ strain. Carotenoids dropped to CS levels, but glutathione content remained higher than in CS (Paper III). The expression of carotenoid or glutathione biosynthesis genes was similar in CS and  $\Delta$ rpoZ, but some anti-sense RNAs of genes involved in carotenoid biosynthesis were upregulated in  $\Delta$ rpoZ (Paper IV). The  $\Delta$ rpoZ contained more flavodiiron proteins and the orange carotenoid protein than CS in high CO<sub>2</sub>. The signal obtained from the hydrogen peroxide, hydroxyl and hydroperoxyl radicals and peroxyxynitrite sensitive CM-H<sub>2</sub>DCFDA was slightly higher in  $\Delta$ rpoZ than in CS after high CO<sub>2</sub> treatment, whereas singlet oxygen content was lower (Paper III). Less protein carbonylation was detected in  $\Delta$ rpoZ than in CS after high CO<sub>2</sub> treatments showing that more oxidative damage occurred in CS than in  $\Delta$ rpoZ in high CO<sub>2</sub> (Paper III). Thus, oxidative damage is unlikely to explain poor growth of  $\Delta$ rpoZ in high CO<sub>2</sub>.

*Synechocystis* cells can store carbon skeletons to decrease the carbon flux to the TCA cycle, which balances the C/N ratio (Forchhammer and Schwarz 2019). Glycogen and polyhydroxybutyrate are typical carbon storage compounds in

*Synechocystis* (Hein et al. 1998; Ball and Morell 2003; Koch et al. 2020). In  $\Delta$ rpoZ, 3.5 fold more glycogen was detected in high CO<sub>2</sub> than in CS. Glycogen usually increases when cells suffer from nitrogen deficiency (Schwarz and Forchhammer 2005; Antal et al. 2016), and genes coding for nitrogen uptake and assimilation complexes (*nrtABCD*, *amt1*, *nirA*, *narB*, *glnA*, *glnN*, *glsF*) were downregulated in  $\Delta$ rpoZ compared to CS in high CO<sub>2</sub> (Paper IV). However, the consumption of nitrate from the BG-11 medium was similar in both strains, and replacement of nitrate with ammonium did not enhance the growth of  $\Delta$ rpoZ in high CO<sub>2</sub> (Paper III). Nitrogen utilization might be slower in  $\Delta$ rpoZ than in CS since many genes encoding nitrogen assimilation enzymes were downregulated in  $\Delta$ rpoZ (Paper IV). In addition, the transcripts of negative regulators GifA and GifB of glutamine synthetase were upregulated in  $\Delta$ rpoZ after 24 h treatment in high CO<sub>2</sub> (Paper IV). CS balanced the excess carbon flux in high CO<sub>2</sub> by increasing nitrogen assimilation but based on transcriptomic data, in  $\Delta$ rpoZ nitrogen uptake and assimilation genes are downregulated, although plenty of Ci is available. Thus, carbon skeletons in  $\Delta$ rpoZ were not directed to GS-GOGAT cycle, but instead carbon skeletons were stored as glycogen and were not used for growth.

In addition to abnormalities in photosynthesis and nitrogen metabolism,  $\Delta$ rpoZ obviously shows deficiencies in cell division, as almost all  $\Delta$ rpoZ cells were as doublets in high CO<sub>2</sub>. The observed cell doublets were probably indications of defects in septum site closing that requires the inward growth of the cell membrane, synthesis of peptidoglycan layer, outer membrane structures and finally reconstruction of the outermost carbohydrate envelope. Some genes involved in peptidoglycan synthesis (*galE*, *rfbU*, *murB*, *murC*) and septum site determination (*minD* and *minE*) were downregulated in  $\Delta$ rpoZ in high CO<sub>2</sub> (Paper IV). In addition, many asRNAs (*as-murA*, *as-murC*, *as-murD*, *as-murF*) of genes involved in cell division were upregulated in  $\Delta$ rpoZ in high CO<sub>2</sub>. Completing cell division is not working in  $\Delta$ rpoZ and it is possible that there is not enough peptidoglycan to close the septum site between two daughter cells. This might keep daughter cells together for a long time, which obviously slows growth. In addition,  $\Delta$ rpoZ cells might have problems to start new cell divisions in high CO<sub>2</sub>, as slow cell division would lead to accumulation of butterfly shaped cells if cell divisions would be initiated with a typical high CO<sub>2</sub> frequency (Paper IV). Furthermore, as SigC recruitment was altered in  $\Delta$ rpoZ, it is proposed that SigC is involved in the downregulation of genes related to photosynthesis, nitrogen uptake and metabolism and peptidoglycan synthesis.

## 4.5 Suppressor mutations in the *ssr1600* gene encoding an anti- $\sigma$ factor antagonist rescue the acclimation capacity of $\Delta$ rpz to high CO<sub>2</sub> and to high temperature.

When  $\Delta$ rpz was kept on plates for months, some patch cultures were able to grow almost like the CS in high CO<sub>2</sub>. To find out why  $\Delta$ rpz cells could tolerate high CO<sub>2</sub>, single-cell originated high CO<sub>2</sub> tolerant suppressor lines were isolated. The isolated suppressor lines grew like CS in ambient air and only slightly slower than CS in high CO<sub>2</sub>. Three of the suppressor lines were sequenced together with CS and  $\Delta$ rpz strains (Paper IV). Only one unique mutation was found from each of the suppressor mutant line, and these missense mutations were located in the coding region of the *ssr1600* gene. In one strain,  $\Delta$ rpz-S1, leucine 24 was changed to serine and in two other strains glycine 43 was changed to valine; only one of these identical suppressor lines,  $\Delta$ rpz-S2, was further analyzed. Interestingly, the *ssr1600* gene encodes a homolog of an anti- $\sigma$ -factor antagonist of *Bacillus subtilis* (Paper IV).

To study the Ssr1600 protein, a polyclonal antibody against Ssr1600 was produced. In a previous phosphoproteome analysis in *Synechocystis* cells, the Ssr1600 protein was detected as a phosphoprotein (Angeleri et al. 2016). In accordance with that, the Ssr1600 antibody detected two bands from total proteins, an abundant 12 kDa protein and a slower moving low amount 14 kDa protein that could be the phosphorylated form of Ssr1600 (Paper IV). Only the 14 kDa protein was immunoprecipitated with the Ssr1600 antibody, but when the precipitated Ssr1600 protein was treated with alkaline phosphatase, the 12 kDa protein appeared. When *Synechocystis* proteins were denatured prior to immunoprecipitation, the abundant 12 kDa protein was precipitated. These results suggest that the 12 kDa protein is the non-phosphorylated form of the Ssr1600 protein, and the 14 kDa protein is the phosphorylated form of Ssr1600. The non-phosphorylated Ssr1600 might interact with other protein(s) in native samples, and these interactions mask the epitope detected by the Ssr1600 antibody.

The effects of high CO<sub>2</sub> treatments on the amount of the Ssr1600 protein were studied. The amount of the Ssr1600 protein decreased in CS and increased in  $\Delta$ rpz in high CO<sub>2</sub> when compared to ambient air grown cells. In suppressor mutant lines, only faint signals were observed. In  $\Delta$ rpz-S1, only phosphorylated Ssr1600 was detected, whereas in  $\Delta$ rpz-S2 both forms were detected (Paper IV). The *ssr1600* transcripts did not respond to high CO<sub>2</sub> in CS or  $\Delta$ rpz, but some increase was detected in suppressor lines (Paper IV).

As Ssr1600 is a homolog of an anti- $\sigma$  factor antagonist, the most intriguing thing was to study the  $\sigma$ -factor recruitment in the suppressor mutants. It was striking to discover that in suppressor mutants the amount of RNAP-SigC holoenzyme was similar as in CS and lower than in  $\Delta$ rpz in high CO<sub>2</sub>, but no differences were

detected between the strains in ambient air (Paper IV). In addition, the SigC contents of total protein samples were similar in suppressor mutants, CS and  $\Delta$ rpoZ, suggesting that the Ssr1600 protein indeed regulates the formation of the RNAP-SigC holoenzyme. Similar amounts of the RNAP-SigB and RNAP-SigE holoenzymes were detected in the suppressor lines as in CS and  $\Delta$ rpoZ, whereas the RNAP-SigD holoenzyme that was hardly detectable in CS in high CO<sub>2</sub> was below the detection limit in the suppressor lines. The amounts of RNAP holoenzymes bearing SigF, SigG, SigH or SigI remained also below the detection limits in all strains.

A DNA microarray was used to compare the transcriptome of the  $\Delta$ rpoZ-S1 suppressor line in ambient air and after 1 h or 24 h of high CO<sub>2</sub> treatments to those of CS and  $\Delta$ rpoZ strains (Paper IV). Genes encoding the photosystems and the phycobilisome antenna were expressed similarly in  $\Delta$ rpoZ-S1 as in CS in high CO<sub>2</sub> and the photosynthetic activity was fairly similar in  $\Delta$ rpoZ-S1 and CS in high CO<sub>2</sub> (Paper IV). In addition, genes coding for cell division proteins were expressed similarly in CS and  $\Delta$ rpoZ-S1, and a similar low proportion of cell doublets were found in the suppressor mutant lines as in CS (Paper IV). However, some genes, especially nitrogen metabolism and *ndh* genes, were similarly downregulated in  $\Delta$ rpoZ-S1 as in  $\Delta$ rpoZ in ambient air. In high CO<sub>2</sub>, the similarity between  $\Delta$ rpoZ-S1 and  $\Delta$ rpoZ diminished, and it is possible that the lower recruitment of SigC in the suppressor mutant caused normal expression of nitrogen uptake and assimilation (*nrtBCD*, *amt1*, *nirA*, *narB*, *glnN*, *glnA*) genes (Paper IV). Taking together, it is proposed that Ssr1600 is an anti-SigC-antagonist and very low amounts of Ssr1600 in suppressor mutants decrease the RNAP-SigC holoenzyme in high CO<sub>2</sub>, which rescues suppressor mutants in high CO<sub>2</sub>.

# 5 Discussion

## 5.1 Role of the $\omega$ -subunit of the RNA polymerase core in *Synechocystis*

The autotrophic nature of *Synechocystis* establishes an interesting frame to study the  $\omega$  subunit. The  $\omega$  subunit is non-essential for *Synechocystis* in standard laboratory growth conditions (Paper I), but in high temperature (Paper II) and high CO<sub>2</sub> (Papers III and IV)  $\omega$  is essential. The  $\omega$ -subunit inactivation strains of *E. coli* (Gentry and Burgess 1989), *S. kasugaensis* (Kojima et al. 2002), *M. smegmatis* (Mathew et al. 2005), *S. coelicolor* (Santos-Beneit et al. 2011), *S. aureus* (Weiss et al. 2016) and *R. capsulatus* (Westbye et al. 2017) are viable, at least in standard growth conditions. However, in some species including *M. smegmatis*, *S. coelicolor* and *R. capsulatus*,  $\omega$ -less strains grow more slowly than the respective parental strains (Mathew et al. 2005; Santos-Beneit et al. 2011; Westbye et al. 2017). A slower growth of  $\Delta$ rpoZ strain of *E. coli* was recognized as well, but more detailed studies indicated that the growth reduction is mainly due to a polarity effect on the *spoT* gene located in the same operon (Gentry and Burgess 1989).

A chaperon-like function has been suggested for the  $\omega$  subunit in *E. coli* (Minakhin et al. 2001). In *E. coli*, the  $\omega$  subunit mainly interacts with  $\beta'$  (Gentry and Burgess 1993; Murakami 2013) and facilitates the docking of  $\beta'$  to the  $\alpha_2\beta$  sub-complex (Ghosh et al. 2001; Minakhin et al. 2001). In cyanobacteria,  $\beta'$  has been split to two parts (Schneider and Haselkorn 1988) and some of the amino acids putatively interacting with the  $\omega$  subunit are located in the  $\gamma$  subunit and some in the  $\beta'$  subunit. However, the actual structure of cyanobacterial RNAP is still not known, and due to low sequence similarity, the  $\omega$  subunit was omitted from the RNAP model produced by homologous modeling (Pollari et al. 2008). Thus, interactions of the  $\omega$  subunit with the other core subunits remains to be solved. In blue native gels, free  $\omega$  subunit was more abundant than free forms of the other RNAP core subunits, suggesting that the  $\omega$  subunit might not always be attached to the RNAP core in *Synechocystis*.

Controversial results challenge the chaperone role of the  $\omega$  subunit in bacteria. Assembly studies have pointed to the importance of the  $\omega$  subunit in *R. capsulatus* (Westbye et al. 2017) and especially in *M. tuberculosis*, whose RNAP was not

assembled *in vitro* or *in vivo* without the  $\omega$  subunit (Mao et al. 2018). However,  $\omega$ -less mutants are viable (Gentry and Burgess 1989; Kojima et al. 2002; Mathew et al. 2005; Santos-Beneit et al. 2011; Weiss et al. 2016; Westbye et al. 2017), pointing out that  $\omega$  is not essential chaperone, like the well studied GroES and GroEL (Fayet et al. 1989). Actually in the  $\omega$ -less strain of *E. coli*, the amount of GroEL is significantly increased and suggested to help the assembly of the  $\omega$ -less RNAP core (Mukherjee et al. 1999). However, overexpressed RNAP core subunits can be assembled without the  $\omega$  subunit *in vitro* (Gentry and Burgess 1989). On the other hand, heat sensitivity of  $\omega$ -less strains of *Synechocystis* (Paper II), *E. coli* (Minakhin et al. 2001) and *S. coelicolor* (Santos-Beneit et al. 2011) fits well to the suggested chaperone like function of  $\omega$ . However, there was no indication of impaired RNAP assembly in the  $\Delta$ rpoZ strain of *Synechocystis* at high temperature, and actually  $\Delta$ rpoZ cells contained more RNA than CS. Instead, the transcription pattern of  $\Delta$ rpoZ differs a lot from that of CS (Paper II).

The  $\omega$  subunit might play a regulatory role in *Synechocystis*, as the  $\omega$ -less RNAP seems to select  $\sigma$  factors for the formation of the transcription initiation competent RNAP holoenzyme differently than the intact RNAP (Papers I and IV). In *E. coli* and in *S. aureus*, the  $\omega$ -less RNAP recruited alternative  $\sigma^S$  and  $\sigma^B$  factors, respectively, more efficiently than the intact RNAP (Geertz et al. 2011; Weiss et al. 2016). Upregulated formation of RNAP- $\sigma^S$  in the  $\Delta$ rpoZ strain of *E. coli* is accompanied with upregulation of many genes of the  $\sigma^S$  regulon, and also to a diminished formation of RNAP- $\sigma^{70}$  (Geertz et al. 2011). Interestingly, overproduction of  $\sigma^{70}$  suppresses  $\Delta$ rpoZ phenotype in *E. coli* (Geertz et al. 2011). Although RNAP holoenzymes have not been analyzed in all  $\omega$ -less strains, these strains typically show alterations that are targeted to the outer layers of the cell and that are typically regulated by alternative  $\sigma$ -factors. In *S. kasugaensis* and *S. coelicolor* aerial hyphae, an extracellular mesh that sticks cells on surfaces was poorly formed in  $\omega$ -less strains (Kojima et al. 2002; Santos-Beneit et al. 2011). The  $\omega$ -less strains of *S. aureus* and *M. smegmatis* showed defects in biofilm formation and in the latter, also reduced sliding motility (Mathew and Chatterji 2006; Weiss et al. 2016). In *Synechocystis*, altered cell envelope properties and cell wall synthesis in  $\Delta$ rpoZ were also demonstrated (Papers I and IV). Furthermore, a mutated  $\omega$  subunit (N60D) that has a stronger binding affinity to RNAP core than the native  $\omega$  in *E. coli*, alters the  $\sigma$  factor recruitment *in vitro* (Bhowmik et al. 2017) also showing the influence of the  $\omega$  subunit on  $\sigma$  factors.

As an autotroph, *Synechocystis* has a complete sets of genes that are not found in heterotrophic bacteria, including genes coding for components of the photosynthetic machinery. Furthermore, these genes are considered to be household genes in autotrophs, and they are among the most highly expressed genes in *Synechocystis* (Paper I, Kopf et al. 2014). In heterotrophic bacteria, household genes

typically comprise translational and transcriptional machinery genes. Interestingly, genes involved in photosynthesis, CCMs and nitrogen assimilation were downregulated in  $\Delta\text{rpoZ}$ , whereas transcriptional and translational machinery genes were not (Papers I and IV). Therefore, it could be hypothesized that in cyanobacteria possessing photosynthetic lifestyle, the  $\omega$  subunit might regulate a specific set of household genes. It was discovered that the changes in gene expression level were probably due to different promoter selectivity and different  $\sigma$ -factor recruitment of the  $\omega$ -less RNAP holoenzyme (Papers I and IV).

The  $\Delta\text{rpoZ}$  strain showed serious growth impairment and cell death in high  $\text{CO}_2$  (Papers III and IV) and an explanation for this is described in Fig. 7. The amount of the anti-SigC antagonist Ssr1600 increases in  $\Delta\text{rpoZ}$  in high  $\text{CO}_2$ , the yet unidentified anti-SigC factor forms a complex with abundant anti-SigC antagonist Ssr1600, releasing SigC from the anti-SigC/SigC complex. Then free SigC is recruited by the RNAP core and a high amount of the RNAP-SigC holoenzyme is formed (Fig. 7, Paper IV). Transcriptomic data points out that the high amount of the RNAP-SigC holoenzyme in  $\Delta\text{rpoZ}$  in high  $\text{CO}_2$  leads to abnormally low expression of photosynthesis and nitrogen acquisition and assimilation genes (Fig. 7). This causes deficiencies in light harvesting capacity, light reactions and nitrogen assimilation leading to abnormal C/N balance and glycogen accumulation (Papers III and IV). In addition, the results indicate that SigC negatively regulates cell division and hence  $\Delta\text{rpoZ}$  has a high amount of cell doublets (Fig. 7, Papers III and IV).

The SigC factor has been connected to the stationary phase, heat stress tolerance and to the regulation of nitrogen metabolism in earlier studies (Caslake et al. 1997; Gruber and Bryant 1998; Imamura et al. 2003a; Asayama et al. 2004; Tuominen et al. 2008). A single mutant lacking SigC shows defects in mild heat treatments or when the inorganic carbon level is below that in ambient air (Gunnelius et al. 2010). Interestingly, the lack of the RNAP-SigC holoenzyme ( $\Delta\text{sigC}$ ) or high amounts of the RNAP-SigC holoenzyme ( $\Delta\text{rpoZ}$ ) both cause problems in growth rate adjustment when either temperature increases or  $\text{C}_i$  concentration changes (Gunnelius et al. 2010, Papers II and III). Enhanced formation of the RNAP-SigC holoenzyme during nitrogen starvation in  $\Delta\text{sigBDE}$  or  $\Delta\text{ssaA}$  strains causes slower recovery of growth after nitrogen sufficient conditions are reintroduced (Antal et al. 2016, Heilmann et al. 2017), suggesting that as long as the RNAP-SigC holoenzyme is abundant, cells remains in the non-growing mode.

Originally the  $\omega$  subunit was connected to stringent response in *E. coli* (An et al. 1979; Igarashi et al. 1989). It was shown that *in vitro* the  $\omega$ -less RNAP was not responding to the alarmone molecule ppGpp, and complementation or overproduction  $\omega$  strains restored the sensitivity to ppGpp *in vivo* (Vrentas et al. 2005). The ppGpp was shown to bind to the interface between  $\beta'$  and  $\omega$  in RNAP (Zuo et al. 2013, Ross et al. 2013). The essentiality of  $\omega$  in stringent response was

later challenged by the discovery of new ppGpp binding site which was located far from  $\beta'$  and  $\omega$  interface (Ross et al. 2016). The new binding site is located between  $\beta'$  and DksA transcription factor and this site was shown to affect stringent response genes more than the previously discovered ppGpp binding site (Ross et al. 2013, 2016). More importantly, the later discovered binding site does not require  $\omega$ , and actually the  $\omega$ -less RNAP can perform stringent response in the presence DksA *in vitro* (Vrentas et al. 2005). Nevertheless, it seems that both sites are needed for the normal stringent response in *E.coli* (Ross et al. 2016). In gram-positive bacteria, the conserved binding sites for ppGpp are missing from the RNAP and no DksA protein has been found (Krásny and Gourse 2004; Weiss et al. 2016). In *B. subtilis*, ppGpp reduces the activity of GTP synthesizing enzymes (Kriel et al., 2012; Liu et al., 2015), and GTP concentration directly regulates the activity of rRNA genes (Krasny and Gourse 2004) without the  $\omega$  subunit playing any role. Additionally, an  $\omega$  deletion strain of *S. aureus* performs a normal stringent response (Weiss et al. 2016).

In cyanobacteria, stringent response remains poorly understood, not to mention its connection to the  $\omega$  subunit. Typical stringent-response-type changes of the gene expression profiles, including downregulation of ribosomal operons and upregulation of amino acid synthesis genes, were observed after UV-B treatment of *Synechocystis* (Huang et al., 2002). The ppGpp concentration of *Synechococcus elongatus* cells increases in darkness and simultaneously growth is restricted (Hood et al. 2016) suggesting that ppGpp might be involved in growth regulation in cyanobacteria. In the filamentous cyanobacterium *Anabaena* sp. PCC 7120, ppGpp might regulate heterocyst formation (Zhang et al. 2013). However, no DksA protein homologs have been found in cyanobacteria, and the initial nucleotide in rRNA operons is GTP (Koskinen et al. 2018). In chloroplasts, the plastid encoded RNAP (PEP) was suggested to be directly regulated by ppGpp (Takahashi et al. 2004; Sato et al. 2009), but PEP does not contain an  $\omega$  subunit (Field 2018) and the DksA protein has not been found in chloroplasts. Thus, further studies are needed to figure what roles the  $\omega$  subunit plays during stringent response in cyanobacteria.

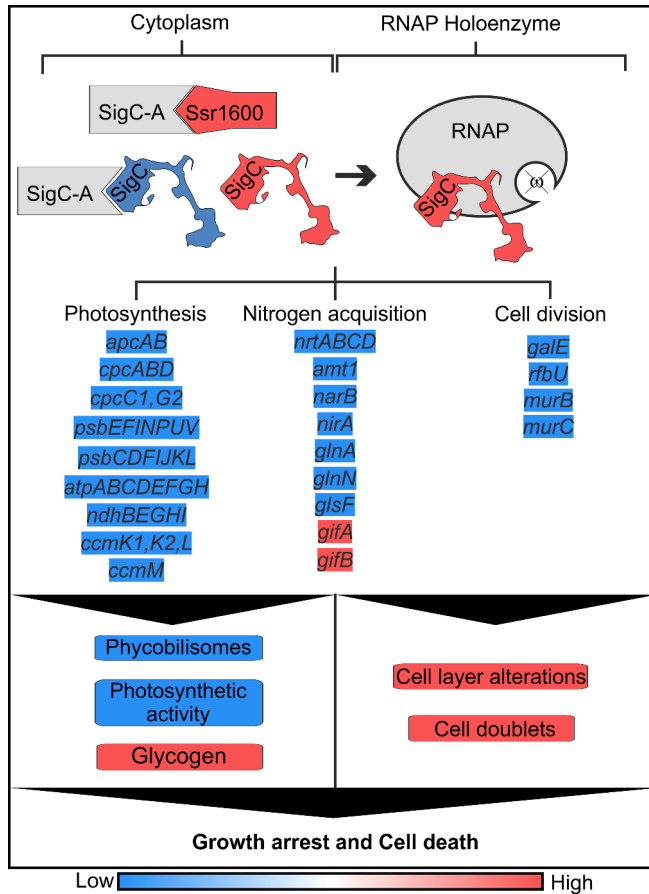


**Figure 7.** Regulation of gene expression by the Ssr1600 mediated signalling cascade in  $\Delta\rho Z$  cells in high  $\text{CO}_2$ . Abundant of anti-SigC antagonist (Ssr1600) forms a complex with an as yet unidentified anti-SigC (SigC-A) protein, releasing free SigC factor, and high amounts of the RNAP-SigC holoenzyme is formed. Elevated RNAP-SigC holoenzyme levels cause downregulation of many nitrogen acquisition, cell division and photosynthesis genes in  $\Delta\rho Z$ , leading to reduced photosynthetic activity, accumulation of cell doublets, glycogen accumulation, growth arrest and finally cell death. Blue/red indicate lower/higher amount of protein or transcript or process activity in  $\Delta\rho Z$  compared to CS, respectively.

## 5.2 Mutations in the anti-SigC antagonist Ssr1600 rescue $\Delta\rho Z$ in high $\text{CO}_2$

High  $\text{CO}_2$  and high temperature tolerant suppressor mutants of the  $\Delta\rho Z$  strain appeared regularly in standard growth conditions. Both suppressor mutant lines contain a single mutation in the *ssr1600* gene, and the point mutations L24S and G43V in  $\Delta\rho Z$ -S1 and  $\Delta\rho Z$ -S2, respectively, reduce the amount of Ssr1600 protein drastically (Paper IV). Figure 8 presents a hypothesis on how mutations in the Ssr1600 protein rescue the high  $\text{CO}_2$  sensitive phenotype of  $\Delta\rho Z$ . As the

amount of the anti-SigC antagonist Ssr1600 is low in suppressor lines, the formation of the anti-SigC/SigC complex is efficient and the amount of free SigC that can be recruited by the RNAP core remains low in high CO<sub>2</sub>, and thus only a low amount of the RNAP-SigC holoenzyme is formed (Fig. 8). According to transcriptomic data, this enables CS-like regulation of photosynthetic, nitrogen acquisition and cell division related genes, which allows fast growth of the suppressor lines in high CO<sub>2</sub> (Fig. 8, Paper IV). In addition to the suggested regulation mechanism, the phosphorylation of Ssr1600 probably plays a role.

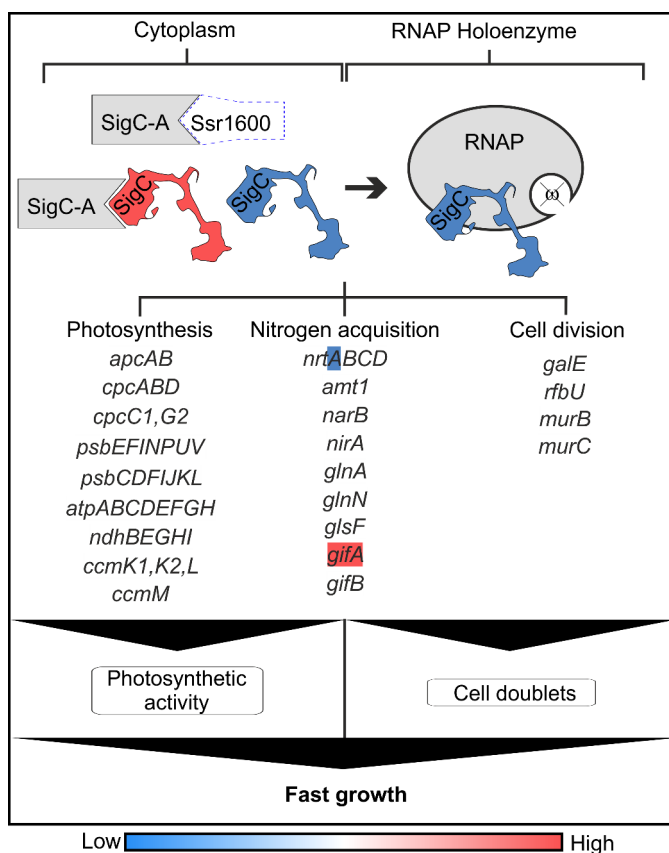


**Figure 8.** Regulation of gene expression by the Ssr1600 mediated signalling cascade in  $\Delta rpoZ$ -S1 cells in high CO<sub>2</sub>.  $\Delta rpoZ$ -S1 cells contains only traces of anti-SigC antagonist (Ssr1600) and because of that, the majority of the SigC protein forms a complex with an as yet unidentified anti-SigC protein. Thus, only a low amount of RNAP-SigC holoenzyme is formed, and the expression of nitrogen acquisition, cell division and photosynthesis genes are comparable to that of CS in high CO<sub>2</sub> allowing normal acclimation of  $\Delta rpoZ$ -S1 cells to high CO<sub>2</sub>. Blue/red indicate lower/higher amount of protein or transcript or process activity in  $\Delta rpoZ$ -S1 compared to CS, respectively.

Attempts to solve other key players in the Ssr1600 mediated regulatory pathway are currently in progress. The Ssr1600 is a homolog of anti- $\sigma^F$  antagonist SpoIIAA of *Bacillus subtilis*. In *B. subtilis* SpoIIAA functions along with an anti- $\sigma$  factor SpoIIAB, phosphatase SpoIIIE and the  $\sigma^F$ -factor in a regulatory pathway that activates sporulation specific genes (Duncan and Losick 1993; Min et al. 1993; Diederich et al. 1994; Arigoni et al. 1996). This pathway works in the forespore that is divided to two daughter cells in unequal cell division. The accumulation of SpoIIIE in the forespore activates the inactive phosphorylated SpoIIAA by dephosphorylation (Duncan et al. 1995; Bradshaw and Losick 2015). The non-phosphorylated SpoIIAA forms a complex with SpoIIAB, releasing  $\sigma^F$  from the SpoIIAB/ $\sigma^F$  complex (Diederich et al. 1994). This is followed by the recruitment of the free  $\sigma^F$  to the RNAP core, which initiates the expression of genes needed for unequal cell division. In standard growth conditions, SpoIIAB phosphorylates SpoIIAA, which keeps  $\sigma^F$  bound to SpoIIAB and silences cell division related genes (Bradshaw and Losick 2015).

The SpoIIIE homolog in *Synechocystis* is the IcfG protein that has been suggested to be a carbon metabolism regulator (Beuf et al. 1994; Shi et al. 1999). Moreover, the *icfG* gene is located in a gene cluster that contains two homologs of anti- $\sigma$  factor antagonists (*slr1859* and *slr1856*) and an anti- $\sigma$  factor (*slr1861*). According to Shi et al., IcfG dephosphorylates Slr1856, but not Slr1859 *in vitro* (Shi et al. 1999). The putative anti- $\sigma$ -factor Slr1861 is a Ser kinase like SpoIIAB, and it phosphorylates efficiently Slr1856 (Shi et al. 1999; Gonzalez et al. 2001) but Slr1859 only poorly (Shi et al. 1999). Some factors in the IcfG gene cluster might also play roles in the Ssr1600 mediated regulatory pathway, and this would be the target of further studies. In addition to the putative anti- $\sigma$  factor Slr1861, a blast search for SpoIIAB homologous proteins resulted in numerous possible candidates including Slr6001, Sll1457, Slr1212/PixA/UirS, Sll0798/RppB, Sll1945/Dxs, Slr0210, Slr0222/Hik29, Slr2098, Slr1167/GldA, Slr1289/Icd, Sll1563 and Slr2102/FtsY in *Synechocystis* making it difficult to resolve the identity of anti-SigC with bioinformatics.

The Ssr1600 is the first anti- $\sigma$ -factor antagonist found from cyanobacteria. Two anti- $\sigma$ -factors have been previously found from cyanobacteria, the SigE anti- $\sigma$ -factor ChlH (Osanai et al. 2009) and the SigG anti- $\sigma$ -factor SapG (Bell et al. 2017). In *Synechocystis* ChlH is the H subunit of Mg-chelatase that functions in chlorophyll biosynthesis and also as an anti- $\sigma$ -factor for SigE. In the proposed mechanism, darkness causes a decrease in  $Mg^{2+}$  concentration and detachment of ChlH from SigE. Free SigE can be recruited by the RNAP core, and the RNAP-SigE holoenzyme then activates sugar catabolic genes (Osanai et al. 2005c, 2007, 2009). The  $\Delta$ poZ contains less SigE protein in high  $CO_2$  than CS, and that might be related to lower chlorophyll amount observed in  $\Delta$ poZ in high  $CO_2$  (Papers III and IV). The SigG-SapG interaction in *Nostoc punctiforme* is related to the damage of cell

envelope (Bell et al. 2017). The SapG protein is a typical anti- $\sigma$ -factor, belonging to the category of extra cytoplasmic function anti- $\sigma$ -factor, whereas ChlH is not a typical anti- $\sigma$ -factor due to its dual function. Anti- $\sigma$ -factor mediated signal transduction systems have been studied in heterotrophic bacteria. The Rsb system contains an anti- $\sigma$ -factor RsbW and an anti- $\sigma$ -factor antagonist RsbV, which regulates the availability of a common stress response factor  $\sigma^B$  in *B. subtilis* (Hecker et al. 2007). Two possible phosphatases are also required to activate RsbV (Hecker et al. 2007). In addition, the Rsd protein was found to be an anti- $\sigma$ -factor of  $\sigma^{70}$  in *E. coli* (Jishage and Ishihama 1998; Mitchell et al. 2007). Later it was shown that the HPr protein works as an antagonist for Rsd (Park et al. 2013, 2015).

### 5.3 A novel signaling cascade of high CO<sub>2</sub> acclimation in *Synechocystis*

Acclimation of *Synechocystis* to high CO<sub>2</sub> is an active, regulated process. At the transcriptional level, CCMs are downregulated but nitrogen and phosphorus acquisition, light harvesting and photosynthetic light reactions are upregulated, which leads to more efficient light harvesting and enhancement of light reactions to provide NADPH and ATP to highly efficient carbon fixation in high CO<sub>2</sub> (Papers III and IV). As production of carbon skeletons increases, transcripts of uptake machineries of nitrogen and phosphorus are upregulated (Paper IV). Obviously, production of carbon skeletons exceeds consumption by growth as carbon is stored as glycogen (Paper III). Photoprotective mechanisms are less abundant in high CO<sub>2</sub> than in ambient air, probably because of the increased electron flux to the CBB cycle (Paper III).

The results of this Thesis show that the anti-SigC antagonist Ssr1600 and SigC are part of a novel signalling pathway that connects carbon signalling and growth rate directly to the function of RNAP. Interestingly, the  $\omega$  subunit of RNAP is a phosphoprotein (Angeleri et al. 2016), but whether or not phosphorylation of the  $\omega$  subunit of RNAP plays a role in the anti-SigC antagonist (Ssr1600) and SigC mediated pathway remains to be solved.

Figure 9 presents the suggested function and targets of a novel signalling cascade. In ambient air, the anti-SigC antagonist Ssr1600 is abundant and forms a complex with an as yet unidentified anti-SigC factor, releasing moderate amounts of free SigC. A moderate amount of RNAP-SigC holoenzyme is formed, which allows normal growth. In high CO<sub>2</sub>, the amount of the anti-SigC antagonist Ssr1600 decreases releasing the anti-SigC factor that forms a complex with the SigC protein and only a low amount of the growth arresting RNAP-SigC holoenzyme is formed. It remains to be solved what is the signal that is recognized by this novel signalling pathway.

Several metabolites relay information about the energy status and C/N balance to signalling factors that control the required acclimation responses. Cyclic AMP is a signal of carbon sufficient conditions, whereas in carbon deprivation the amount of AMP increases (Selim et al. 2018). The C/N balance is sensed by two central metabolites 2-OG and 2-PG. A high amount of 2-OG functions as a signal of increased C:N (Carrieri et al. 2015) ratio and a high amount of 2-PG is a signal of a low C:N ratio (Hackenberg et al. 2012). The PII-like signalling protein SbtB controls membrane binding of the SbtA protein in a Ci dependent manner, maybe by sensing the ratio of cAMP/AMP (Selim et al. 2018). The cAMP levels were not studied in this Thesis, but interestingly, a previous study shows that cAMP levels are low in a  $\Delta$ sigC mutant in ambient air when compared to CS (Gunnelius et al. 2010). This indicates that  $\Delta$ sigC might suffer from Ci deprivation in ambient air, which also suggests that SigC might play a role in carbon signalling.

The previously known carbon signalling factors like NdhR, CmpR and SbtB were strongly downregulated at transcriptional level in CS after 1 h treatment in high CO<sub>2</sub> (Paper IV). The strong downregulation of the negative regulator *ndhR* did not lead to upregulation of NDH-1<sub>3</sub> encoding genes, *sbtAB*, *mnh* or *bicA* (Paper IV). However, the activity of NdhR is regulated by the ratio of 2-OG to 2-PG (Jiang et al. 2018). The 2-OG level might increase temporarily, as the upregulation of nitrogen uptake might be slower than the transportation of Ci into cells upon shifting from ambient air to high CO<sub>2</sub>. This means that NdhR is likely to bind 2-OG and in this form it binds strongly to two tandem consensus motifs ATAG-N<sub>8</sub>-CTAT around -10 sites (Klähn et al. 2015) blocking the RNAP binding site. Hence even if *ndhR* is downregulated in high CO<sub>2</sub>, at the protein level NdhR might still repress NdhR-dependent genes. Downregulation of transcripts of the CmpR activator was followed by downregulation of *cmpABCD* genes when cells were shifted from ambient air to high CO<sub>2</sub> (Paper IV). In *Synechocystis*, the mechanism of CmpR regulation still remains to be studied, but in *Synechococcus elongatus*, CmpR might sense the amount of 2-PG (Nishimura et al. 2008).

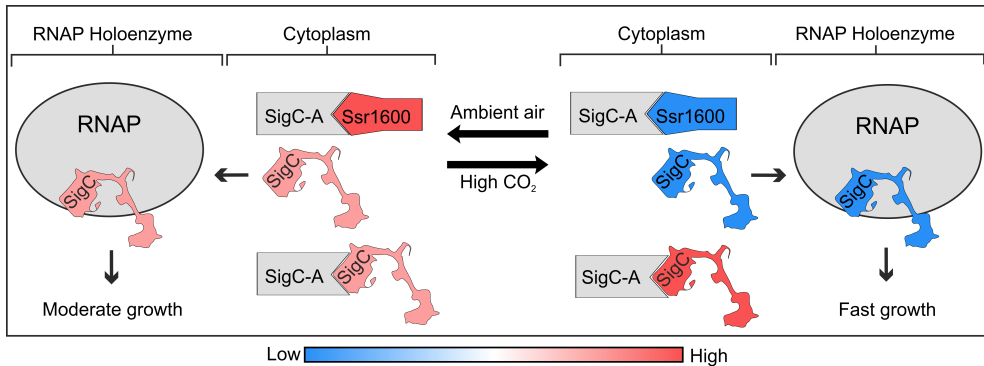


**Figure 9.** Signalling pathway controlling the growth rate according to available Ci. In ambient air, the moderate amount of an anti-SigC antagonist (Ssr1600) interacts with an as yet unidentified anti-SigC protein and the rest of the anti-SigC protein forms complexes with SigC, thereby reducing the amount of free SigC to a moderate level. A moderate amount of RNAP-SigC holoenzyme is formed, which allows balanced gene expression and moderate growth. In high CO<sub>2</sub>, the low amount of the anti-SigC antagonist (Ssr1600) facilitates the formation of the anti-SigC/SigC complex, which leads to formation of the low amount of the stationary phase specific RNAP-SigC holoenzyme, thus enabling fast growth. The intensities of blue and red indicate the amount of protein.

## 6 Conclusions and future perspectives

This PhD work was set to solve the role of the enigmatic  $\omega$ -subunit of the cyanobacterial RNAP. The results show that the  $\omega$  subunit is non-essential in *Synechocystis* in standard growth conditions in ambient air, but cell doublets are common in  $\Delta$ rpoZ, light saturated photosynthetic activity is low and some of the photoprotective mechanisms are upregulated.  $\Delta$ rpoZ cells contain a normal amount of RNA but part of the household genes including CCMs, Rubisco, ATP synthase, and nitrogen acquisition genes are downregulated, whereas transcription and translation machinery genes and photosynthetic light reaction genes are expressed normally. Thus, the  $\omega$  subunit affects the expression of a particular set of genes, not the overall transcription rate.

The  $\omega$  subunit is essential in moderately high temperatures in *Synechocystis*. The  $\omega$ -less RNAP is functional in heat stress, as  $\Delta$ rpoZ contains more rRNA than CS but the transcriptome of  $\Delta$ rpoZ was different from that of CS, which leads to the general conclusion that upon heat treatment  $\Delta$ rpoZ lacks proper adjustment of gene expression.

The  $\omega$  subunit is essential in high CO<sub>2</sub>. Four fold more of the stationary phase specific RNAP-SigC holoenzyme is formed in  $\Delta$ rpoZ than in CS in high CO<sub>2</sub>, and normal upregulation of genes coding for subunits of the light harvesting systems, photosynthetic light reactions, and nitrogen uptake and assimilation is missing in  $\Delta$ rpoZ in high CO<sub>2</sub>. Furthermore, a set of cell division genes shows low expression in  $\Delta$ rpoZ. These characteristics in  $\Delta$ rpoZ lead to low photosynthetic activity, accumulation of cell doublets, slow growth and finally to cell death in high CO<sub>2</sub>.

Suppressor mutations rescuing high CO<sub>2</sub> and heat acclimation of  $\Delta$ rpoZ cells appear regularly. Sequencing of suppressor lines revealed localization of mutations in the Ssr1600 protein. Due to mutations, the amount of Ssr1600 is drastically decreased, which leads to similar formation of the RNAP-SigC holoenzyme as in CS, disappearance of cell doublets and normal acclimation to high CO<sub>2</sub>. The Ssr1600 protein functions as an anti- $\sigma$  factor antagonist regulating the recruitment of the SigC factor by the RNAP core.

The results suggest that the anti-SigC factor antagonist (Ssr1600), and an as yet unidentified anti-SigC factor and SigC form a signaling cascade that controls the growth rate in *Synechocystis*. In ambient air, abundant anti-SigC antagonist forms a complex with the anti-SigC factor, releasing part of SigC from the SigC/anti-SigC complex, and a moderate amount of the RNAP-SigC holoenzyme is formed, which keeps the growth rate moderate. In high CO<sub>2</sub>, the amount of the anti-SigC antagonist decreases, anti-SigC binds to SigC and a low amount of the RNAP-SigC holoenzyme is formed, which leads to upregulation of transcription of photosynthesis, nitrogen and phosphate assimilation and cell division genes, and thus to an increase in the growth rate (Fig. 9, Paper IV).

The next step of the study will be the identification of the anti-SigC factor. As coimmunoprecipitation with the Ssr1600 antibody was not successful, coimmunoprecipitation will be performed with the SigC antibody, and precipitated proteins will be identified with mass spectrometry. Alternatively, a His-tagged SigC or His-tagged Ssr1600 could be overexpressed in *E. coli*, purified and attached to nickel columns, which can then be used to bind interacting proteins from isolated *Synechocystis* proteins. From eluted samples, interacting proteins will be recognized with mass spectrometry. A more direct method would be to test if the putative anti- $\sigma$  factor Slr1861 or some other of the SpoIIAB homologs interacts with Ssr1600 or SigC.

To complete the analysis of the anti-SigC factor antagonist, inactivation and overexpression strains of Ssr1600 with CS background will be constructed. It is already known that Ssr1600 is phosphorylated from two serine residues, and phosphomimetic and non-phosphorylatable strains would also provide crucial data to solve the mechanism of the novel signaling cascade. According to *B. subtilis* studies, a specific phosphatase and kinase for Ssr1600 are expected to exist. The IcfG is a promising candidate for Ssr1600 specific phosphatase, and to analyze it, Ssr1600 and IcfG are overexpressed in *E. coli* and purified for *in vitro* experiments. The IcfG gene cluster also has an interesting putative anti- $\sigma$  factor, the serine kinase *slr1861*. Slr1861 would be good candidate for protein interaction studies, as Ssr1600 is phosphorylated from serine residues. The  $\Delta$ sigC strain could be used in above mentioned experiments for additional data.

Cyanobacteria are under extensive research related to biotechnological applications, and many aspects are nowadays considered. (1) Carbon neutral production of valuable compounds in genetically engineered cyanobacteria. (2) Waster water treatment with cyanobacteria. (3) Production of sustainable energy like hydrogen by cyanobacteria. One approach would be to use the knowledge about the cyanobacterial transcription machinery and  $\sigma$  factors that control the acclimatory responses to create new expression systems usable in cyanobacteria. Considering findings in this Thesis, the growth rate could be controlled by engineering

cyanobacterial strains overexpressing Ssr1600. According to the hypothesis presented in this Thesis, Ssr1600-overexpression should slow down growth even in high CO<sub>2</sub>.

# Acknowledgements

This Thesis was completed in the laboratories of Molecular Plant Biology unit of the Department of Biochemistry in the faculty of Science and Engineering. I want to thank University of Turku Graduate School and Finnish Cultural Foundation for the financial support.

I would like to express my most sincere gratitude to my supervisor Dr. Taina Tyystjärvi. Your passion in science has always been important source of motivation for me. All the invaluable comments to manuscripts, presentations, abstracts and posters have been essential for me to get here. I have also enjoyed for our numerous discussion about science and life in general and for those and all the things you have taught to me, I will be always grateful. A long journey from summer employee to PhD is now finished and you made it possible. Thank you!

I want to acknowledge Prof. Eevi Rintamäki for all the guidance with administrative things. Assoc. Prof. Takashi Osanai and Dr. Franck Chauvat are thanked for reviewing and improving the content of this Thesis. I would also like to thank Prof. Karl Forchhammer for accepting the invitation to be my opponent during my doctoral disputation. Advices and suggestions given by my advisory committee members Dr. Georgi Belogurov and Assoc. Prof. Yagut Allahverdiyeva-Rinne have been a great help in my PhD studies and for these I thank you.

All co-authors and especially former group members are thankfully acknowledged for their valuable roles in publications. Dr. Liisa Gunnelius is thanked for starting the  $\omega$  subunit research in cyanobacteria, Dr. Kaisa Hakkila is warmly thanked for all the help and support in designing and performing experiments and Satu Koskinen is thanked for teaching and helping me with bioinformatics.

I'm also very grateful for the assistance of Dr. Esa Tyystjärvi. Thank you for offering your criticism in joint publications and when rehearsing important presentations. Your advices have been very helpful and thoughtful for me. Furthermore your singing and poetry moments in the coffee room have also been entertaining to witness.

“Help will always be given in our unit, to those who ask for it.” I would like to offer my thanks to technical staff (past and present) Anniina, Mika, Kurt, Tapio and Eve for taking good care of our labs and lab equipments. In addition big thanks to

Jouko Sandholm from Cell Imaging Core of Turku Bioscience for assisting me with flow cytometry and cell imaging.

I would like to express my very great appreciation to past and present colleagues in Molecular Plant Biology unit: Heta, Janne, Olli, Pooneh, Dimitar, Hari, Lauri N, Daniel, Julia, Martina A, Martina J, Tuomas, Matleena, Pekka, Moona, Duncan, Pasi, Andrea, Jesus, Steffen, Sara, Sanna, Marjaana, Guido, Aiste, Anita, Azfar, Lauri K. With you I have either shared hundreds of coffee moments, or had too many chicken piffis for lunch or too few “afterworks”. Thank you also for your help in the lab, all the laughs in planning karonkka programs and thanks for sharing all the tears and suffering during shitty movie nights.

Special thanks goes to Vesa Havurinne who has been a close friend since the beginning of our university studies. There has always been a friendly competition between us that has definitely had a positive impact to my studies. Somehow we have ended working in the same unit, same office and almost in the same group. In addition to work we have had good time, singing karaoke and partying wherever we have ended up. Thank you for your friendship and all the best for you!

Many thanks to my friends Teemu, Emppu, Jaakko, Miika, Henkka Irene and Selina for listening my monologues about cyanobacteria and for showing also genuine interest in my work. Sorry that I still don't know all the Latin names for each organism 😊

I want to express my gratitude to my family for encouraging me throughout my study. Kiitos, olette tärkeitä minulle.

Finally I wish to thank Meri for sharing this time with me. You are important person in my life. My heartfelt thanks.

September 2020

A handwritten signature in black ink, appearing to read 'Juha Kurkela', with a long, sweeping horizontal line extending to the right.

# List of References

- Allahverdiyeva, Y., Ermakova, M., Eisenhut, M., Zhang, P., Richaud, P., Hagemann, M., Cournac, L., and Aro, E.-M. (2011). Interplay between Flavodiiron Proteins and Photorespiration in *Synechocystis* sp. PCC 6803. *J. Biol. Chem.* *286*, 24007–24014.
- An, G., Justesen, J., Watson, R.J., and Friesen, J.D. (1979). Cloning the *spoT* Gene of *Escherichia coli*: Identification of the *spoT* Gene Product. *J. Bacteriol.* *137*, 1100–1110.
- Anderson, S.L., and McIntosh, L. (1991). Light-Activated Heterotrophic Growth of the Cyanobacterium *Synechocystis* sp. Strain PCC 6803: a Blue-Light-Requiring Process. *J. Bacteriol.* *173*, 2761–2767.
- Angeleri, M., Muth-Pawlak, D., Aro, E.-M., and Battchikova, N. (2016). Study of O-Phosphorylation Sites in Proteins Involved in Photosynthesis-Related Processes in *Synechocystis* sp. Strain PCC 6803: Application of the SRM Approach. *J. Proteome Res.* *15*, 4638–4652.
- Antal, T., Kurkela, J., Parikainen, M., Kårlund, A., Hakkila, K., Tyystjärvi, E., and Tyystjärvi, T. (2016). Roles of Group 2 Sigma Factors in Acclimation of the Cyanobacterium *Synechocystis* sp. PCC 6803 to Nitrogen Deficiency. *Plant Cell Physiol.* *57*, 1309–1318.
- Arigoni, F., Duncan, L., Alper, S., Losick, R., and Stragier, P. (1996). SpoIIE governs the phosphorylation state of a protein regulating transcription factor  $\sigma^F$  during sporulation in *Bacillus subtilis*. *Proc. Natl. Acad. Sci. U. S. A.* *93*, 3238–3242.
- Asayama, M., and Imamura, S. (2008). Stringent promoter recognition and autoregulation by the group 3  $\sigma$ -factor SigF in the cyanobacterium *Synechocystis* sp strain PCC 6803. *Nucleic Acids Res.* *36*, 5297–5305.
- Asayama, M., Imamura, S., Yoshihara, S., Miyazaki, A., Yoshida, N., Sazuka, T., Kaneko, T., Ohara, O., Tabata, S., Osanai, T., et al. (2004). SigC, the Group 2 Sigma Factor of RNA Polymerase, Contributes to the Late-stage Gene Expression and Nitrogen Promoter Recognition in the Cyanobacterium *Synechocystis* sp. Strain PCC 6803. *Biosci. Biotechnol. Biochem.* *68*, 477–487.
- Azuma, M., Osanai, T., Hirai, M.Y., and Tanaka, K. (2011). A Response Regulator Rre37 and an RNA Polymerase Sigma Factor SigE Represent Two Parallel Pathways to Activate Sugar Catabolism in a Cyanobacterium *Synechocystis* sp. PCC 6803. *Plant Cell Physiol.* *52*, 404–412.
- Ball, S.G., and Morell, M.K. (2003). From Bacterial Glycogen To Starch: Understanding the Biogenesis of the Plant Starch Granule. *Annu. Rev. Plant Biol.* *54*, 207–233.
- Battchikova, N., Eisenhut, M., and Aro, E.-M. (2011). Cyanobacterial NDH-1 complexes: Novel insights and remaining puzzles. *Biochim. Biophys. Acta-Bioenergetics* *1807*, 935–944.
- Battistuzzi, F.U., Feijao, A., and Hedges, S.B. (2004). A genomic timescale of prokaryote evolution: Insights into the origin of methanogenesis, phototrophy, and the colonization of land. *BMC Evol. Biol.* *4*, 1–14.
- Bell, N., Lee, J.J., and Summers, M.L. (2017). Characterization and *in vivo* regulon determination of an ECF sigma factor and its cognate anti-sigma factor in *Nostoc punctiforme*. *Mol. Microbiol.* *104*, 179–194.
- Belogurov, G.A., and Artsimovitch, I. (2019). The Mechanisms of Substrate Selection, Catalysis, and Translocation by the Elongating RNA Polymerase. *J. Mol. Biol.* *431*, 3975–4006.

- Berner, R.A. (2003). The long-term carbon cycle, fossil fuels and atmospheric composition. *Nature* 426, 323–326.
- Berry, S., Schneider, D., Vermaas, W.F.J., and Rögner, M. (2002). Electron Transport Routes in Whole Cells of *Synechocystis* sp. Strain PCC 6803: The Role of the Cytochrome *bd*-Type Oxidase. *Biochemistry* 41, 3422–3429.
- Bersanini, L., Battchikova, N., Jokel, M., Rehman, A., Vass, I., Allahverdiyeva, Y., and Aro, E.-M. (2014). Flavodiiron Protein Flv2/Flv4-Related Photoprotective Mechanism Dissipates Excitation Pressure of PSII in Cooperation with Phycobilisomes in Cyanobacteria. *Plant Physiol.* 164, 805–818.
- Beuf, L., Bédu, S., Durand, M.C., and Joset, F. (1994). A protein involved in co-ordinated regulation of inorganic carbon and glucose metabolism in the facultative photoautotrophic cyanobacterium *Synechocystis* PCC6803. *Plant Mol. Biol.* 25, 855–864.
- Bhardwaj, N., Syal, K., and Chatterji, D. (2018). The role of  $\omega$ -subunit of *Escherichia coli* RNA polymerase in stress response. *Genes to Cells* 23, 357–369.
- Bhaya, D., Watanabe, N., Ogawa, T., and Grossman, A.R. (1999). The role of an alternative sigma factor in motility and pilus formation in the cyanobacterium *Synechocystis* sp. strain PCC6803. *Proc. Natl. Acad. Sci. U. S. A.* 96, 3188–3193.
- Bhowmik, D., Bhardwaj, N., and Chatterji, D. (2017). Influence of Flexible “ $\omega$ ” on the Activity of *E. coli* RNA Polymerase: A Thermodynamic Analysis. *Biophys. J.* 112, 901–910.
- den Blaauwen, T., Hamoen, L.W., and Levin, P.A. (2017). The divisome at 25: the road ahead. *Curr. Opin. Microbiol.* 36, 85–94.
- Bolay, P., Muro-Pastor, M.I., Florencio, F.J., and Klähn, S. (2018). The distinctive regulation of cyanobacterial glutamine synthetase. *Life* 8.
- Booth, S., and Lewis, R.J. (2019). Structural basis for the coordination of cell division with the synthesis of the bacterial cell envelope. *Protein Sci.* 28, 2042–2054.
- Borukhov, S., Sagitov, V., and Goldfarb, A. (1993). Transcript cleavage factors from *E. coli*. *Cell* 72, 459–466.
- Bouillet, S., Arabet, D., Jourlin-Castelli, C., Méjean, V., and Iobbi-Nivol, C. (2018). Regulation of  $\sigma$  factors by conserved partner switches controlled by divergent signalling systems. *Environ. Microbiol. Rep.* 10, 127–139.
- Boulay, C., Wilson, A., D’Haene, S., and Kirilovsky, D. (2010). Identification of a protein required for recovery of full antenna capacity in OCP-related photoprotective mechanism in cyanobacteria. *Proc. Natl. Acad. Sci. U. S. A.* 107, 11620–11625.
- Bradshaw, N., and Losick, R. (2015). Asymmetric division triggers cell-specific gene expression through coupled capture and stabilization of a phosphatase. *Elife* 4, 1–18.
- Brocks, J.J., Logan, G.A., Buick, R., and Summons, R.E. (1999). Archean molecular fossils and the early rise of eukaryotes. *Science* (80- ). 285, 1033–1036.
- Bryant, D.A. (2003). The beauty in small things revealed. *Proc. Natl. Acad. Sci. U. S. A.* 100, 9647–9649.
- Burillo, S., Luque, I., Fuentes, I., and Contreras, A. (2004). Interactions between the nitrogen signal transduction protein PII and N-acetyl glutamate kinase in organisms that perform oxygenic photosynthesis. *J. Bacteriol.* 186, 3346–3354.
- Burnap, R.L., Nambudiri, R., and Holland, S. (2013). Regulation of the carbon-concentrating mechanism in the cyanobacterium *Synechocystis* sp. PCC6803 in response to changing light intensity and inorganic carbon availability. *Photosynth. Res.* 118, 115–124.
- Cai, F., Menon, B.B., Cannon, G.C., Curry, K.J., Shively, J.M., and Heinhorst, S. (2009). The Pentameric Vertex Proteins Are Necessary for the Icosahedral Carboxysome Shell to Function as a CO<sub>2</sub> Leakage Barrier. *PLoS One* 4, e7521.
- Cameron, J.C., and Pakrasi, H.B. (2010). Essential Role of Glutathione in Acclimation to Environmental and Redox Perturbations in the Cyanobacterium *Synechocystis* sp. PCC 6803. *Plant Physiol* 154, 1672–1685.

- Cameron, J.C., and Pakrasi, H.B. (2011a). Glutathione facilitates antibiotic resistance and photosystem I stability during exposure to gentamicin in cyanobacteria. *Appl. Environ. Microbiol.* *77*, 3547–3550.
- Cameron, J.C., and Pakrasi, H.B. (2011b). Glutathione in *Synechocystis* 6803. *Plant Signal. Behav.* *6*, 89–92.
- Carrieri, D., Broadbent, C., Carruth, D., Paddock, T., Ungerer, J., Maness, P.C., Ghirardi, M., and Yu, J. (2015). Enhancing photo-catalytic production of organic acids in the cyanobacterium *Synechocystis* sp. PCC 6803  $\Delta$ glgC, a strain incapable of glycogen storage. *Microb. Biotechnol.* *8*.
- Caslake, L.F., Gruber, T.M., and Bryant, D.A. (1997). Expression of two alternative sigma factors of *Synechococcus* sp. strain PCC 7002 is modulated by carbon and nitrogen stress. *Microbiology* *143*, 3807–3818.
- Cavalier-Smith, T. (2006). Cell evolution and Earth history: stasis and revolution. *Philos. Trans. R. Soc. B-Biological Sci.* *361*, 969–1006.
- Chitnis, V.P., and Chitnis, P.R. (1993). PsaL subunit is required for the formation of photosystem I trimers in the cyanobacterium *Synechocystis* Sp. PCC 6803. *FEBS Lett.* *336*, 330–334.
- Chitnis, V.P., Xu, Q., Yu, L., Golbeck, J.H., Nakamoto, H., Xie, D.L., and Chitnis, P.R. (1993). Targeted Inactivation of the Gene *psaL* Encoding a Subunit of Photosystem I of the Cyanobacterium *Synechocystis* sp. PCC 6803. *J. Biol. Chem.* *268*, 11678–11684.
- D’Heygere, F., Rabhi, M., and Boudvillain, M. (2013). Phyletic distribution and conservation of the bacterial transcription termination factor Rho. *Microbiology-Sgm* *159*, 1423–1436.
- Daley, S.M.E., Kappell, A.D., Carrick, M.J., and Burnap, R.L. (2012). Regulation of the Cyanobacterial CO<sub>2</sub>-Concentrating Mechanism Involves Internal Sensing of NADP<sup>+</sup> and  $\alpha$ -Ketoglutarate Levels by Transcription Factor CcmR. *PLoS One* *7*, e41286.
- Diederich, B., Wilkinson, J.F., Magnin, T., Najafi, S.M.A., Errington, J., and Yudkin, M.D. (1994). Role of Interactions between SpoIIAA and SpoIIAB in Regulating Cell-Specific Transcription Factor  $\sigma^F$  of *Bacillus Subtilis*. *Genes Dev.* *8*, 2653–2663.
- Dou, Z., Heinhorst, S., Williams, E.B., Murin, C.D., Shively, J.M., and Cannon, G.C. (2008). CO<sub>2</sub> fixation kinetics of *Halothiobacillus neapolitanus* mutant carboxysomes lacking carbonic anhydrase suggest the shell acts as a diffusional barrier for CO<sub>2</sub>. *J. Biol. Chem.* *283*, 10377–10384.
- Duncan, L., and Losick, R. (1993). SpoIIAB is an anti- $\sigma$  factor that binds to and inhibits transcription by regulatory protein  $\sigma^F$  from *Bacillus subtilis*. *Proc. Natl. Acad. Sci. U. S. A.* *90*, 2325–2329.
- Duncan, L., Alper, S., Arigoni, F., Losick, R., and Stragier, P. (1995). Activation of cell-specific transcription by a serine phosphatase at the site of asymmetric division. *Science* (80-. ). *270*, 641–644.
- Eisenhut, M., Kahlon, S., Hasse, D., Ewald, R., Lieman-Hurwitz, J., Ogawa, T., Ruth, W., Bauwe, H., Kaplan, A., and Hagemann, M. (2006). The plant-like C2 glycolate cycle and the bacterial-like glycerate pathway cooperate in phosphoglycolate metabolism in cyanobacteria. *Plant Physiol.* *142*, 333–342.
- Eisenhut, M., Aguirre von Wobeser, E., Jonas, L., Schubert, H., Ibelings, B.W., Bauwe, H., Matthijs, H.C.P.P., Hagemann, M., Von Wobeser, E.A., Jonas, L., et al. (2007). Long-term response toward inorganic carbon limitation in wild type and glycolate turnover mutants of the cyanobacterium *Synechocystis* sp. strain PCC 6803. *Plant Physiol.* *144*, 1946–1959.
- Eisenhut, M., Ruth, W., Haimovich, M., Bauwe, H., Kaplan, A., and Hagemann, M. (2008). The photorespiratory glycolate metabolism is essential for cyanobacteria and might have been conveyed endosymbiotically to plants. *Proc. Natl. Acad. Sci. U. S. A.* *105*, 17199–17204.
- Espinosa, J., Forchhammer, K., Burillo, S., and Contreras, A. (2006). Interaction network in cyanobacterial nitrogen regulation: PipX, a protein that interacts in a 2-oxoglutarate dependent manner with PII and NtcA. *Mol. Microbiol.* *61*, 457–469.
- Espinosa, J., Forchhammer, K., and Contreras, A. (2007). Role of the *Synechococcus* PCC 7942 nitrogen regulator protein PipX in NtcA-controlled processes. *Microbiology* *153*, 711–718.

- Espinosa, J., Labella, J.I., Cantos, R., and Contreras, A. (2018). Energy drives the dynamic localization of cyanobacterial nitrogen regulators during diurnal cycles. *Environ. Microbiol.* *20*, 1240–1252.
- Fan, J., Leroux-Coyau, M., Savery, N.J., and Strick, T.R. (2016). Reconstruction of bacterial transcription-coupled repair at single-molecule resolution. *Nature* *536*, 234–237.
- Fayet, O., Ziegelhoffer, T., Georgopoulos, C., Bukau, B., Donnelly, C.E., Walker, G.C., L Pardue, in M., Feramisco, J., and Lindquist, S. (1989). The groES and groEL Heat Shock Gene Products of *Escherichia coli* Are Essential for Bacterial Growth at All Temperatures Manipulations involving bacteriophage A derivatives. *J. Bacteriol.* *171*, 1379–1385.
- Field, B. (2018). Green magic: Regulation of the chloroplast stress response by (p)ppGpp in plants and algae. *J. Exp. Bot.* *69*, 2797–2807.
- Figge, R.M., Cassier-Chauvat, C., Chauvat, F., and Cerff, R. (2000). The carbon metabolism-controlled *Synechocystis* *gap2* gene harbours a conserved enhancer element and a Gram-positive-like -16 promoter box retained in some chloroplast genes. *Mol. Microbiol.* *36*, 44–54.
- Figge, R.M., Cassier-Chauvat, C., Chauvat, F., and Cerff, R. (2001). Characterization and analysis of an NAD(P)H dehydrogenase transcriptional regulator critical for the survival of cyanobacteria facing inorganic carbon starvation and osmotic stress. *Mol. Microbiol.* *39*, 455–468.
- Flores, C., Santos, M., Pereira, S.B., Mota, R., Rossi, F., De Philippis, R., Couto, N., Karunakaran, E., Wright, P.C., Oliveira, P., et al. (2018). The alternative sigma factor SigF is a key player in the control of secretion mechanisms in *Synechocystis* sp. PCC 6803. *Environ. Microbiol.* *21*, 343–359.
- Flores, E., Frías, J.E., Rubio, L.M., and Herrero, A. (2005). Photosynthetic nitrate assimilation in cyanobacteria. *Photosynth. Res.* *83*, 117–133.
- Forcada-Nadal, A., Forchhammer, K., and Rubio, V. (2014). SPR analysis of promoter binding of *Synechocystis* PCC6803 transcription factors NtcA and CRP suggests cross-talk and sheds light on regulation by effector molecules. *FEBS Lett.* *588*, 2270–2276.
- Forcada-Nadal, A., Llácer, J.L., Contreras, A., Marco-Marín, C., and Rubio, V. (2018). The P<sub>II</sub>-NAGK-PipX-NtcA regulatory axis of cyanobacteria: A tale of changing partners, allosteric effectors and non-covalent interactions. *Front. Mol. Biosci.* *5*, 91.
- Forchhammer, K., and Schwarz, R. (2019). Nitrogen chlorosis in unicellular cyanobacteria – a developmental program for surviving nitrogen deprivation. *Environ. Microbiol.* *21*, 1173–1184.
- Forchhammer, K., and Selim, K.A. (2019). Carbon/nitrogen homeostasis control in cyanobacteria. *FEMS Microbiol. Rev.* *44*, 33–53.
- Fujisawa, T., Narikawa, R., Maeda, S.I., Watanabe, S., Kanesaki, Y., Kobayashi, K., Nomata, J., Hanaoka, M., Watanabe, M., Ehira, S., et al. (2017). CyanoBase: A large-scale update on its 20th anniversary. *Nucleic Acids Res.* *45*, 551–554.
- García-Domínguez, M., Reyes, J.C., and Florencio, F.J. (2000). NtcA represses transcription of *gifA* and *gifB*, genes that encode inhibitors of glutamine synthetase type I from *Synechocystis* sp. PCC 6803. *Mol. Microbiol.* *35*, 1192–1201.
- Geertz, M., Travers, A., Mehandziska, S., Sobetzko, P., Janga, S.C., Shimamoto, N., and Muskhelishvili, G. (2011). Structural Coupling between RNA Polymerase Composition and DNA Supercoiling in Coordinating Transcription: a Global Role for the Omega Subunit? *MBio* *2*, e00034-11-e00034-11.
- Gentry, D.R., and Burgess, R.R. (1989). Rpoz, Encoding the Omega Subunit of *Escherichia coli* RNA Polymerase, is in the Same Operon as spot. *J. Bacteriol.* *171*, 1271–1277.
- Gentry, D.R., and Burgess, R.R. (1993). Cross-Linking of *Escherichia coli* RNA Polymerase Subunits: Identification of  $\beta'$  as the Binding Site of  $\omega$ . *Biochemistry* *32*, 11224–11227.
- Georg, J., Voß, B., Scholz, I., Mitschke, J., Wilde, A., and Hess, W.R. (2009). Evidence for a major role of antisense RNAs in cyanobacterial gene regulation. *Mol. Syst. Biol.* *5*, 305.
- Gerhardt, E.C.M., Rodrigues, T.E., Müller-Santos, M., Pedrosa, F.O., Souza, E.M., Forchhammer, K., and Huergo, L.F. (2015). The Bacterial signal transduction protein GlnB regulates the committed

- step in fatty acid biosynthesis by acting as a dissociable regulatory subunit of acetyl-CoA carboxylase. *Mol. Microbiol.* *95*, 1025–1035.
- Ghosh, P., Ishihama, A., and Chatterji, D. (2001). *Escherichia coli* RNA polymerase subunit  $\omega$  and its N-terminal domain bind full-length  $\beta'$  to facilitate incorporation into the  $\alpha_2\beta$  subassembly. *Eur. J. Biochem.* *268*, 4621–4627.
- Giner-Lamia, J., Robles-Rengel, R., Hernández-Prieto, M.A., Isabel Muro-Pastor, M., Florencio, F.J., Futschik, M.E., Muro-Pastor, M.I., Florencio, F.J., and Futschik, M.E. (2017). Identification of the direct regulon of NtcA during early acclimation to nitrogen starvation in the cyanobacterium *Synechocystis* sp. PCC 6803. *Nucleic Acids Res.* *45*, 11800–11820.
- Gonzalez, L., Basso, O., Bedu, S., and Zhang, C.C. (2001). Characterization of the icfG Gene Cluster Implicated in the Regulation of Carbon Metabolism in the Cyanobacterium *Synechocystis* Sp. PCC 6803. *Algae Their Biotechnol. Potential* 251–261.
- Gruber, T.M., and Bryant, D.A. (1998). Characterization of the alternative  $\sigma$ -factors SigD and SigE in *Synechococcus* sp. strain PCC 7002. SigE is implicated in transcription of post-exponential-phase-specific genes. *Arch. Microbiol.* *169*, 211–219.
- Gruber, T.M., and Gross, C.A. (2003). Multiple Sigma Subunits and the Partitioning of Bacterial Transcription Space. *Annu. Rev. Microbiol.* *57*, 441–466.
- Guergova-Kuras, M., Boudreaux, B., Joliot, A., Joliot, P., and Redding, K. (2001). Evidence for two active branches for electron transfer in photosystem I. *Proc. Natl. Acad. Sci. U. S. A.* *98*, 4437–4442.
- Gunnelius, L., Tuominen, I., Rantamäki, S., Pollari, M., Ruotsalainen, V., Tyystjärvi, E., and Tyystjärvi, T. (2010). SigC sigma factor is involved in acclimation to low inorganic carbon at high temperature in *Synechocystis* sp. PCC 6803. *Microbiology* *156*, 220–229.
- Gwizdala, M., Berera, R., Kirilovsky, D., Van Grondelle, R., and Krüger, T.P.J. (2016). Controlling Light Harvesting with Light. *J. Am. Chem. Soc.* *138*, 11616–11622.
- Hackenberg, C., Huege, J., Engelhardt, A., Wittink, F., Laue, M., Matthijs, H.C.P., Kopka, J., Bauwe, H., and Hagemann, M. (2012). Low-carbon acclimation in carboxysome-less and photorespiratory mutants of the cyanobacterium *Synechocystis* sp. strain PCC 6803. *Microbiology* *158*, 398–413.
- Hakkila, K., Antal, T., Gunnelius, L., Kurkela, J., Matthijs, H.C.P., Tyystjärvi, E., and Tyystjärvi, T. (2013). Group 2 Sigma Factor Mutant  $\Delta$ sigCDE of the Cyanobacterium *Synechocystis* sp. PCC 6803 Reveals Functionality of Both Carotenoids and Flavodiiron Proteins in Photoprotection of Photosystem II. *Plant Cell Physiol.* *54*, 1780–1790.
- Hakkila, K., Antal, T., Rehman, A.U., Kurkela, J., Wada, H., Vass, I., Tyystjärvi, E., and Tyystjärvi, T. (2014). Oxidative stress and photoinhibition can be separated in the cyanobacterium *Synechocystis* sp. PCC 6803. *Biochim. Biophys. Acta - Bioenerg.* *1837*, 217–225.
- Hakkila, K., Valev, D., Antal, T., Tyystjärvi, E., and Tyystjärvi, T. (2019). Group 2 Sigma Factors are Central Regulators of Oxidative Stress Acclimation in Cyanobacteria. *Plant Cell Physiol.* *60*, 436–447.
- Hauf, W., Schmid, K., Gerhardt, E.C.M., Huergo, L.F., and Forchhammer, K. (2016). Interaction of the nitrogen regulatory protein GlnB (P<sub>II</sub>) with biotin carboxyl carrier protein (BCCP) controls acetyl-Coa levels in the cyanobacterium *Synechocystis* sp. PCC 6803. *Front. Microbiol.* *7*, 1700.
- Hecker, M., Pané-Farré, J., and Uwe, V. (2007). SigB-Dependent General Stress Response in *Bacillus subtilis* and Related Gram-Positive Bacteria. *Annu. Rev. Microbiol.* *61*, 215–236.
- Hedges, S.B., Blair, J.E., Venturi, M.L., and Shoe, J.L. (2004). A molecular timescale of eukaryote evolution and the rise of complex multicellular life. *BMC Evol. Biol.* *4*, 1–9.
- Heil, A., and Zillig, W. (1970). Reconstitution of bacterial DNA-dependent RNA-polymerase from isolated subunits as a tool for the elucidation of the role of the subunits in transcription. *FEBS Lett.* *11*, 165–168.
- Heilmann, B., Hakkila, K., Georg, J., Tyystjärvi, T., Hess, W.R., Axmann, I.M., and Dienst, D. (2017). 6S RNA plays a role in recovery from nitrogen depletion in *Synechocystis* sp PCC 6803. *Bmc Microbiol.* *17*, 229.

- Hein, S., Tran, H., and Steinbüchel, A. (1998). *Synechocystis* sp. PCC6803 possesses a two-component polyhydroxyalkanoic acid synthase similar to that of anoxygenic purple sulfur bacteria. *Arch. Microbiol.* *170*, 162–170.
- Helman, Y., Tchernov, D., Reinhold, L., Shibata, M., Ogawa, T., Schwarz, R., Ohad, I., and Kaplan, A. (2003). Genes encoding A-type flavoproteins are essential for photoreduction of O<sub>2</sub> in cyanobacteria. *Curr. Biol.* *13*, 230–235.
- Hodgskiss, M.S.W., Crockford, P.W., Peng, Y., Wing, B.A., and Horner, T.J. (2019). A productivity collapse to end Earth's Great Oxidation. *Proc. Natl. Acad. Sci. U. S. A.* *116*, 17207–17212.
- Hood, R.D., Higgins, S.A., Flamholz, A., Nichols, R.J., and Savage, D.F. (2016). The stringent response regulates adaptation to darkness in the cyanobacterium *Synechococcus elongatus*. *Proc. Natl. Acad. Sci. U. S. A.* *113*, E4867-76.
- Houot, L., Floutier, M., Marteyn, B., Michaut, M., Picciocchi, A., Legrain, P., Aude, J.C., Cassier-Chauvat, C., and Chauvat, F. (2007). Cadmium triggers an integrated reprogramming of the metabolism of *Synechocystis* PCC6803, under the control of the Slr1738 regulator. *BMC Genomics* *8*, 350.
- Howitt, C.A., and Vermaas, W.F.J. (1998). Quinol and cytochrome oxidases in the cyanobacterium *Synechocystis* sp. PCC 6803. *Biochemistry* *37*, 17944–17951.
- Howitt, C.A., Udall, P.K., and Vermaas, W.F.J. (1999). Type 2 NADH dehydrogenases in the cyanobacterium *Synechocystis* sp. Strain PCC 6803 are involved in regulation rather than respiration. *J. Bacteriol.* *181*, 3994–4003.
- Huckauf, J., Nomura, C., Forchhammer, K., and Hagemann, M. (2000). Stress responses of *Synechocystis* sp. strain PCC 6803 mutants impaired in genes encoding putative alternative sigma factors. *Microbiology* *146*, 2877–2889.
- Igarashi, K., Fujita, N., and Ishihama, A. (1989). Promoter selectivity of *Escherichia coli* RNA polymerase: omega factor is responsible for the ppGpp sensitivity. *Nucleic Acids Res.* *17*, 5461–5476.
- Imamura, S., and Asayama, M. (2009). Sigma Factors for Cyanobacterial Transcription. *Gene Regul. Syst. Bio.* *3*, GRSB.S2090.
- Imamura, S., Yoshihara, S., Nakano, S., Shiozaki, N., Yamada, A., Tanaka, K., Takahashi, H., Asayama, M., and Shirai, M. (2003a). Purification, characterization, and gene expression of all sigma factors of RNA polymerase in a cyanobacterium. *J. Mol. Biol.* *325*, 857–872.
- Imamura, S., Asayama, M., Takahashi, H., Tanaka, K., Takahashi, H., and Shirai, M. (2003b). Antagonistic dark/light-induced SigB/SigD, group 2 sigma factors, expression through redox potential and their roles in cyanobacteria. *FEBS Lett.* *554*, 357–362.
- Imashimizu, M., Tanaka, K., and Shimamoto, N. (2011). Comparative Study of Cyanobacterial and *E. coli* RNA Polymerases: Misincorporation, Abortive Transcription, and Dependence on Divalent Cations. *Genet. Res. Int.* *2011*, 1–11.
- Iyer, L.M., and Aravind, L. (2012). Insights from the architecture of the bacterial transcription apparatus. *J. Struct. Biol.* *179*, 299–319.
- Jiang, Y.-L., Wang, X.-P., Sun, H., Han, S.-J., Li, W.-F., Cui, N., Lin, G.-M., Zhang, J.-Y., Cheng, W., Cao, D.-D., et al. (2018). Coordinating carbon and nitrogen metabolic signaling through the cyanobacterial global repressor NdhR. *Proc. Natl. Acad. Sci.* *115*, 403–408.
- Jishage, M., and Ishihama, A. (1998). A stationary phase protein in *Escherichia coli* with binding activity to the major  $\sigma$  subunit of RNA polymerase. *Proc. Natl. Acad. Sci. U. S. A.* *95*, 4953–4958.
- Johnston, E.B., Lewis, P.J., and Griffith, R. (2009). The interaction of *Bacillus subtilis*  $\sigma^A$  with RNA polymerase. *Protein Sci.* *18*, 2287–2297.
- Kacar, B., Hanson-Smith, V., Adam, Z.R., and Boekelheide, N. (2017). Constraining the timing of the Great Oxidation Event within the Rubisco phylogenetic tree. *Geobiology* *15*, 628–640.
- Kaczmarzyk, D., Anfelt, J., Sarnegrim, A., and Hudson, E.P. (2014). Overexpression of sigma factor SigB improves temperature and butanol tolerance of *Synechocystis* sp. PCC6803. *J. Biotechnol.* *182*, 54–60.

- Kammerscheit, X., Chauvat, F., and Cassier-Chauvat, C. (2019). First in vivo evidence that glutathione-S-transferase operates in photo-oxidative stress in cyanobacteria. *Front. Microbiol.* *10*, 1899.
- Kaneko, T., Sato, S., Kotani, H., Tanaka, A., Asamizu, E., Nakamura, Y., Miyajima, N., Hirosawa, M., Sugiura, M., Sasamoto, S., et al. (1996). Sequence Analysis of the Genome of the Unicellular Cyanobacterium *Synechocystis* sp. Strain PCC6803. II. Sequence Determination of the Entire Genome and Assignment of Potential Protein-coding Regions. *DNA Res.* *3*, 109–136.
- Kaneko, T., Nakamura, Y., Sasamoto, S., Watanabe, A., Kohara, M., Matsumoto, M., Shimpo, S., Yamada, M., and Tabata, S. (2003). Structural analysis of four large Plasmids harboring in a unicellular cyanobacterium, *Synechocystis* sp. PCC 6803. *Dna Res.* *10*, 221–228.
- Kanesaki, Y., Suzuki, I., Allakhverdiev, S.I., Mikami, K., and Murata, N. (2002). Salt stress and hyperosmotic stress regulate the expression of different sets of genes in *Synechocystis* sp. PCC 6803. *Biochem. Biophys. Res. Commun.* *290*, 339–348.
- Kaplan, A. (2017). On the cradle of CCM research: discovery, development, and challenges ahead. *J. Exp. Bot.* *68*, 3785–3796.
- Kerfeld, C.A., and Melnicki, M.R. (2016). Assembly, function and evolution of cyanobacterial carboxysomes. *Curr. Opin. Plant Biol.* *31*, 66–75.
- Kettenberger, H., Armache, K.J., and Cramer, P. (2003). Architecture of the RNA polymerase II-TFIIS complex and implications for mRNA cleavage. *Cell* *114*, 347–357.
- Kim, J.E., Choi, J.S., Kim, J.S., Cho, Y.H., and Roe, J.H. (2020). Lysine acetylation of the housekeeping sigma factor enhances the activity of the RNA polymerase holoenzyme. *Nucleic Acids Res.* *48*, 2401–2411.
- Kizawa, A., and Osanai, T. (2020). Overexpression of the response regulator rpaA causes an impaired cell division in the Cyanobacterium *Synechocystis* sp. PCC 6803. *J. Gen. Appl. Microbiol.* *66*, 121–128.
- Klähn, S., Orf, I., Schwarz, D., Matthiessen, J.K.F., Kopka, J., Hess, W.R., and Hagemann, M. (2015). Integrated Transcriptomic and Metabolomic Characterization of the Low-Carbon Response Using an *ndhR* Mutant of *Synechocystis* sp. PCC 6803. *Plant Physiol.* *169*, 1540–1556.
- Klotz, A., Georg, J., Bučinská, L., Watanabe, S., Reimann, V., Januszewski, W., Sobotka, R., Jendrossek, D., Hess, W.R., and Forchhammer, K. (2016). Awakening of a Dormant Cyanobacterium from Nitrogen Chlorosis Reveals a Genetically Determined Program. *Curr. Biol.* *26*, 2862–2872.
- Koch, M., Berendzen, K.W., and Forchhammer, K. (2020). On the Role and Production of Polyhydroxybutyrate (PHB) in the Cyanobacterium *Synechocystis* sp. pcc 6803. *Life* *10*, 47.
- Kojima, I., Kasuga, K., Kobayashi, M., Fukasawa, A., Mizuno, S., Arisawa, A., and Akagawa, H. (2002). The *rpoZ* gene, encoding the RNA polymerase omega subunit, is required for antibiotic production and morphological differentiation in *Streptomyces kasugaensis*. *J. Bacteriol.* *184*, 6417–6423.
- Koksharova, O.A., and Wolk, C.P. (2002). A novel gene that bears a DnaJ motif influences cyanobacterial cell division. *J. Bacteriol.* *184*, 5524–5528.
- Kondo, K., Conrad, A.E., and Mullineaux, W. (2009). Distinct roles of CpcG1-phycobilisome and CpcG2-phycobilisome in state transitions in a cyanobacterium *Synechocystis* sp. PCC 6803. *Photosynth. Res.* *99*, 217–225.
- Kopf, M., Klähn, S., Scholz, I., Matthiessen, J.K.F., Hess, W.R., and Voß, B. (2014). Comparative Analysis of the Primary Transcriptome of *Synechocystis* sp. PCC 6803. *DNA Res.* *21*, 527–539.
- Kopp, R.E., Kirschvink, J.L., Hilburn, I.A., and Nash, C.Z. (2005). Paleoproterozoic snowball Earth: Extreme climatic and geochemical global change and its biological consequences. *PNAS* *97*, 1400–1405.
- Koskinen, S., Hakkila, K., Gunnelius, L., Kurkela, J., Wada, H., and Tyystjärvi, T. (2016). *In vivo* recruitment analysis and a mutant strain without any group 2  $\sigma$  factor reveal roles of different  $\sigma$  factors in cyanobacteria. *Mol. Microbiol.* *99*, 43–54.

- Koskinen, S., Hakkila, K., Kurkela, J., Tyystjärvi, E., and Tyystjärvi, T. (2018). Inactivation of group 2  $\sigma$  factors upregulates production of transcription and translation machineries in the cyanobacterium *Synechocystis* sp. PCC 6803. *Sci. Rep.* *8*, 10305.
- Kouba, T., Pospíšil, J., Hnilicová, J., Šanderová, H., Barvík, I., and Krásný, L. (2019). The core and holoenzyme forms of RNA polymerase from mycobacterium smegmatis. *J. Bacteriol.* *201*, e00583-18.
- Krásny, L., and Gourse, R.L. (2004). An alternative strategy for bacterial ribosome synthesis: *Bacillus subtilis* rRNA transcription regulation. *EMBO J.* *23*, 4473–4483.
- Kupriyanova, E., Villarejo, A., Markelova, A., Gerasimenko, L., Zavarzin, G., Samuelsson, G., Los, D.A., and Pronina, N. (2007). Extracellular carbonic anhydrases of the stromatolite-forming cyanobacterium *Microcoleus chthonoplastes*. *Microbiology* *153*, 1149–1156.
- Kupriyanova, E. V., Sinetova, M.A., Cho, S.M., Park, Y.-I., Los, D.A., and Pronina, N.A. (2013). CO<sub>2</sub>-concentrating mechanism in cyanobacterial photosynthesis: organization, physiological role, and evolutionary origin. *Photosynth. Res.* *117*, 133–146.
- Kurian, D., Phadwal, K., and Mäenpää, P. (2006). Proteomic characterization of acid stress response in *Synechocystis* sp. PCC 6803. *Proteomics* *6*, 3614–3624.
- Latifi, A., Ruiz, M., and Zhang, C.-C. (2009). Oxidative stress in cyanobacteria. *FEMS Microbiol. Rev.* *33*, 258–278.
- Lea-Smith, D.J., Bombelli, P., Vasudevan, R., and Howe, C.J. (2016). Photosynthetic, respiratory and extracellular electron transport pathways in cyanobacteria. *Biochim. Biophys. Acta - Bioenerg.* *1857*, 247–255.
- Lehtimäki, N., Shunmugam, S., Jokela, J., Wahlsten, M., Carmel, D., Keränen, M., Sivonen, K., Aro, E.M., Allahverdiyeva, Y., and Mulo, P. (2011). Nodularin uptake and induction of oxidative stress in spinach (*Spinachia oleracea*). *J. Plant Physiol.* *168*, 594–600.
- Llácer, J.L., Contreras, A., Forchhammer, K., Marco-Marín, C., Gil-Ortiz, F., Maldonado, R., Fita, I., and Rubio, V. (2007). The crystal structure of the complex of P<sub>II</sub> and acetylglutamate kinase reveals how P<sub>II</sub> controls the storage of nitrogen as arginine. *Proc. Natl. Acad. Sci. U. S. A.* *104*, 17644–17649.
- Llácer, J.L., Espinosa, J., Castells, M.A., Contreras, A., Forchhammer, K., and Rubio, V. (2010). Structural basis for the regulation of NtcA-dependent transcription by proteins PipX and P<sub>II</sub>. *Proc. Natl. Acad. Sci. U. S. A.* *107*, 15397–15402.
- Lüddecke, J., and Forchhammer, K. (2013). From P<sub>II</sub> signaling to metabolite sensing: A novel 2-oxoglutarate sensor that details P<sub>II</sub> - NAGK complex formation. *PLoS One* *8*, e83181.
- Lutkenhaus, J. (2007). Assembly Dynamics of the Bacterial MinCDE System and Spatial Regulation of the Z Ring. *Annu. Rev. Biochem.* *76*, 539–562.
- Lyons, T.W., Reinhard, C.T., and Planavsky, N.J. (2014). The rise of oxygen in Earth's early ocean and atmosphere. *Nature* *506*, 307–315.
- Maeda, H., Sakuragi, Y., Bryant, D.A., and DellaPenna, D. (2005). Tocopherols protect *Synechocystis* sp. strain PCC 6803 from lipid peroxidation. *Plant Physiol.* *138*, 1422–1435.
- Maheswaran, M., Ziegler, K., Lockau, W., Hagemann, M., and Forchhammer, K. (2006). P<sub>II</sub>-Regulated Arginine Synthesis Controls Accumulation of Cyanophycin in *Synechocystis* sp. Strain PCC 6803. *J. Bacteriol.* *188*, 2730–2734.
- Mahounga, D.M., Sun, H., and Jiang, Y.L. (2018). Crystal structure of the effector-binding domain of *Synechococcus elongatus* CmpR in complex with ribulose 1,5-bisphosphate. *Acta Crystallogr. Sect. F Struct. Biol. Commun.* *74*, 506–511.
- Malik, S., Zalenskaya, K., and Goldfarb, A. (1987). Competition between Sigma Factors for Core RNA Polymerase. *Nucleic Acids Res.* *15*, 8521–8530.
- Mao, C., Zhu, Y., Lu, P., Feng, L., Chen, S., and Hu, Y. (2018). Association of  $\omega$  with the C-terminal region of the  $\beta'$  subunit is essential for assembly of RNA polymerase in *Mycobacterium tuberculosis*. *J. Bacteriol.* *200*, e00159-18.

- Marbouty, M., Saguez, C., Cassier-Chauvat, C., and Chauvat, F. (2009a). Characterization of the FtsZ-interacting septal proteins SepF and Ftn6 in the spherical-celled cyanobacterium *Synechocystis* strain PCC 6803. *J. Bacteriol.* *191*, 6178–6185.
- Marbouty, M., Mazouni, K., Saguez, C., Cassier-Chauvat, C., and Chauvat, F. (2009b). Characterization of the *Synechocystis* strain PCC 6803 penicillin-binding proteins and cytokinetic proteins FtsQ and FtsW and their network of interactions with ZipN. *J. Bacteriol.* *191*, 5123–5133.
- Marteyn, B., Domain, F., Legrain, P., Chauvat, F., and Cassier-Chauvat, C. (2009). The thioredoxin reductase-glutaredoxins-ferredoxin crossroad pathway for selenate tolerance in *Synechocystis* PCC6803. *Mol. Microbiol.* *71*, 520–532.
- Mathew, R., and Chatterji, D. (2006). The evolving story of the omega subunit of bacterial RNA polymerase. *Trends Microbiol.* *14*, 450–455.
- Mathew, R., Ramakanth, M., and Chatterji, D. (2005). Deletion of the gene *rpoZ*, encoding the  $\omega$  subunit of RNA polymerase, in *Mycobacterium smegmatis* results in fragmentation of the  $\beta'$  subunit in the enzyme assembly. *J. Bacteriol.* *187*, 6565–6570.
- Matsui, M., Yoshimura, T., Wakabayashi, Y., Imamura, S., Tanaka, K., Takahashi, H., Munchiko, A., and Shirai, M. (2007). Interference Expression at Levels of the Transcript and Protein among Group 1, 2, and 3 Sigma Factors Genes in a Cyanobacterium. *Microbes Environ.* *22*, 32–43.
- Mazouni, K., Bulteau, S., Cassier-Chauvat, C., and Chauvat, F. (1998). Promoter element spacing controls basal expression and light inducibility of the cyanobacterial *secA* gene. *Mol. Microbiol.* *30*, 1113–1122.
- Mazouni, K., Domain, F., Cassier-chauvat, C., and Chauvat, F. (2004). Molecular analysis of the key cytokinetic components of cyanobacteria : FtsZ , ZipN and MinCDE. *Mol. Microbiol.* *52*, 1145–1158.
- Mazumder, A., and Kapanidis, A.N. (2019). Recent Advances in Understanding  $\sigma$ 70-Dependent Transcription Initiation Mechanisms. *J. Mol. Biol.* *431*, 3947–3959.
- McConnell, M.D., Koop, R., Vasil'ev, S., and Bruce, D. (2002). Regulation of the distribution of chlorophyll and phycobilin-absorbed excitation energy in cyanobacteria. A structure-based model for the light state transition. *Plant Physiol.* *130*, 1201–1212.
- Mcgurn, L.D., Moazami-Goudarzi, M., White, S.A., Suwal, T., Brar, B., Tang, J.Q., Espie, G.S., and Kimber, M.S. (2016). The structure, kinetics and interactions of the  $\beta$ -carboxysomal  $\beta$ -carbonic anhydrase, CcaA. *Biochem. J.* *473*, 4559–4572.
- Meeks, J.C., Wolk, C.P., and Thomas, J. (1977). The pathways of assimilation of  $^{13}\text{NH}_4^+$  by the cyanobacterium, *Anabaena cylindrica*. *J. Biol. Chem.* *252*, 7894–7900.
- Mi, H.L., Endo, T., Schreiber, U., Ogawa, T., and Asada, K. (1992). Electron Donation from Cyclic and Respiratory Flows to the Photosynthetic Intersystem Chain is Mediated by Pyridine Nucleotide Dehydrogenase in the Cyanobacterium *Synechocystis* PCC 6803. *Plant Cell Physiol.* *33*, 1233–1237.
- Mills, L.A., McCormick, A.J., and Lea-Smith, D.J. (2020). Current knowledge and recent advances in understanding metabolism of the model cyanobacterium *Synechocystis* sp. PCC 6803. *Biosci. Rep.* *40*, 1–33.
- Min, K.-T., Hilditch, C.M., Diederich, B., Errington, J., and Yudkin, M.D. (1993).  $\sigma^F$ , the first compartment-specific transcription factor of *B. subtilis*, is regulated by an anti- $\sigma$  factor that is also a protein kinase. *Cell* *74*, 735–742.
- Minakhin, L., Bhagat, S., Brunning, A., Campbell, E.A., Darst, S.A., Ebright, R.H., and Severinov, K. (2001). Bacterial RNA polymerase subunit  $\omega$  and eukaryotic polymerase subunit RPB6 are sequence, structural, and functional homologs and promote RNA polymerase assembly. *Proc. Natl. Acad. Sci. U. S. A.* *98*, 892–897.
- Mitchell, J.E., Oshima, T., Piper, S.E., Webster, C.L., Westblade, L.F., Karimova, G., Ladant, D., Kolb, A., Hobman, J.L., Busby, S.J.W., et al. (2007). The *Escherichia coli* regulator of sigma 70 protein, Rsd, can up-regulate some stress-dependent promoters by sequestering sigma 70. *J. Bacteriol.* *189*, 3489–3495.

- Mohamed, H.E., Van De Meene, A.M.L., Roberson, R.W., and Vermaas, W.F.J. (2005). Myxoxanthophyll is required for normal cell wall structure and thylakoid organization in the cyanobacterium *Synechocystis* sp. strain PCC 6803. *J. Bacteriol.* *187*, 6883–6892.
- Mohammadi, T., van Dam, V., Sijbrandi, R., Vernet, T., Zapun, A., Bouhss, A., Diepeveen-de Bruin, M., Nguyen-Distèche, M., de Kruijff, B., and Breukink, E. (2011). Identification of FtsW as a transporter of lipid-linked cell wall precursors across the membrane. *EMBO J.* *30*, 1425–1432.
- Montesinos, M.L., Muro-Pastor, A.M., Herrero, A., and Flores, E. (1998). Ammonium/methylammonium permeases of a cyanobacterium: Identification and analysis of three nitrogen-regulated *amt* genes in *Synechocystis* sp. PCC 6803. *J. Biol. Chem.* *273*, 31463–31470.
- Mostofa, K.M.G., Liu, C.Q., Zhai, W., Minella, M., Vione, D., Gao, K., Minakata, D., Arakaki, T., Yoshioka, T., Hayakawa, K., et al. (2016). Reviews and Syntheses: Ocean acidification and its potential impacts on marine ecosystems. *Biogeosciences* *13*, 1767–1786.
- Mukherjee, K., Nagai, H., Shimamoto, N., and Chatterji, D. (1999). GroEL is involved in activation of *Escherichia coli* RNA polymerase devoid of the omega subunit *in vivo*. *Eur. J. Biochem.* *266*, 228–235.
- Mullineaux, C.W. (2014). Electron transport and light-harvesting switches in cyanobacteria. *Front. Plant Sci.* *5*, 7.
- Murakami, K.S. (2013). X-ray Crystal Structure of *Escherichia coli* RNA Polymerase  $\sigma^{70}$  Holoenzyme. *J. Biol. Chem.* *288*, 9126–9134.
- Murakami, K., Murakami, and S., K. (2015). Structural Biology of Bacterial RNA Polymerase. *Biomolecules* *5*, 848–864.
- Murakami, K.S., Masuda, S., and Darst, S.A. (2003). Crystallographic Analysis of *Thermus aquaticus* RNA Polymerase Holoenzyme and a Holoenzyme/Promoter DNA Complex. *Methods Enzymol.* *370*, 42–53.
- Muro-Pastor, A.M., Herrero, A., and Flores, E. (2001). Nitrogen-regulated group 2 sigma factor from *Synechocystis* sp. strain PCC 6803 involved in survival under nitrogen stress. *J. Bacteriol.* *183*, 1090–1095.
- Narainsamy, K., Marteyn, B., Sakr, S., Cassier-Chauvat, C., and Chauvat, F. (2013). Genomics of the Pleiotropic Glutathione System in Cyanobacteria. In *Advances in Botanical Research*, (Academic Press Inc.), pp. 157–188.
- Nikaido, H. (2003). Molecular Basis of Bacterial Outer Membrane Permeability Revisited. *Microbiol. Mol. Biol. Rev.* *67*, 593–656.
- Nikkinen, H.-L.L., Hakikila, K., Gunnelius, L., Huokko, T., Pollari, M., and Tyystjärvi, T. (2012). The SigB  $\sigma$  factor regulates multiple salt acclimation responses of the cyanobacterium *Synechocystis* sp. PCC 6803. *Plant Physiol.* *158*, 514–523.
- Nishimura, T., Takahashi, Y., Yamaguchi, O., Suzuki, H., Maeda, S.I., and Omata, T. (2008). Mechanism of low CO<sub>2</sub>-induced activation of the *cmp* bicarbonate transporter operon by a LysR family protein in the cyanobacterium *Synechococcus elongatus* strain PCC 7942. *Mol. Microbiol.* *68*, 98–109.
- Noctor, G., Mhamdi, A., Chaouch, S., Han, Y., Neukermans, J., Marquez-Garcia, B., Queval, G., and Foyer, C.H. (2012). Glutathione in plants: an integrated overview. *Plant. Cell Environ.* *35*, 454–484.
- Ogawa, T., Marco, E., and Orus, M.I. (1994). A gene (*ccmA*) required for carboxysome formation in the cyanobacterium *Synechocystis* sp. strain PCC6803. *J. Bacteriol.* *176*, 2374–2378.
- Ohkawa, H., Pakrasi, H.B., and Ogawa, T. (2000). Two types of functionally distinct NAD(P)H dehydrogenases in *Synechocystis* sp. strain PCC6803. *J. Biol. Chem.* *275*, 31630–31634.
- Omata, T., Price, G.D., Badger, M.R., Okamura, M., Gohta, S., and Ogawa, T. (1999). Identification of an ATP-binding cassette transporter involved in bicarbonate uptake in the cyanobacterium *Synechococcus* sp. strain PCC 7942. *Proc. Natl. Acad. Sci. U. S. A.* *96*, 13571–13576.

- Omata, T., Gohta, S., Takahashi, Y., Harano, Y., and Maeda, S.I. (2001). Involvement of a CbbR homolog in low CO<sub>2</sub>-induced activation of the bicarbonate transporter operon in cyanobacteria. *J. Bacteriol.* *183*, 1891–1898.
- Orf, I., Schwarz, D., Kaplan, A., Kopka, J., Hess, W.R., Hagemann, M., and Klähn, S. (2016). CyAbrB2 Contributes to the Transcriptional Regulation of Low CO<sub>2</sub> Acclimation in *Synechocystis* sp. PCC 6803. *Plant Cell Physiol.* *57*, 2232–2243.
- Osanai, T., Kanesaki, Y., Nakano, T., Takahashi, H., Asayama, M., Shirai, M., Kanehisa, M., Suzuki, I., Murata, N., and Tanaka, K. (2005a). Positive regulation of sugar catabolic pathways in the cyanobacterium *Synechocystis* sp. PCC 6803 by the group 2 sigma factor sigE. *J. Biol. Chem.* *280*, 30653–30659.
- Osanai, T., Sato, S., Tabata, S., and Tanaka, K. (2005b). Identification of PamaA as a PII-binding membrane protein important in nitrogen-related and sugar-catabolic gene expression in *Synechocystis* sp. PCC 6803. *J. Biol. Chem.* *280*, 34684–34690.
- Osanai, T., Kanesaki, Y., Nakano, T., Takahashi, H., Asayama, M., Shirai, M., Kanehisa, M., Suzuki, I., Murata, N., and Tanaka, K. (2005c). Positive regulation of sugar catabolic pathways in the cyanobacterium *Synechocystis* sp. PCC 6803 by the group 2  $\sigma$  factor SigE. *J. Biol. Chem.* *280*, 30653–30659.
- Osanai, T., Imamura, S., Asayama, M., Shirai, M., Suzuki, I., Murata, N., and Tanaka, K. (2006). Nitrogen induction of sugar catabolic gene expression in *Synechocystis* sp. PCC 6803. *Dna Res.* *13*, 185–195.
- Osanai, T., Azuma, M., and Tanaka, K. (2007). Sugar catabolism regulated by light- and nitrogen-status in the cyanobacterium *Synechocystis* sp. PCC 6803. *Photochem. Photobiol. Sci.* *6*, 508.
- Osanai, T., Ikeuchi, M., and Tanaka, K. (2008). Group 2 sigma factors in cyanobacteria. *Physiol. Plant.* *133*, 490–506.
- Osanai, T., Imashimizu, M., Seki, A., Sato, S., Tabata, S., Imamura, S., Asayama, M., Ikeuchi, M., and Tanaka, K. (2009). ChlH, the H subunit of the Mg-chelatase, is an anti-sigma factor for SigE in *Synechocystis* sp. PCC 6803. *Proc. Natl. Acad. Sci. U. S. A.* *106*, 6860–6865.
- Osanai, T., Oikawa, A., Azuma, M., Tanaka, K., Saito, K., Hirai, M.Y., and Ikeuchi, M. (2011). Genetic Engineering of Group 2  $\sigma$  Factor SigE Widely Activates Expressions of Sugar Catabolic Genes in *Synechocystis* Species PCC 6803. *J. Biol. Chem.* *286*, 30962–30971.
- Osanai, T., Numata, K., Oikawa, A., Kuwahara, A., Iijima, H., Doi, Y., Tanaka, K., Saito, K., and Hirai, M.Y. (2013). Increased bioplastic production with an RNA polymerase sigma factor SigE during nitrogen starvation in *Synechocystis* sp. PCC 6803. *DNA Res.* *20*, 525–535.
- Osanai, T., Oikawa, A., Shirai, T., Kuwahara, A., Iijima, H., Tanaka, K., Ikeuchi, M., Kondo, A., Saito, K., and Hirai, M.Y. (2014a). Capillary electrophoresis-mass spectrometry reveals the distribution of carbon metabolites during nitrogen starvation in *Synechocystis* sp. PCC 6803. *Environ. Microbiol.* *16*, 512–524.
- Osanai, T., Oikawa, A., Numata, K., Kuwahara, A., Iijima, H., Doi, Y., Saito, K., and Hirai, M.Y. (2014b). Pathway-level acceleration of glycogen catabolism by a response regulator in the cyanobacterium *Synechocystis* species PCC 6803. *Plant Physiol.* *164*, 1831–1841.
- Park, Y.H., Lee, C.R., Choe, M., and Seok, Y.J. (2013). HPr antagonizes the anti- $\sigma^{70}$  activity of Rsd in *Escherichia coli*. *Proc. Natl. Acad. Sci. U. S. A.* *110*, 21142–21147.
- Park, Y.H., Um, S.H., Song, S., Seok, Y.J., and Ha, N.C. (2015). Structural basis for the sequestration of the anti- $\sigma^{70}$  factor Rsd from  $\sigma^{70}$  by the histidine-containing phosphocarrier protein HPr. *Acta Crystallogr. Sect. D Biol. Crystallogr.* *71*, 1998–2008.
- Peltier, G., Aro, E.-M., and Shikanai, T. (2016). NDH-1 and NDH-2 Plastoquinone Reductases in Oxygenic Photosynthesis. *Annu. Rev. Plant Biol.* *67*, 55–80.
- Peng, L., and Shikanai, T. (2011). Supercomplex formation with photosystem I is required for the stabilization of the chloroplast NADH dehydrogenase-like complex in Arabidopsis. *Plant Physiol.* *155*, 1629–1639.

- Pentecost, A., and Whitton, B.A. (2012). Ecology of cyanobacteria II: Their diversity in space and time. Springer Sci. Bus. Media.
- Petit, J.R., Jouzel, J., Raynaud, D., Barkov, N.I., Barnola, J.-M., Basile, I., Bender, M., Chappellaz, J., Davis, M., Delaygue, G., et al. (1999). Climate and atmospheric history of the past 420,000 years from the Vostok ice core, Antarctica. *Nature* 399, 429–436.
- Pinto, F., Thapper, A., Sontheim, W., and Lindblad, P. (2009). Analysis of current and alternative phenol based RNA extraction methodologies for cyanobacteria. *BMC Mol. Biol.* 10, 79.
- Pollari, M., Gunnelius, L., Tuominen, I., Ruotsalainen, V., Tyystjärvi, E., Salminen, T., and Tyystjärvi, T. (2008). Characterization of single and double inactivation strains reveals new physiological roles for group 2  $\sigma$  factors in the cyanobacterium *Synechocystis* sp. PCC 6803. *Plant Physiol.* 147, 1994–2005.
- Pollari, M., Ruotsalainen, V., Rantamäki, S., Tyystjärvi, E., and Tyystjärvi, T. (2009). Simultaneous inactivation of sigma factors B and D interferes with light acclimation of the cyanobacterium *Synechocystis* sp. strain PCC 6803. *J. Bacteriol.* 191, 3992–4001.
- Pollari, M., Rantamäki, S., Huokko, T., Kårlund-Marttila, A., Virjamo, V., Tyystjärvi, E., and Tyystjärvi, T. (2011). Effects of deficiency and overdose of group 2 sigma factors in triple inactivation strains of *Synechocystis* sp. strain PCC 6803. *J. Bacteriol.* 193, 265–273.
- Price, G.D., Maeda, S.I., Omata, T., and Badger, M.R. (2002). Modes of active inorganic carbon uptake in the cyanobacterium, *Synechococcus* sp. PCC7942. *Funct. Plant Biol.* 29, 131–149.
- Price, G.D., Badger, M.R., Woodger, F.J., and Long, B.M. (2008). Advances in understanding the cyanobacterial CO<sub>2</sub>-concentrating-mechanism (CCM): functional components, Ci transporters, diversity, genetic regulation and prospects for engineering into plants. *J. Exp. Bot.* 59, 1441–1461.
- Rakhimberdieva, M.G., Boichenko, V.A., Karapetyan, N. V., and Stadnichuk, I.N. (2001). Interaction of phycobilisomes with photosystem II dimers and photosystem I monomers and trimers in the cyanobacterium *Spirulina platensis*. *Biochemistry* 40, 15780–15788.
- Rasmussen, B., Fletcher, I.R., Brocks, J.J., and Kilburn, M.R. (2008). Reassessing the first appearance of eukaryotes and cyanobacteria. *Nature* 455, 1101–1104.
- Rehman, A.U., Cser, K., Sass, L., and Vass, I. (2013). Characterization of singlet oxygen production and its involvement in photodamage of Photosystem II in the cyanobacterium *Synechocystis* PCC 6803 by histidine-mediated chemical trapping. *Biochim. Biophys. Acta - Bioenerg.* 1827, 689–698.
- Riaz-Bradley, A. (2019). Transcription in cyanobacteria: A distinctive machinery and putative mechanisms. *Biochem. Soc. Trans.* 47, 679–689.
- Riaz-Bradley, A., James, K., and Yuzenkova, Y. (2020). High intrinsic hydrolytic activity of cyanobacterial RNA polymerase compensates for the absence of transcription proofreading factors. *Nucleic Acids Res.* 48, 1341–1352.
- Richard, C.L., Tandon, A., Sloan, N.R., and Kranz, R.G. (2003). RNA polymerase subunit requirements for activation by the enhancer-binding protein *Rhodobacter capsulatus* NtrC. *J. Biol. Chem.* 278, 31701–31708.
- Rippka, R., Deruelles, J., and Waterbury, J.B. (1979). Generic assignments, strain histories and properties of pure cultures of cyanobacteria. *J. Gen. Microbiol.* 111, 1–61.
- Roberts, J.W. (2019). Mechanisms of Bacterial Transcription Termination. *J. Mol. Biol.* 431, 4030–4039.
- Rögner, M., Mühlenhoff, U., Boekema, E.J., and Witt, H.T. (1990). Mono-, di- and trimeric PS I reaction center complexes isolated from the thermophilic cyanobacterium *Synechococcus* sp. *Biochim. Biophys. Acta - Bioenerg.* 1015, 415–424.
- Ross, W., Vrentas, C.E., Sanchez-Vazquez, P., Gaal, T., and Gourse, R.L. (2013). The Magic Spot: A ppGpp Binding Site on E. coli RNA Polymerase Responsible for Regulation of Transcription Initiation. *Mol. Cell* 50, 420–429.

- Ross, W., Sanchez-Vazquez, P., Chen, A.Y., Lee, J.H., Burgos, H.L., and Gourse, R.L. (2016). PpGpp Binding to a Site at the RNAP-DksA Interface Accounts for Its Dramatic Effects on Transcription Initiation during the Stringent Response. *Mol. Cell* 62, 811–823.
- Rowlett, V.W., and Margolin, W. (2013). The bacterial Min system. *Curr. Biol.* 23, R553–R556.
- Rye, R., Kuo, P.H., and Holland, H.D. (1995). Atmospheric carbon dioxide concentrations before 2.2 billion years ago. *Nature* 378, 603–605.
- Sabareesh, V., Sarkar, P., Sardesai, A.A., and Chatterji, D. (2010). Identifying N60D mutation in  $\omega$  subunit of *Escherichia coli* RNA polymerase by bottom-up proteomic approach. *Analyst* 135, 2723–2729.
- Sandrini, G., Cunsolo, S., Schuurmans, J.M., Matthijs, H.C.P., and Huisman, J. (2015). Changes in gene expression, cell physiology and toxicity of the harmful cyanobacterium *Microcystis aeruginosa* at elevated CO<sub>2</sub>. *Front. Microbiol.* 6, 401.
- Santos-Beneit, F., Barriuso-Iglesias, M., Fernández-Martínez, L.T., Martínez-Castro, M., Sola-Landa, A., Rodríguez-García, A., and Martín, J.F. (2011). The RNA polymerase omega factor RpoZ is regulated by Phop and has an important role in antibiotic biosynthesis and morphological differentiation in *Streptomyces coelicolor*. *Appl. Environ. Microbiol.* 77, 7586–7594.
- Sarkar, P., Sardesai, A.A., Murakami, K.S., and Chatterji, D. (2013). Inactivation of the bacterial RNA polymerase due to acquisition of secondary structure by the  $\omega$  subunit. *J. Biol. Chem.* 288, 25076–25087.
- Sato, M., Takahashi, K., Ochiai, Y., Hosada, T., Ochi, K., and Nabeta, K. (2009). Bacterial alarmone, guanosine 5'-diphosphate 3'-diphosphate (ppGpp), predominantly binds the  $\beta'$  subunit of plastid-encoded plastid RNA polymerase in chloroplasts. *ChemBioChem* 10, 1227–1233.
- Schneider, G.J., and Haselkorn, R. (1988). RNA-Polymerase Subunit Homology among Cyanobacteria, Other Eubacteria, and Archaeobacteria. *J. Bacteriol.* 170, 4136–4140.
- Schramm, F.D., Schroeder, K., and Jonas, K. (2019). Protein aggregation in bacteria. *FEMS Microbiol. Rev.* 44, 54–72.
- Schuller, J.M., Birrell, J.A., Tanaka, H., Konuma, T., Wulfhorst, H., Cox, N., Schuller, S.K., Thiemann, J., Lubitz, W., Sétif, P., et al. (2019). Structural adaptations of photosynthetic complex I enable ferredoxin-dependent electron transfer. *Science* 363, 257–260.
- Schwarz, R., and Forchhammer, K. (2005). Acclimation of unicellular cyanobacteria to macronutrient deficiency: emergence of a complex network of cellular responses. *Microbiology-Sgm* 151, 2503–2514.
- Selby, C.P., and Sancar, A. (1993). Molecular mechanism of transcription-repair coupling. *Science* (80- ). 260, 53–58.
- Selim, K.A., Haase, F., Hartmann, M.D., Hagemann, M., and Forchhammer, K. (2018). P<sub>II</sub>-like signaling protein SbtB links cAMP sensing with cyanobacterial inorganic carbon response. *Proc. Natl. Acad. Sci.* 115, E4861–E4869.
- Sengupta, A., Sunder, A.V., Sohoni, S. V., and Wangikar, P.P. (2019). The effect of CO<sub>2</sub> in enhancing photosynthetic cofactor recycling for alcohol dehydrogenase mediated chiral synthesis in cyanobacteria. *J. Biotechnol.* 289, 1–6.
- Sham, L.T., Butler, E.K., Lebar, M.D., Kahne, D., Bernhardt, T.G., and Ruiz, N. (2014). MurJ is the flippase of lipid-linked precursors for peptidoglycan biogenesis. *Science* (80- ). 345, 220–222.
- Sheldon, N.D. (2006). Precambrian paleosols and atmospheric CO<sub>2</sub> levels. *Precambrian Res.* 147, 148–155.
- Shi, L., Bischoff, K.M., and Kennelly, P.J. (1999). The *icfG* gene cluster of *Synechocystis* sp. strain PCC 6803 encodes an Rsb/Spo-like protein kinase, protein phosphatase, and two phosphoproteins. *J. Bacteriol.* 181, 4761–4767.
- Shibata, M., Ohkawa, H., Kaneko, T., Fukuzawa, H., Tabata, S., Kaplan, A., and Ogawa, T. (2001). Distinct constitutive and low-CO<sub>2</sub>-induced CO<sub>2</sub> uptake systems in cyanobacteria: Genes involved and their phylogenetic relationship with homologous genes in other organisms. *Proc. Natl. Acad. Sci. U. S. A.* 98, 11789–11794.

- Shibata, M., Katoh, H., Sonoda, M., Ohkawa, H., Shimoyama, M., Fukuzawa, H., Kaplan, A., and Ogawa, T. (2002). Genes essential to sodium-dependent bicarbonate transport in cyanobacteria - Function and phylogenetic analysis. *J. Biol. Chem.* *277*, 18658–18664.
- Shih, P.M., and Matzke, N.J. (2013). Primary endosymbiosis events date to the later Proterozoic with cross-calibrated phylogenetic dating of duplicated ATPase proteins. *Proc. Natl. Acad. Sci. U. S. A.* *110*, 12355–12360.
- Sieger, B., Schubert, K., Donovan, C., and Bramkamp, M. (2013). The lipid II flippase RodA determines morphology and growth in *Corynebacterium glutamicum*. *Mol. Microbiol.* *90*, 966–982.
- Silhavy, T.J., Kahne, D., and Walker, S. (2010). The bacterial cell envelope. *Cold Spring Harb. Perspect. Biol.* *2*.
- So, A.K.-C., and Espie, G.S. (2005). Cyanobacterial carbonic anhydrases. *Can. J. Bot.* *83*, 721–734.
- Sonoda, M., Katoh, H., Vermaas, W., Schmetterer, G., and Ogawa, T. (1998). Photosynthetic electron transport involved in PxcA-dependent proton extrusion in *Synechocystis* sp. strain PCC6803: Effect of pxcA inactivation on CO<sub>2</sub>, HCO<sub>3</sub><sup>-</sup>, and NO<sub>3</sub><sup>-</sup> uptake. *J. Bacteriol.* *180*, 3799–3803.
- Soppa, J., Ludt, K., and Zerulla, K. (2016). The ploidy level of *Synechocystis* sp. PCC 6803 is highly variable and is influenced by growth phase and by chemical and physical external parameters. *Microbiology* *162*, 730–739.
- Sozer, O., Komenda, J., Ughy, B., Domonkos, I., Laczkó-Dobos, H., Malec, P., Gombos, Z., and Kis, M. (2010). Involvement of Carotenoids in the Synthesis and Assembly of Protein Subunits of Photosynthetic Reaction Centers of *Synechocystis* sp. PCC 6803. *Plant Cell Physiol.* *51*, 823–835.
- Srivastava, A., Summers, M.L., and Sobotka, R. (2020). Cyanobacterial sigma factors: Current and future applications for biotechnological advances. *Biotechnol. Adv.* *40*, 107517.
- Suga, M., Akita, F., Sugahara, M., Kubo, M., Nakajima, Y., Nakane, T., Yamashita, K., Umena, Y., Nakabayashi, M., Yamane, T., et al. (2017). Light-induced structural changes and the site of O=O bond formation in PSII caught by XFEL. *Nature* *543*, 131–135.
- Summerfield, T.C., and Sherman, L.A. (2007). Role of sigma factors in controlling global gene expression in Light/Dark transitions in the cyanobacterium *Synechocystis* sp. strain PCC 6803. *J. Bacteriol.* *189*, 7829–7840.
- Takahashi, K., Kasai, K., and Ochi, K. (2004). Identification of the bacterial alarmone guanosine 5'-diphosphate 3'-diphosphate (ppGpp) in plants. *Proc. Natl. Acad. Sci. U. S. A.* *101*, 4320–4324.
- Trautmann, D., Voß, B., Wilde, A., Al-Babili, S., and Hess, W.R. (2012). Microevolution in cyanobacteria: Re-sequencing a motile substrain of *Synechocystis* sp. PCC 6803. *DNA Res.* *19*, 435–448.
- Tsunekawa, K., Shijuku, T., Hayashimoto, M., Kojima, Y., Onai, K., Morishita, M., Ishiura, M., Kuroda, T., Nakamura, T., Kobayashi, H., et al. (2009). Identification and characterization of the Na<sup>+</sup>/H<sup>+</sup> antiporter Nhas3 from the thylakoid membrane of *Synechocystis* sp. PCC 6803. *J. Biol. Chem.* *284*, 16513–16521.
- Tuominen, I., Tyystjärvi, E., and Tyystjärvi, T. (2003). Expression of primary sigma factor (PSF) and PSF-like sigma factors in the cyanobacterium *Synechocystis* sp. strain PCC 6803. *J. Bacteriol.* *185*, 1116–1119.
- Tuominen, I., Pollari, M., Tyystjärvi, E., and Tyystjärvi, T. (2006). The SigB  $\sigma$  factor mediates high-temperature responses in the cyanobacterium *Synechocystis* sp. PCC6803. *FEBS Lett.* *580*, 319–323.
- Tuominen, I., Pollari, M., von Wobeser, E.A., Tyystjärvi, E., Ibelings, B.W., Mattheijs, H.C.P., and Tyystjärvi, T. (2008). Sigma factor SigC is required for heat acclimation of the cyanobacterium *Synechocystis* sp. strain PCC 6803. *FEBS Lett.* *582*, 346–350.
- Türkeri, H., Schweer, J., and Link, G. (2012). Phylogenetic and functional features of the plastid transcription kinase cpCK2 from *Arabidopsis* signify a role of cysteinyl SH-groups in regulatory phosphorylation of plastid sigma factors. *FEBS J.* *279*, 395–409.

- Turmo, A., Gonzalez-Esquer, C.R., and Kerfeld, C.A. (2017). Carboxysomes: metabolic modules for CO<sub>2</sub> fixation. *FEMS Microbiol. Lett.* *364*, 1–7.
- Tyystjärvi, T., Herranen, M., and Aro, E.-M. (2001). Regulation of translation elongation in cyanobacteria: Membrane targeting of the ribosome nascent-chain complexes controls the synthesis of D1 protein. *Mol. Microbiol.* *40*, 476–484.
- Tyystjärvi, T., Huokko, T., Rantamäki, S., and Tyystjärvi, E. (2013). Impact of Different Group 2 Sigma Factors on Light Use Efficiency and High Salt Stress in the Cyanobacterium *Synechocystis* sp. PCC 6803. *PLoS One* *8*.
- Valev, D., Kurkela, J., Tyystjärvi, E., and Tyystjärvi, T. (2020). Testing the Potential of Regulatory Sigma Factor Mutants for Wastewater Purification or Bioreactor Run in High Light. *Curr. Microbiol.* *77*, 1590–1599.
- Valladares, A., Montesinos, M.L., Herrero, A., and Flores, E. (2002). An ABC-type, high-affinity urea permease identified in cyanobacteria. *Mol. Microbiol.* *43*, 703–715.
- Vasil'ev, S., Orth, P., Zouni, A., Owens, T.G., and Bruce, D. (2001). Excited-state dynamics in photosystem II: Insights from the x-ray crystal structure. *Proc. Natl. Acad. Sci. U. S. A.* *98*, 8602–8607.
- Vassilyev, D.G., Sekine, S., Laptenko, O., Lee, J., Vassilyeva, M.N., Borukhov, S., and Yokoyama, S. (2002). Crystal structure of a bacterial RNA polymerase holoenzyme at 2.6 Å resolution. *Nature* *417*, 712–719.
- Vrentas, C.E., Gaal, T., Ross, W., Ebright, R.H., and Gourse, R.L. (2005). Response of RNA polymerase to ppGpp: requirement for the  $\omega$  subunit and relief of this requirement by DksA. *Genes Dev.* *19*, 2378–2387.
- Van De Waal, D.B., Verschoor, A.M., Verspagen, J.M.H., Van Donk, E., and Huisman, J. (2010). Climate-driven changes in the ecological stoichiometry of aquatic ecosystems. *Front. Ecol. Environ.* *8*, 145–152.
- Wang, H.-L., Postier, B.L., and Burnap, R.L. (2004). Alterations in global patterns of gene expression in *Synechocystis* sp. PCC 6803 in response to inorganic carbon limitation and the inactivation of *ndhR*, a LysR family regulator. *J. Biol. Chem.* *279*, 5739–5751.
- Watzer, B., and Forchhammer, K. (2018). Cyanophycin Synthesis Optimizes Nitrogen Utilization in the Unicellular Cyanobacterium *Synechocystis* sp. Strain PCC 6803. *Appl. Environ. Microbiol.* *84*, e01298-18.
- Watzer, B., Spät, P., Neumann, N., Koch, M., Sobotka, R., MacEk, B., Hennrich, O., and Forchhammer, K. (2019). The signal transduction protein PII controls ammonium, nitrate and urea uptake in cyanobacteria. *Front. Microbiol.* *10*, 1428.
- Weiss, A., Moore, B.D., Tremblay, M.H.J., Chaput, D., Kremer, A., and Shaw, L.N. (2016). The  $\omega$  subunit governs RNA polymerase stability and transcriptional specificity in *Staphylococcus aureus*. *J. Bacteriol.* *199*, e00459-16.
- Westbye, A.B., O'Neill, Z., Schellenberg-Beaver, T., and Beatty, J.T. (2017). The *Rhodobacter capsulatus* gene transfer agent is induced by nutrient depletion and the RNAP omega subunit. *Microbiology* *163*, 1355–1363.
- Williams, J.G.K. (1988). Construction of Specific Mutations in Photosystem II Photosynthetic Reaction Center by Genetic Engineering Methods in *Synechocystis* 6803. *Methods Enzymol.* *167*, 766–778.
- Wilson, A., Boulay, C., Wilde, A., Kerfeld, C.A., and Kirilovsky, D. (2007). Light-induced energy dissipation in iron-starved cyanobacteria: Roles of OCP and IsiA proteins. *Plant Cell* *19*, 656–672.
- Wilson, A., Punginelli, C., Gall, A., Bonetti, C., Alexandre, M., Routaboul, J.M., Kerfeld, C.A., Van Grondelle, R., Robert, B., Kennis, J.T.M., et al. (2008). A photoactive carotenoid protein acting as light intensity sensor. *Proc. Natl. Acad. Sci. U. S. A.* *105*, 12075–12080.
- Woodger, F.J., Bryant, D.A., and Price, G.D. (2007). Transcriptional regulation of the CO<sub>2</sub>-concentrating mechanism in a euryhaline, coastal marine cyanobacterium, *Synechococcus* sp. strain PCC 7002: Role of NdhR/CcmR. *J. Bacteriol.* *189*, 3335–3347.

- Xu, M., Ogawa, T., Pakrasi, H.B., and Mi, H. (2008a). Identification and Localization of the CupB Protein Involved in Constitutive CO<sub>2</sub> Uptake in the Cyanobacterium, *Synechocystis* sp. Strain PCC 6803. *Plant Cell Physiol.* *49*, 994–997.
- Xu, M., Bernát, G., Singh, A., Mi, H., Rögner, M., Pakrasi, H.B., and Ogawa, T. (2008b). Properties of Mutants of *Synechocystis* sp. Strain PCC 6803 Lacking Inorganic Carbon Sequestration Systems. *Plant Cell Physiol.* *49*, 1672–1677.
- Yamamoto, H., Peng, L., Fukao, Y., and Shikanai, T. (2011). An Src homology 3 domain-like fold protein forms a ferredoxin binding site for the chloroplast NADH dehydrogenase-like complex in *Arabidopsis*. *Plant Cell* *23*, 1480–1493.
- Yeremenko, N., Jeanjean, R., Prommeenate, P., Krasikov, V., Nixon, P.J., Vermaas, W.F.J., Havaux, M., and Matthijs, H.C.P. (2005). Open Reading Frame *ssr2016* is Required for Antimycin A-sensitive Photosystem I-driven Cyclic Electron Flow in the Cyanobacterium *Synechocystis* sp. PCC 6803. *Plant Cell Physiol.* *46*, 1433–1436.
- Yoon, H.S., Hackett, J.D., Ciniglia, C., Pinto, G., and Bhattacharya, D. (2004). A Molecular Timeline for the Origin of Photosynthetic Eukaryotes. *Mol. Gen. Genet.* *271*, 809–818.
- Zakar, T., Kovacs, L., Vajravel, S., Herman, E., Kis, M., Laczko-Dobos, H., and Gombos, Z. (2018). Determination of PS I oligomerisation in various cyanobacterial strains and mutants by non-invasive methods. *Photosynthetica* *56*, 294–299.
- Zeth, K., Fokinas, O., and Forchhammers, K. (2014). Structural basis and target-specific modulation of ADP sensing by the *Synechococcus elongatus* P<sub>II</sub> signaling protein. *J. Biol. Chem.* *289*, 8960–8972.
- Zhang, G., and Darst, S.A. (1998). Structure of the *Escherichia coli* RNA polymerase  $\alpha$  subunit amino-terminal domain. *Science* (80-. ). *281*, 262–266.
- Zhang, C.C., Zhou, C.Z., Burnap, R.L., and Peng, L. (2018). Carbon/Nitrogen Metabolic Balance: Lessons from Cyanobacteria. *Trends Plant Sci.* *23*, 1116–1130.
- Zhang, P., Battchikova, N., Jansen, T., Appel, J., Ogawa, T., and Aro, E.-M. (2004). Expression and functional roles of the two distinct NDH-1 complexes and the carbon acquisition complex NdhD3/NdhF3/CupA/Sll1735 in *Synechocystis* sp PCC 6803. *Plant Cell* *16*, 3326–3340.
- Zhang, P., Allahverdiyeva, Y., Eisenhut, M., and Aro, E.-M. (2009). Flavodiiron Proteins in Oxygenic Photosynthetic Organisms: Photoprotection of Photosystem II by Flv2 and Flv4 in *Synechocystis* sp. PCC 6803. *PLoS One* *4*, e5331.
- Zhang, P., Eisenhut, M., Brandt, A.M., Carmel, D., Silén, H.M., Vass, I., Allahverdiyeva, Y., Salminen, T.A., and Aro, E.M. (2012a). Operon *flv4-flv2* provides cyanobacterial photosystem II with flexibility of electron transfer. *Plant Cell* *24*, 1952–1971.
- Zhang, S.R., Lin, G.M., Chen, W.L., Wang, L., and Zhang, C.C. (2013). ppGpp metabolism is involved in heterocyst development in the Cyanobacterium *Anabaena* sp. Strain pcc 7120. *J. Bacteriol.* *195*, 4536–4544.
- Zhang, X., Chen, G., Qin, C., Wang, Y., and Wei, D. (2012b). Slr0643, an S2P homologue, is essential for acid acclimation in the cyanobacterium *Synechocystis* sp. PCC 6803. *Microbiol. (United Kingdom)* *158*, 2765–2780.
- Zhao, M.X., Jiang, Y.L., Xu, B.Y., Chen, Y., Zhang, C.C., and Zhou, C.Z. (2010). Crystal structure of the cyanobacterial signal transduction protein P<sub>II</sub> in complex with PipX. *J. Mol. Biol.* *402*, 552–559.
- Zuo, Y., Wang, Y., and Steitz, T.A. (2013). The Mechanism of E. coli RNA Polymerase Regulation by ppGpp Is Suggested by the Structure of their Complex. *Mol. Cell* *50*, 430–436.





**UNIVERSITY  
OF TURKU**

ISBN 978-951-29-8149-6 (PRINT)  
ISBN 978-951-29-8148-9 (PDF)  
ISSN 0082-7002 (Print)  
ISSN 2343-3175 (Online)